CZECH TECHNICAL UNIVERSITY IN PRAGUE

Faculty of Electrical Engineering
Department of Electrical Power Engineering

# Power Quality in Industrial Distribution Systems

Doctoral thesis

Author: Ing. Martin Čerňan

Supervisor: Prof. Ing. Josef Tlustý CSc.
Supervisor specialist: Prof. Ing. Viktor Valouch CSc.

Study program: Electrical Engineering and Information Technology (P2612)
Branch of study: Electric Power Engineering (3907V001)

May 2021, Prague

# Acknowledgement

At this point, I would like to thank everyone who allowed me to complete this work and complete my studies. Many thanks to my family, especially to my parents for their great support throughout the study. Special thanks to my supervisor Prof. Ing. Josef Tlustý CSc. for valuable advice, countless ideas and excellent access to work management. My gratitude also belongs to my supervisor specialist Prof. Ing. Viktor Valouch CSc. for valuable advice, ideas and very valuable consultations. Thanks also go to the Head of the Department of Electrical Power Engineering, Faculty of Electrical Engineering, Czech Technical University in Prague Doc. Ing. Zdeněk Müller PhD. for the creation of excellent conditions and a creative environment within the collective of the department during my studies. My thanks also go to Ing. Peter Šimek PhD. from the Institute of Thermomechanics of the Czech Academy of Sciences for assistance in setting up laboratory experiments and measurements. Special thanks also go to the company Železiarne Podbrezová a.s. to enable practical measurements to be made. Thanks also the Department of Electrical Engineering and Electrophysics at the Institute of Thermomechanics of the Czech Academy of Sciences for enabling the use of the power electronics laboratory.

# Declaration

I hereby declare I have written this doctoral thesis independently and quoted all the sources of information used in accordance with methodological instructions on ethical principles for writing an academic thesis. Moreover, I state that this thesis has neither been submitted nor accepted for any other degree.

Prague, 31th May 2021 …….

Martin Čerňan

# Abstrakt

K tématu bylo přistoupeno tak, aby byla v úvodu zpracována problematika kvality elektrické energie z hlediska legislativy, následně byly definovány parametry kvality elektrické energie (měření i vyhodnocování) a dále uvedeny principy šíření rušení v distribučních soustavách s důrazem na hledisko zdrojů rušení. Jako nejvýznamnější zdroj rušení v průmyslových distribučních soustavách se projevují elektrické obloukové pece (EOP), na které se práce dále specializuje. Pro efektivní uchopení této problematiky práce obsahuje představení technologie EOP a odvození pracovních charakteristik EOP, na základě kterých jsou snadno pochopitelné hlavní mechanismy vzniku flicker efektu. Tato část práce rovněž obsahuje ukázku srovnání teoretických charakteristik s daty z reálného provozu. V návaznosti na příčiny vzniku a mechanismy šíření rušení jsou v práci popsané základní možnosti zlepšení kvality elektrické energie na základě základních opatření bez využití přídavných zařízení. Tyto opatření spočívají ve volbě vhodného místa připojení problematických odběratelů v distribuční soustavě, dále ve volbě vhodných komponentů a ve volbě vhodné konfigurace dané distribuční soustavy. Další možnosti je ještě zásah do výrobní technologie problematického odběratele s cílem omezení problému s kvalitou elektrické energie bez negativního dopadu na produkci odběratele. Potenciál pro výraznější omezení rušení přináší přídavná kompenzační zařízení. Práce podává přehled o současně používaných kompenzačních zařízení pro různorodé aplikace. Na základě vymezení této dizertační práce na průmyslové distribuční soustavy a problematiku spojenou s EOP je další část této práce zaměřená na polovodičově řízené kompenzační zařízení velkých výkonu na bázi výkonových tyristorů – SVC (Static VAr Compensator) a na bázi výkonových tranzistorů – STATCOM (Static Synchronous Compensator). U uvedené dvojice technologií je kladen důraz i na srovnání realizačních a provozních aspektů. Jádro práce se zaměřuje na modifikaci řídicího systému SVC s cílem efektivnějšího omezení flicker efektu. Analyzovaný řídicí systém SVC se skládá z otevřené regulační smyčky, která poskytuje rychlou odezvu na dynamické změny výkonu EOP, a uzavřené regulační smyčky, která poskytuje přesnou regulaci k zajištění požadované hodnoty účiníku v předávacím místě – PCC (Point of Common Coupling). Vylepšení spočívá v použití alternativních technik pro zpracování signálu vstupních řídicích proměnných. První alternativní technikou je použití SOGI (Second Order Generalized Integrator), který se také používá v jiných souvisejících aplikacích. Druhou alternativní technikou je použití váhovací funkce flicker efektu, která odpovídá funkci použité k měření flicker efektu pomocí standardizovaného flickermetru. K ověření vlastností navrhovaných technik bylo použito experimentální laboratorní pracoviště. K simulaci dynamického chování EOP byla použita data měřená ze skutečného provozu, která byla implementována do experimentu pomocí VSC (Voltage Source Converter). Analýza naměřených dat a dat získaných z laboratorních přístrojů vykazuje vysokou podobnost. Pokusy byly prováděny v několika variantách, aby odrážely rozdíly v různých fázích výrobního procesu v EOP. U všech variant byl vyhodnocen výsledný efekt blikání a jednotlivé techniky byly porovnány navzájem a s výsledky jiných prací. Práce navíc obsahuje případovou studií, která je prakticky zaměřena na konkrétní oblast. Popisuje podmínky a rozsah problémů s kvalitou elektrické energie ve studované oblasti a vyhodnocuje přínos již realizovaných opatření.

# Klíčová slova

Kvalita elektrické energie, elektrická oblouková pec, Static Var Compensator, omezování flicker efektu, průmyslová distribuční soustava, řízení SVC, vylepšené řízení SVC, šíření flicker efektu.

# Abstract

The topic was approached in such a way that the issue of electricity quality from the point of view of legislation was dealt in the introduction. Subsequently, the parameters of electricity quality were defined (measurement and evaluation). Furthermore, the principles of interference propagation in distribution systems were presented with emphasis on the aspect of interference sources. Electric arc furnaces (EAF), on which the work further specializes, are the most significant source of interference in industrial distribution systems. To effectively grasp this issue, the work contains an introduction to EAF technology and the derivation of EAF performance characteristics, based on which the main mechanisms of the flicker effect are easily understood. This part of the work also contains an example of the comparison of theoretical characteristics with data from real operation. In connection with the causes and mechanisms of interference propagation, the work describes the basic possibilities of improving the power quality on the basis of basic measures without the use of additional equipment. These measures consist in the selection of a suitable connection point for problematic customers in the distribution system, as well as in the selection of suitable components and the selection of a suitable configuration of the given distribution system. Another possibility is to intervene in the production technology of the problematic customer in order to reduce the problem with the power quality without a negative impact on the customer's production. Additional compensation devices provide the potential for more significant interference reduction. The work provides an overview of currently used compensation devices for various applications. Based on the definition of this dissertation on industrial distribution systems and issues related to EAFs, another part of this work focuses on semiconductor-controlled high power compensation devices based on power thyristors - SVC (Static VAr Compensator) and power transistors – STATCOM (Static Synchronous Compensator). Emphasis is also placed on the comparison of implementation and operational aspects of these technologies. The core of the work focuses on the modification of the SVC control system in order to more effectively reduce the flicker effect. The analyzed SVC control system consists of an open control loop, which provides a fast response to dynamic changes in EAF power, and a closed control loop, which provides precise control to ensure the required power factor value in the PCC (Point of Common Coupling). The improvement lies in the use of alternative techniques for signal processing of the input control variables. The first alternative technique is to use SOGI (Second Order Generalized Integrator), which is also used in other related applications. The second alternative technique is to use the weighting function of the flicker effect, which corresponds to the function used to measure the flicker effect using a standardized flickmeter. An experimental laboratory was used to verify the properties of the proposed techniques. Data from real operation were used to simulate the dynamic behavior of the EAF and were implemented in the experiment using VSC(Voltage Source Converter). The analysis of measured data and data obtained from laboratory instruments shows a high similarity. The experiments were performed in several variants to reflect the differences at different stages of the production process in the EAF. For all variants, the resulting flicker effect was evaluated and the individual techniques were compared with each other and with the results of other work. In addition, the work contains a case study, which is practically focused on a specific area. It describes the conditions and extent of problems with the power quality in the studied area and evaluates the benefits of already implemented measures.

# Keywords

Power Quality, Electric Arc Furnace, Static Var Compensator, Flicker Effect, Industrial Distribution system, SVC Control, Improved SVC control, Flicker Effect Propagation.

# Content

# List of abbreviations

| | |
|---|---|
| **AC** | Alternated Current |
| **ANN** | Artificial Neural Network |
| **DC** | Direct Current |
| **DRI** | Direct Reduced Iron |
| **DSO** | Distribution System Operator |
| **EAF** | Electric Arc Furnace |
| **EHV** | Extra High Voltage |
| **EMC** | Electromagnetic Compatibility |
| **EU** | European Union |
| **FACTS** | Flexible AC Transmission systems |
| **FCD** | Filtration-Compensation Device |
| **FF** | Flicker Filter |
| **FLL** | Frequency Locked Loop |
| **GIU** | Graphical User Interface |
| **HBI** | Hot Briqueted Iron |
| **HV** | High Voltage |
| **HVDC** | High Voltage Direct Current |
| **LF** | Ladle Furnace |
| **LPF** | Low Pass filter |
| **LV** | Low Voltage |
| **MSC** | Mechanically Switched Capacitors |
| **MSR** | Mechanically Switched Reactor |
| **MV** | Medium Voltage |
| **NARX** | Nonlinear Autoregressive Exogenous Model |
| **OL** | Overhead Line |
| **OLTC** | On Load Tap Changer |
| **PCC** | Point of Common Coupling |
| **PI** | Proportional - Integral |
| **RMS** | Root Mean Square |
| **SAIDI** | System Average Interruption Duration Index |
| **SAIFI** | System Average Interruption Frequency Index |
| **SOGI** | Second Order Generalized Integrator |
| **SOGI-QSG** | Second-Order Generalized Integrator based Quadrature Signal Generator |
| **SSR** | Solid-state Relay |
| **STATCOM** | Static Synchronous Compensator |
| **SVC** | Static VAr Compensator |
| **SVS** | Static VAr System |
| **TCR** | Thyristor Controlled Reactor |
| **THD** | Total Harmonic Distortion |
| **TSC** | Thyristor Switched Capacitors |
| **TSO** | Transmission System Operator |
| **UHP** | Ultra Heat Power |
| **VSC** | Voltage Source Converter |

# List of figures

# List of tables

# 1 Introduction

## 1.1 Thesis organization

The dissertation is divided into ten chapters, including the introduction and conclusion. The introductory chapter "**Power quality**" is focused on approaching the issue of power quality in terms of legislation, defining the parameters of power quality (measurement and evaluation), the principles of propagation of interference in distribution systems, and in terms of sources of interference. The most significant source of interference in industrial distribution systems is the electric arc furnace (EAF), on which this work will specialize. The chapter "**Electric arc furnace**" specializes in arc furnaces in more detail, which presents this technology with a deeper focus on the electrical part. For a more effective grasp of the issue of power quality, this chapter is further limited to the performance characteristics of EAF, based on which the main mechanisms of the flicker effect are easily understood. The chapter also contains an example of comparing theoretical characteristics with data from real EAF operation. The following chapter "**Basic methods for power quality improvement**" describes the basic measures for improving the power quality without the use of additional equipment. These include the selection of a suitable connection point for problematic customers in the distribution system, the selection of suitable components, and the selection of a suitable configuration of the distribution system. Another possibility is to intervene in the production technology of the problematic customer in order to reduce the problem of power quality without a negative impact on the customer's production. This chapter is followed by the chapter "**Use of compensation devices to improve the power quality**", which describes possible measures to improve the power quality with the use of additional compensating devices. The initial part of this chapter provides an overview of currently used compensation devices for various applications. Based on the definition of this dissertation on industrial distribution systems and issues related to electric arc furnaces, the next part of this chapter focuses on semiconductor-controlled high power compensation devices based on SVC (Static Var Compensator) power thyristors and STATCOM (Static Synchronous Compensator) power transistors. The mentioned pair of technologies also emphasizes the comparison of implementation and operational aspects. The chapter "**Enhanced possibilities of deploying FACTS systems in industrial distribution systems**" brings new knowledge about the possibilities of extended deployment of compensation devices based on power semiconductor elements. These systems were derived from Flexible AC Transmission Systems (FACTS) devices, which are the domain of applications in transmission systems. There are fundamental differences in the control system of these devices. This chapter provides an overview of these differences and suggestions for further improvements to streamline the power quality improvement feature in specified applications. The next chapter "**Case study of an industrial power system in a problematic area**" is practically focused on a specific area. It describes the conditions and extent of power quality problems in the studied area and evaluates the benefits of already implemented measures. Potential measures with a closer look at the use of compensation devices are provided in the following practically oriented chapter "**FACTS utilization in the problematic area**". To test the proposed changes in the SVC compensation control system, a laboratory-scale SVC device was designed and assembled. VSC (Voltage Source Converter) was used to simulate the behavior of the electric arc furnace, which was controlled on the basis of reference data sets, which were obtained by measurements from real EAF operation. A methodology was developed for the use of test data, facilitating the subsequent evaluation of the results. The following chapter "**Evaluation of the result of simulations and measurements**" presents the evaluation of the achieved results and the contribution of the work, their comparison with other works, and discussion.

## 1.2 State of art

Power quality is one of the basic pillars for satisfying the requirements of electricity consumers. In the past, the most important parameters of power quality were the size of the supply voltage and the system frequency [1]. The fluctuation of these indicators was caused by insufficiently built infrastructure and the growing number of connected customers and increasing electricity consumption. With regard to the sustainability of the electricity system, considerable development has been made in the area of electricity savings, which has brought a number of new technologies [2]. These technologies mostly include devices with non-linear or highly variable operating characteristics (semiconductor converters [3], electric arc furnaces, etc.). This group of equipment brought significant savings in electricity, but in terms of electricity quality brought new problems that needed to be addressed. These problems manifested themselves in the form of energy disturbances - higher harmonics, voltage fluctuations, voltage asymmetry, and more [4]. These forms of energy interference have, from a certain level, adverse effects on the functionality of other devices connected to the distribution system. At this time, the concept of electromagnetic compatibility (EMC), which specializes in electromagnetic interference, was introduced [5]. To eliminate undesirable phenomena, the issue of electromagnetic compatibility is based on the assessment of equipment from two perspectives:

- The extent to which equipment connected to the system may be a source of interference.
- The extent to which equipment connected to the distribution system must be resistant to interference.

The term compatible interference level defines that the radiated interference of a particular device must be below this level with a certain margin, and also the immunity of the device to interference must be higher than this level with a certain margin. This methodology ensures reliable operation of the device so that its function is not affected by electromagnetic interference. With the growing importance of equipment, the requirement for a higher level of interference immunity is taken into account for equipment.

The parameters of power quality also include indicators that not only have a negative effect on the functionality of the device but also have a negative effect on the users of these devices. A typical example is voltage fluctuations, which result in a flicker effect. Voltage fluctuations, even to a small extent, can cause observable changes in the luminous flux of light sources. At a certain frequency of these changes, due to their perception through the human eye, there are unpleasant feelings that adversely affect human activities (concentration, increased fatigue, nervousness,…). The flicker effect is therefore an important area of electricity quality issues and deserves considerable attention.

The issue of the flicker effect most often appears in electrical systems in three areas:

- **Flicker effect in the low voltage distribution system** [6] - most often occurs together with unsatisfactory values of other power quality parameters (voltage magnitude, higher harmonics, voltage asymmetry). This problem most often occurs on long LV (low voltage) feeders with a gradual increase in the number of customers or an increase in the size of consumption without the necessary strengthening of the infrastructure. In this case, the flicker effect is not conditioned by the presence of a source of interference. Interference is caused by accidental switching of appliances within the LV feeder, which causes large changes in the "soft" network, resp. voltage fluctuations. In the long run, the only solution to eliminate this problem is to strengthen networks. This can be achieved by replacing the wires (not always a sufficient measure) or by thickening the distribution system by building a new distribution substation and thus shortening the LV feeders (an effective solution, but more costly). The flicker effect in a low

voltage distribution system may also occur due to an increase in the number of connected photovoltaic systems [7].

- **Flicker effect in the areas of wind power plants** [8], [9] - In wind power plants, voltage fluctuations and the flicker effect occur principally due to the formation of a wind shadow formed by the tube of the wind power plant structure. Another cause may be changes in wind speed and direction. Compared to the previous one, this issue is already more significant due to the fact that wind power plants are connected to higher voltage levels, which means that the resulting interference affects a much larger distribution area. In this case, problems with the flicker effect are solved effectively using wind turbines connected to the system using an inverter or HVDC system or additional compensation equipment. The mentioned measures in the case of wind power plants work effectively because the generated interference is mostly periodic in nature.
- **Flicker effect in industrial distribution systems with large sources of interference** [10] - most often these are large loads with nonlinear volt-ampere characteristics. On the one hand, they are typically semiconductor converters of various drives, especially in the heavy and mining industries, on the other hand, it is the electric arc furnaces that are the most problematic. Electric arc furnaces are problematic in two respects. The first aspect is the stochastic behavior of electric arcs (highly variable consumption and other problems), the second aspect is the high performance of equipment (from units up to hundreds of MW). Due to the connection of these technological units to higher voltage levels (HV distribution, or transmission system), there is a significant risk of interference propagation (flicker effect) in a large area with a significant impact on the number of other customers in the area. There are several possibilities to reduce the flicker effect in industrial distribution systems, and this work will specialize in them in more detail.

Electric arc furnaces (EAF) are a very important technology for the production of steel with more than 120 years of history. In the total world steel production of 1869 million tons, the EAF accounted for 27.7% [11] in 2019, in the case of the EU, the total steel production in 2019 was 158.8 million tons and the EAF production share was 40.9%. The main advantage of EAF is the recycling and refining of steel scrap of all kinds. EAF can process a wide range of input materials - HBI (hot briquetted iron), DRI (direct reduced iron), pig iron, molten liquid metal, and all types of steel scrap. The EAF output material can be processed by a continuous casting process, ingot casting, or other casting processes. EAF technology has undergone great development and the following parameters are typical for current equipment - batch weight up to 350 t, energy consumption from 345 kWh/t, melting time from 40 minutes, and consumption of graphite electrodes from 1.1 kg/t [12].

The main cause of power quality problems in EAFs is the nonlinear nature of impedance and highly variable nature [13]. These properties are caused by the physical nature of the electric arc, which is significantly reflected in its nonlinear volt-ampere characteristics. In addition, the arc environment in the case of EAF has many specifics, which we will explain at the various stages of the production process in EAF. The phases of the production process can be divided according to the character into two basic types [14].

The first type is the melting of the input material of the batch, which is the most problematic in terms of power quality. Scrap and other input materials are inserted into the furnace space, through which the electrodes are gradually re-melted to the bottom of the furnace, where molten liquid metal collects. This process is accompanied by alternating arc extinguishing and short-circuit states as scrap slides occur. To mitigate the negative effects of this process (power fluctuations, wear of furnace linings, and electrodes), a lower arc voltage (thus lower power) is used. When the electrodes reach the bottom of the liquid metal furnace, some stabilization of the process occurs, a layer of slag begins to

form on the liquid metal, which begins to cover the electric arcs. At this point, it is possible to increase the stress of the arcs (longer arcs and higher power), which helps to shorten the melting time. This phase of the process continues until the batch is completely melted. During melting, the process of melting the input material is usually repeated three times with further charges always being milder than the first (a considerable amount of liquid metal is already present in the furnace). [12]

The second type is the refining phase, which is less problematic in terms of power quality, as the furnace works only with liquid metal and the electric arcs are completely covered with slag. During this production phase, various chemical processes take place (extraction of undesirable substances, the addition of alloys, adjustment of carbon content) and reaching the required melt temperature before the material passes to the next process of ladle metallurgy. The ladle furnace (LF) is similar in nature to the EAF refining phase, but with an electrical output of 10 - 20% of the EAF output, as it only serves to maintain the melt temperature during the addition of other alloys and additives. [12]

The problem with power quality in electric arc furnaces manifests itself to varying degrees, depending on the stage of the production process [15]. The most significant problems include odd higher harmonics (due to nonlinear volt-ampere characteristics of the arc), subharmonic, even higher harmonics, consumption asymmetries (due to process variability in EAF), and reactive power consumption (due to short-circuit power limitation and EAF working range position for stable burning of electric arcs). The most significant problem and the most difficult to limit is voltage fluctuations (flicker effect), which is primarily caused by variable EAF consumption. For this reason, other parts of the work are focused exclusively on the flicker effect.

To reduce the flicker effect in industrial distribution systems with EAF, 3 components are typically involved: the steel plant operator, the distribution system operator (DSO), and the transmission system operator (TSO). To effectively improve the situation, the cooperation of all named entities is needed, while each entity has possible corrective measures at its disposal. The cooperation of these entities is important from the beginning of the EAF construction plan and subsequently also during the operation of the facility. Stakeholders can take a number of measures to reduce the flicker effect. The involvement of individual entities in partial measures is summarized in Table 1.1. In the following specialized chapters of this dissertation, the individual measures will be described in detail.

| Measure | Involved entity | | |
|---|---|---|---|
| | TSO | DSO | Steelworks |
| Increasing short-circuit power in PCC | Yes | Yes | No |
| Separation of EAF section power supply | Yes | Yes | Partly |
| SVC utilization | Partly | Partly | Yes |
| STATCOM utilization | Partly | Partly | Yes |
| Customized EAF design | No | No | Yes |
| Improving the production process in EAF | No | No | Yes |

*Table 1.1: Involvement of subjects in reducing the flicker effect in the industrial distribution system with EAF.*

On the part of the TSO and DSO, it is most often a matter of strengthening the systems and separating the section supplying the EAF. These measures have a direct effect on reducing the flicker effect and on minimizing the group of customers that would be affected by the interference. However, it is a time-consuming and investment-intensive process, but with a significant effect.

On the part of the EAF operator, the strongest motivation is for the implementation of measures, especially in the area of design and improvement of the production process. These measures lead both to a reduction in the flicker effect and a reduction in the operating costs of EAF technology and an increase in productivity (reduction of energy consumption, reduction of electrode

consumption, increase of product quality, etc.). These changes can be achieved by appropriate processing, sorting, and storage of input material (crushed scrap), the use of an advanced process control system (dynamic regulation of electrode position), the use of gas and oxygen burners technology, and the use of foamed slag. These measures are now standard for thriving steel producers using EAF.

The last group of measures is the use of compensation devices [16]. This measure is most often carried out under the direction of a steel plant operator with an EAF at the instigation of the DSO / TSO, who may penalize the steel plant operator for reactive power consumption and further require that the generated interference is within certain permits. Filter compensation devices are thus in many cases a necessary measure. This is therefore a necessary investment for steel plant operators, but it does not bring about a significant improvement in the production process. Compensating devices can, to a limited extent, increase the productivity of an electric arc furnace.

In the past, the so-called fixed compensations were most often used, when at the time of melting the compensating elements (passive harmonic filters or capacitor banks) were switched on directly using a circuit breaker without dynamic regulation. This solution was disadvantageous due to the fact that during the operation of the EAF there could be a small amount of supply and consumption of reactive power from industrial distribution systems and this type of equipment did not contribute significantly to reducing the flicker effect.

Currently, dynamic compensation SVC (Static Var Compensator) is most often used. This is the previous variant supplemented by a decompensation converter TCR (Thyristor Controlled Reactor). SVC makes it possible to continuously and dynamically control reactive power, which brings precise control of the power factor, symmetrization of consumption, and a significant reduction of the flicker effect due to dynamic properties. This type of device is tested by long-term reliable operation, robust construction, and availability in a wide range of rated power.

The current and future trend is the use of STATCOM technology (Static Synchronous Compensator). The technology is based on the use of VSC (Voltage Source Converter) technology using IGBT transistor elements. This technology is characterized by the possibility of active and reactive power control, compared to SVC with better dynamic properties and the ability to reduce the flicker effect to a greater extent. The disadvantages of this technology often include greater sensitivity, a small spread of technology in the area, and significantly higher investment intensity compared to SVC technology.

For steelworks operators with EAF, there is often little or no incentive to switch from SVC to STATCOM. This type of change would bring them only significant investment costs, while the financial benefit from the new technology will not be applied. For many electric arc furnace operators, only the operation of SVC technology can be expected in the future. Thus, for more effective flicker reduction, it has significant potential to improve SVC's ability to reduce the flicker effect. Taking into account the financial demands, there is significant potential in improving the SVC control system.

## 1.3 Defining objectives

Following the previous subchapter, the following objectives are set:

1. Introduction to power quality issues from applicable legislation, power quality parameters, causes of power quality problems, power quality measurements, and principles of interference propagation.
2. Elaboration of an overview of basic possibilities of power quality improvement without the use of additional compensation devices - possibilities of modification of system components, possibilities of system reconfiguration, and modification of technological process with focus on industrial distribution systems with EAF.
3. Elaboration of an overview of compensating devices - an overview of used technologies and their specifics.
4. Improvement of SVC equipment for more effective reduction of flicker effect in industrial distribution systems with EAF. The proposed improvement will consist of modifying the control system of the industrial SVC design.
5. Creation of a case study for a selected industrial distribution system with EAF, which demonstrates the effectiveness of the implemented measures.
6. Experimental verification of the proposed improvements based on point 4 and subsequent comparison of the results with other works.

# 2 Power Quality

The concept of power quality is based on the fact that electricity is perceived as a commodity. In the early days of electrification, the main goal of electricity consumers was availability. Over time, operators have realized the importance of the reliability of energy systems. The subsequent rapid development of robust and modern interconnected power systems ensured a sufficient level of power system reliability. Also with the development of new technologies, such as semiconductor power electronics, as well as the use of renewable energy sources, electricity companies have been interested in both environmental and financial issues concerning electricity. This has also created the need to monitor the quality of electricity in electrical systems. The inclusion of energy quality in relation to the reliability and availability of electricity [17] is shown in Figure 2.1.

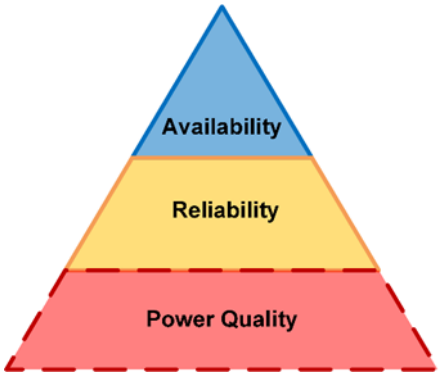


*Figure 2.1: Power quality context illustration. [17]*

## 2.1 Legislation

Power quality monitoring is carried out on the basis of legislation [18], [19], [20], [21] according to the standard ČSN EN 50160 "Characteristics of the voltage of electricity supplied from public distribution networks" [21]. Power quality parameters according to [21]can be divided into two groups:

- Parameters depending on the structure and parameters of electricity generation sources, transmission systems, and distribution systems. These parameters can include the system frequency, supply voltage deviations, voltage phenomena, signal level in the supply voltage, etc.
- Parameters associated with connecting nonlinear loads to the distribution/industrial system. These parameters can include harmonic voltages, the flicker effect, asymmetries in the supply voltage, and subharmonic voltages. These parameters form a significant part of the issue of industrial distribution networks.

## 2.2 Power quality parameters

Power quality requirements in distribution systems are based on the standard [21]. Based on possible complaints from distribution system customers, the distribution system operator shall perform measurements, the output of which is a protocol stating whether or not the requirements specified in [21] have been met. The aim of this subchapter is to briefly present what is one of the requirements according to [21].

The standard [21] describes the voltage characteristics of electricity supplied from the public distribution system. The characteristics are generally divided into two categories:

- Persistent phenomena - a group of parameters capturing permanent deviations of monitored quantities from nominal values. The reasons for these phenomena are load characteristics, load changes, or the presence of nonlinear loads.
- Voltage-related events - a group of parameters that capture sudden and significant deviations from the desired voltage waveform. Reasons include unforeseen events (failures) or external causes.

It should also be noted that the limit values of the specified parameters are separately defined for low voltage (LV), medium voltage (MV), and high voltage (HV) levels.

### 2.2.1 Persistent phenomena

Persistent phenomena include:

- System frequency
- Supply voltage deviations
- Rapid voltage changes - flicker effect
- Supply voltage asymmetry
- Harmonic voltages
- Interharmonic voltages
- Signal voltage in the network

The frequency evaluation is based on the evaluation of the mean frequency value for a 10-second interval. Tolerances are specified for two situations. The first situation concerns a distribution system synchronously interconnected with a transmission system within an interconnected system. The second situation concerns the distribution system in island operation, ie without interconnection with the transmission system within the interconnected system. For the second situation, the tolerances are less strict. In both situations, the tolerances are specified for two different confidence intervals - for the first situation 99.5% and 100% for the second situation 95% and 100%.

The evaluation of supply voltage deviations is based on 10 minutes of mean RMS voltage values. As in the case of network frequency, there are two situations - the first situation is the distribution system synchronously connected to the transmission system within the interconnected system. The second situation is without synchronous interconnection (island operation) or in the case of special remote network users. The second situation allows a larger deviation for the cases $U < U_{nom}$. Only one confidence interval (95%) is used for the supply voltage.

The evaluation of rapid voltage changes is based on the evaluation of the long-term flicker effect perceptibility $P_{lt}$ (value for 2 hours time interval), which is determined on the basis of knowledge of 12 chronologically consecutive values of the short-term flicker perceptibility $P_{st}$ according to (2.1). One confidence interval (95%) is used for this value.

$$P_{\mathrm{lt}} = \sqrt[3]{\sum_{i=1}^{12} \frac{P_{\mathrm{sti}}^3}{12}} \tag{2.1}$$

The supply voltage asymmetry is evaluated on the basis of the ratio of the ten-minute RMS value of the negative sequence and positive sequence voltage components. The maximum permitted share of the feedback component is up to 2%. The evaluation is performed for a period of one week under normal operating conditions for one confidence interval (95%).

Higher harmonic voltages are evaluated on the basis of two approaches, which are applied simultaneously. The first approach is to evaluate the ten-minute mean RMS values of the individual higher harmonics (ranging from 2nd harmonic to 25th harmonic). The evaluation is performed for a period of one week under normal operating conditions for one confidence interval (95%). The second approach is the evaluation of the total harmonic distortion (THD - Total Harmonic Distortion) which is determined according to (2.2).

$$THD = \sqrt{\sum_{h=2}^{40} (v_{\mathrm{h}})^2} \tag{2.2}$$

where $v_h$ is the relative amplitude of the *h*-th higher harmonic. In contrast to the first approach, higher harmonics from the 2nd harmonic to the 40th harmonic are considered for THD. To meet the requirements, the maximum value of the total harmonic distortion of the voltage is determined.

In the case of signal voltages in the network, the 3-second mean value of the signal voltages is evaluated. The maximum permissible value of the signal voltage depends on the signal frequency. One 99% confidence interval is considered in the evaluation.

### 2.2.2 Voltage events

Voltage events include:

- Supply voltage interruption
- Supply voltage drops
- Increased supply voltage
- Transient over voltages

Supply voltage interruptions are manifested by an unpredictable and variable nature. The issue is addressed in an informative annex to the standard [21]. Based on the above appendix, supply voltage interruptions are divided into two groups - long and short voltage interruptions. Long supply voltage interruptions are characterized by interruptions lasting longer than 3 minutes. In terms of expressing the quality of electricity supply, SAIFI, SAIDI, and other indicators are used to evaluate this parameter. The values of the indicators are reported within the distribution system operators and individual countries and have a certain weight in the methodologies for determining the electricity distribution fee (influence on the price decisions of the regulator). These indicators differ for different types of networks (overhead lines vs. underground cables) and also for different types of landscape (flat landscape, mountainous forest landscape, area with an increased incidence of risky meteorological phenomena, etc.). For short interruptions, the indication values can be found in [22]. Most often it is an interruption lasting up to 1 second, otherwise, depending on the approach, interruptions lasting less than 1 minute are considered, resp. 3 minutes - so that events do not fall under long interruptions.

Drops and increases in supply voltage have different causes. Decreases most often occur due to incoming faults in the power supply system or in the equipment of connected customers. The increases are due to switching events and load disconnecting. Evaluation methods are in principle similar for voltage drops and increases. These methods are specifically regulated by the standard [23]. For decreases and increases, threshold values are determined based on the permissible deviations of the supply voltage with a defined hysteresis according to [23]. Events are then classified on the basis of two quantities. The first quantity is the duration of the decrease, where 5 time intervals are distinguished for voltage drops, 3 time intervals are distinguished for voltage increases. The second variable in the voltage drop is the rate of drop - resp. residual voltage (5 intervals) and for voltage increase increased voltage (2 intervals).

Transient over voltages are caused by switching or a direct lightning strike and lightning strike induction.

## 2.3 Measurement of power quality parameters

The measurement of power quality parameters set out in [21] is further specified by the harmonized standard ČSN EN 61000-4-30 "Electromagnetic compatibility (EMC) - Part 4-30: Testing and measurement techniques - Methods for measuring energy quality" [23], which is based on from the International Electrotechnical Commission (IEC) standard [23]. The measurement of the flicker effect is specifically described in the standard ČSN EN 61000-4-15 "Electromagnetic compatibility (EMC) - Part 4-15: Testing and measurement techniques - Flickermeter - Specialization of function and dimensioning" [24]. Measurement of higher harmonics and interharmonics is specifically described in the standard ČSN EN 61000-4-7 "Electromagnetic compatibility (EMC) - Part 4-15: Testing and measurement techniques - General directive on measurement and measurement of harmonics and interharmonics for distribution networks and connected equipment to them" [25]. Table 2.1 summarizes the requirements for measuring individual power quality parameters for systems with a nominal frequency of 50 Hz.

| Parameter | Evaluation interval | | Accuracy class | | Measuring range | | Aggregation |
|---|---|---|---|---|---|---|---|
| | Class A | Class S | Class A | Class S | Class A | Class S | |
| **Frequency** | 10 s | | ±10 mHz | ±50 mHz | 42,5-57,5 Hz | 42,5-57,5 Hz | Not mandatory |
| **Voltage** | 10 periods | | ±0,1 % $V_{din}$ | ±0,5 % $V_{din}$ | 10-150% $V_{din}$ | 20-120% $V_{din}$ | 3s/10min/120min |
| **Flicker effect**[1)] | $P_{st}$ - 10 min (1-15 min) | | ±0,5 % $V_{din}$ | ±0,5 % $V_{din}$ | 0,2-10 $P_{st}$ | 0,4-4 $P_{st}$ | 12 * $t_{st}$ |
| | $P_{lt}$ - 12 * $t_{st}$ | | | | | | |
| **Short-term decreases and short-term increases in supply voltage** | $V_{RMS1/2}$ ($T_{1/2}$ determined based on frequency) | | ±0,2 % $V_{din}$, duration ±1 period | ±1 % $V_{din}$, duration ±1 period | Undefined | Undefined | Not used |
| **Voltage interruptions** | $V_{RMS1/2}$ ($T_{1/2}$ determined based on frequency) | | ±0,2 % $V_{din}$, duration ±1 period, or ±2 period | ±1 % $V_{din}$, duration ±1 period, or ±2 period | Undefined | Undefined | Not used |
| **Supply voltage asymmetry** | 10 periods | | ±0,15 % for $v_2$ and $v_0$ | ±0,3 % for $v_2$ and $v_0$ | 0,5-5 % $v_2$, 0,5-5 % $v_0$ | 1-5 % $v_2$, 1-5 % $v_0$ | 3s/10min/120min |
| **Harmonic voltages**[2)] | 10 periods | | ±5 % $V_m$ | ±5 % $V_m$ | $V_m \geq 1$ % $V_{nom}$ | $V_m \geq 3$ % $V_{nom}$ | 3s/10min/120min |
| | | | ±0,05 % $V_{nom}$ | ±0,15 % $V_{nom}$ | $V_m < 1$ % $V_{nom}$ | $V_m < 3$ % $V_{nom}$ | |
| **Interharmonic voltages**[2)] | 10 periods | | ±5 % $V_m$ | ±5 % $V_m$ | $V_m \geq 1$ % $V_{nom}$ | $V_m \geq 3$ % $V_{nom}$ | 3s/10min/120min |
| | | | ±0,05 % $V_{nom}$ | ±0,15 % $V_{nom}$ | $V_m < 1$ % $V_{nom}$ | $V_m < 3$ % $V_{nom}$ | |
| **Voltage network signals to a power supply voltage** | 10 periods | | ±5 % $V_m$ | Specified by the manufacturer | 3-15 % $V_{din}$ | Specified by the manufacturer | Not mandatory |
| | | | ±0,15 % $V_{din}$ | Specified by the manufacturer | 1-3 % $V_{din}$ | Specified by the manufacturer | Not mandatory |
| | | | without requirement | Specified by the manufacturer | 0-1 % $V_{din}$ | Specified by the manufacturer | Not mandatory |
| **Rapid voltage change (RVC)** | 100 * $V_{RMS1/2}$ | | ±0,1 % $V_{din}$ | ±0,5 % $V_{din}$ | 10-150% $V_{din}$ | 20-120% $V_{din}$ | Not used |
| **Current** | 10 periods | | ±1 % $I_m$ | ±2 % $I_m$ | 10-100 % $I_{nom}$ | 10-100 % $I_{nom}$ | 3s/10min/120min |
| **Current harmonics** | 10 periods | | ±5 % $I_m$ | ±5 % $I_m$ | $I_m \geq 3$ % $I_{nom}$ | $I_m \geq 10$ % $I_{nom}$ | 3s/10min/120min |
| | | | ±0,15 % $I_{nom}$ | ±0,5 % $I_{nom}$ | $I_m < 3$ % $I_{nom}$ | $I_m < 10$ % $I_{nom}$ | |
| **Current interharmonics** | 10 periods | | ±5 % $I_m$ | ±5 % $I_m$ | $I_m \geq 3$ % $I_{nom}$ | $I_m \geq 10$ % $I_{nom}$ | 3s/10min/120min |
| | | | ±0,15 % $I_{nom}$ | ±0,5 % $I_{nom}$ | $I_m < 3$ % $I_{nom}$ | $I_m < 10$ % $I_{nom}$ | |
| **Current asymmetry** | 10 periods | | Undefined | Undefined | Undefined | Undefined | 3s/10min/120min |
| 1) IEC 61000-4-15<br>2) IEC 61000-4-7 | | | | | | | |

*Table 2.1: Overview of requirements for measuring power quality parameters for 50 Hz systems.*

## 2.4 Causes of power quality problems

It is possible to identify a selected group of devices connected to the distribution system, which from the principle of its function generate unwanted interference, as the most important group of causes of power quality problems. A group of these devices can be classified based on two criteria. The first criterion is the classification in terms of the size of consumption, on the basis of which it is possible to divide equipment (or consumption) with interfering effects as follows:

- Households and small consumers - interference affects a small surrounding area, for example within an LV feeder.
- **Industry (large customers)** - interference can affect areas with a larger area, in the worst case the node area of the very HV distribution system, to a lesser extent part of the HV or MV feeder. This dissertation focuses on this area.

The second criterion is the classification based on the characteristics of the equipment. Typically, the division into two groups is used [26], [27], [28]:

- Equipment with non-linear volt-ampere characteristics - based on the principle of the device, for example, electric arc, saturation of magnetic circuits of electrical machines, etc.
- Semiconductor converters - this is essentially a subcategory of the previous group. Partial semiconductor devices are characterized by a nonlinear volt-ampere characteristic. This group is singled out separately, looking for a large number of variants and a large representation at present.

Table 2.2 shows an overview of the types of interference generated by individual types of devices [26], [27], [28]. The overview focuses on power quality parameters that can be most affected by these devices. Many parameters of electricity quality listed in subchapter 2.2 are influenced by other factors (the frequency is influenced by the power balance within the whole power system the size of the supply voltage is influenced by the system dimensioning and the number and parameters of connected customers, fast voltage events are also influenced by events within the whole power system).

| Consumer specification | Device character | Category of device | Harmonics | Flicker effect | Voltage asymmetry |
|---|---|---|---|---|---|
| Industry and large consumers | Nonlinear V-A characteristics | Electric arc furnaces | Yes | Yes | Yes |
| | | Welding devices | Yes | Yes | No |
| | | Transformers | Selected operating states | No | Selected operating states |
| | | Induction furnaces | Selected operating states | No | According to the configuration |
| | | Motors | Selected operating states | No | No |
| | Semiconductor converters | 3-phase controlled drives | Yes | Depending on the process | No |
| | | DC drives | Yes | Depending on the process | No |
| | | Converters for welding devices | Yes | Depending on the process | No |
| | | Converters for wind power plants | Yes | Yes | No |
| | | Converters for photovoltaics | Yes | No | No |
| | | HVDC systems | Yes | No | No |
| | | SSR (switching over whole periods 50 Hz) | No | Depending on the settings | According to the configuration |
| | | Converters for induction furnaces | Yes | No | According to the configuration |
| Households and small consumers | Semiconductor converters | Light sources | Yes | No | No |
| | | Home appliances | Yes | No | No |
| | | Pumps | Yes | No | No |
| | | IT devices | Yes | No | No |
| | | SSR(switching over whole periods 50 Hz) | No | Depending on the settings | No |
| | Nonlinear V-A characteristics | Selected light sources | Yes | No | No |
| | | Small motors | Selected operating states | No | No |

*Table 2.2: An overview of categorized devices and their effects on power quality. [26], [27], [28]*

The following paragraphs (semiconductor converters and EAFs) point to more detailed causes of power quality problems.

### 2.4.1 Examples for semiconductor converters

Semiconductor converters are a large group of interfering devices. In most cases, they are negatively manifested only by higher harmonics. However, other problems may occur, but only depending on the specific application for which they are used (cyclic operation, dynamically changing loads, etc.). A specific example of current waveforms of the one phase taken from the network with thyristor-controlled rectifiers is illustrated in Figure 2.2. The figure compares the waveforms for 6-pulse and 12-pulse connections. Only one stream is illustrated, for clarity. The waveforms were obtained on the basis of a simulation [29].

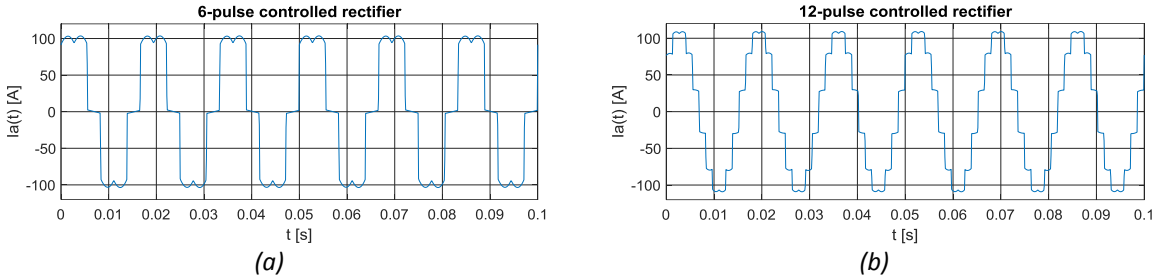


*Figure 2.2: Demonstration of single-phase current waveforms taken from a network with a 6-pulse (a) and a 12-pulse (b) thyristor controlled rectifier.*

Figure 2.3 shows the results of the Fourier analysis of the waveforms shown in Figure 2.2.

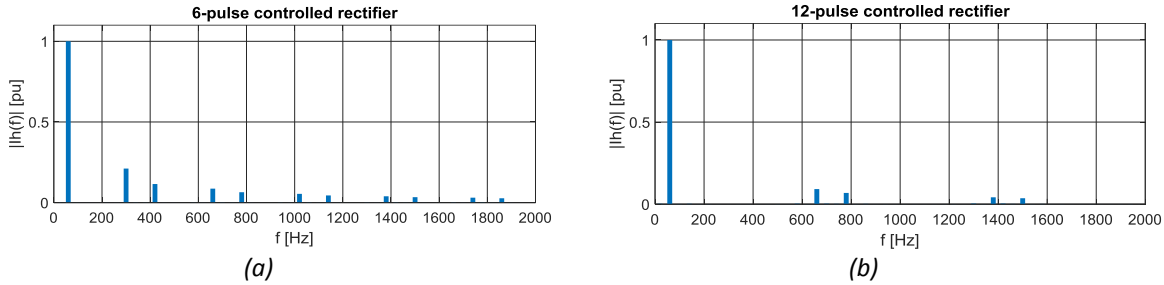


*Figure 2.3: Results of the Fourier analysis of the waveforms shown in Figure 2.2.*

## 2.4.2 Examples for EAF

EAFs have the greatest negative effects on the electricity system. This is due to both their high power and the nature of the interference. EAFs are manifested by higher harmonics, subharmonics, flicker effect, and consumption asymmetry. Figure 2.4 shows the current waveform taken of one phase of the EAF (the waveform was obtained by measuring the supply section of EAF in the MV substation).

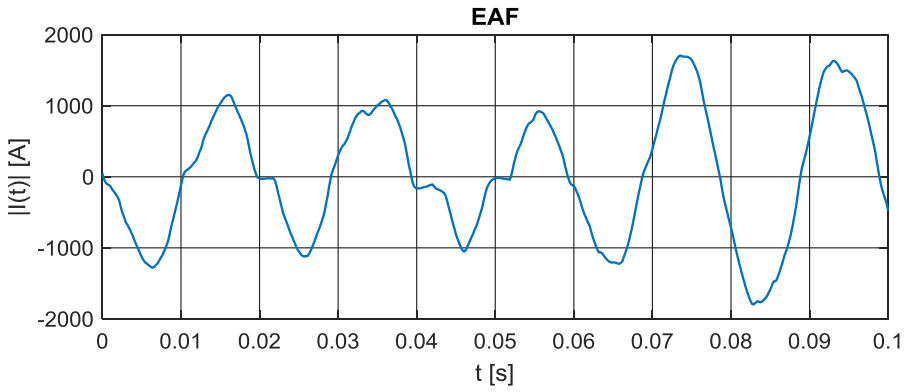


*Figure 2.4: Example of consumed current waveform of EAF (1 phase).*

In comparison with the example of the rectifier (Figure 2.3), the stochastic behavior of the EAF is visible in Figure 2.4. Figure 2.5 illustrates the results of the Fourier analysis of the waveform on Figure 2.4.

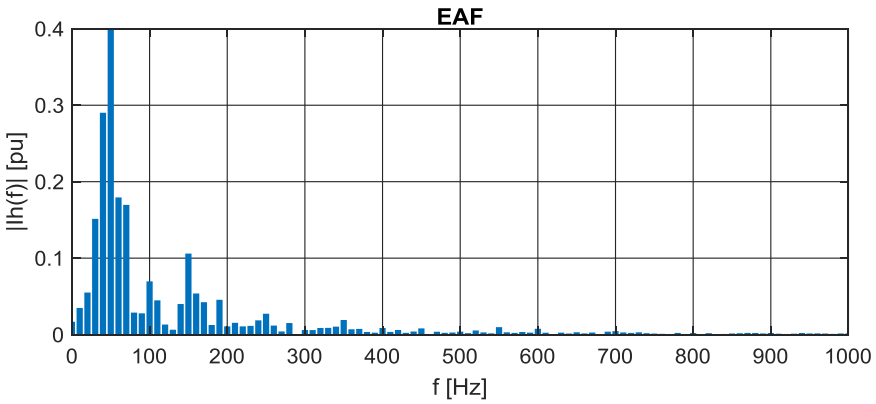


*Figure 2.5: Result of the Fourier analysis of the waveform shown in Figure 2.4.*

## 2.5 Propagation of interference in transmission and distribution systems

The issue of interference propagation in distribution systems is crucial in terms of planning the development of the system and the integration of modern technologies on the side of production and consumption of electricity. The current centralized model of the electricity system is transformed into a decentralized model. The philosophy of the centralized model of the power system is characterized by a robust backbone transmission system into which power enters from large centralized plants and further power is output to transformer stations (electrical stations) of individual node areas. In these power stations, power is transferred between the TSO and the DSO at the HV level. Within the distribution system, small production sources are also considered, which are connected to the LV, MV, and HV system. Furthermore, it is assumed that within the nodal areas of the distribution system, consumption exceeds electricity production. Currently, there is a visible transformation to a decentralized model of the electricity system. For large sources fed into the transmission system, there are more and more arguments for its gradual attenuation. Typical causes include the approaching end of technology life, depletion of available fuel supplies, economic, environmental, and social aspects.

### 2.5.1 Propagation of higher harmonics

Calculating the propagation of higher harmonics is an important analytical tool for monitoring and improving power quality from the initial design of parts of the system and equipment connected to it. In terms of the complexity of the requirements for the analysis of the propagation of higher harmonics, possible methods can be divided into three categories [30]:

1. Methods based on analysis in the frequency and time domain.
2. Methods for modeling direct injection of higher harmonics, capacitive load switching, provided that the equivalents according to Norton's theorem are not affected by switching operations and further where the change of the phase angle affects the results.
3. Analysis of voltage and current waveforms during transients caused by normal switching operations.

For the issue of power quality assessment (interference propagation and its limitation), the analysis in the frequency domain is most often sufficient, where nonlinear loads are represented as current sources for individual higher harmonics. The procedure is based on the description of an *n*-node system using the admittance matrix defined according to (2.3).

$$\hat{\mathbf{Y}}(h) = \begin{bmatrix} \hat{\mathrm{Y}}_{(1,1)}(h) & \dots & \hat{\mathrm{Y}}_{(1,\mathrm{n})}(h) \\ \vdots & \ddots & \vdots \\ \hat{\mathrm{Y}}_{(\mathrm{n},1)}(h) & \dots & \hat{\mathrm{Y}}_{(\mathrm{n},\mathrm{n})}(h) \end{bmatrix} \tag{2.3}$$

Where $\hat{\mathbf{Y}}(h)$ is admittance matrix for h[th] harmonic frequency (f=2πhf$_0$, f$_0$=50 Hz), $n$ is number of network nodes, $\hat{\mathrm{Y}}_{(i,j)}(h);\ i=j;\ i=1,\dots,n; j=1,\dots,n$ are diagonal elements of admittance matrix a $\hat{\mathrm{Y}}_{(i,j)}(h);\ i\neq j;\ i=1,\dots,n; j=1,\dots,n$ are elements of the admittance matrix outside of diagonal. Diagonal elements of the admittance matrix are defined according to (2.4).

$$\hat{\mathrm{Y}}_{(i,i)}(h)=\sum_{\substack{j=0\\ i\neq j}} -\hat{\mathrm{Y}}_{(\mathrm{i,j})}(h) \tag{2.4}$$

where $\hat{\mathrm{Y}}_{(\mathrm{i,j})}(h)$ is mutual admittance between node *i* and nodes $j=0,1,\dots,n$ for h[th] harmonic frequency. For index $j=0$, the admittance is connected between node *i* and ground. Elements of the admittance matrix outside of the diagonal are defined according to (2.5).

$$\hat{\mathrm{Y}}_{(i,j)}(h)=\ \hat{\mathrm{Y}}_{(\mathrm{i,j})}(h) \tag{2.5}$$

where $\hat{\mathrm{Y}}_{(\mathrm{i,j})}(h)$ is mutual admittance between node *i* and nodes $j=0,1,\dots,n$ for h[th] harmonic frequency.

The sign convention for (2.4) and (2.5) is valid for the so-called appliance-oriented system, for which it applies that the power consumed in the node (consumption) is a positive value and the power supplied to the node (generation) is a negative value. In the case of a resource-oriented system, equations (2.4) and (2.5) would have opposite signs and it would be true that the power consumed at the node (consumption) is a negative value and the power supplied to the node (generation) is a positive value.

To build an admittance matrix, it is necessary to know the network topology and element parameters. To ensure results with a sufficient informative value, it is necessary to take into account the detailed parameters of individual elements and also to define a sufficient part of the network for possible analysis. If the network were represented only by problematic consumption, short-circuit equivalent at the point of common coupling (PCC) and possible compensating device, the results could be distorted, which would result from not being visible for such a simplified network all resonant phenomena that they do occur there. This shortcoming can be easily avoided by considering most of the analyzed network.

After assembling the admittance matrix, we can describe the system in the frequency domain by the matrix equation (2.6).

$$\begin{bmatrix}\hat{\mathrm{I}}_{(1)}(h)\\ \vdots\\ \hat{\mathrm{I}}_{(n)}(h)\end{bmatrix}=\begin{bmatrix}\hat{\mathrm{Y}}_{(1,1)}(h) & \dots & \hat{\mathrm{Y}}_{(1,\mathrm{n})}(h)\\ \vdots & \ddots & \vdots\\ \hat{\mathrm{Y}}_{(\mathrm{n},1)}(h) & \dots & \hat{\mathrm{Y}}_{(\mathrm{n,n})}(h)\end{bmatrix}\begin{bmatrix}\hat{\mathrm{V}}_{(1)}(h)\\ \vdots\\ \hat{\mathrm{V}}_{(n)}(h)\end{bmatrix}=\hat{\mathbf{I}}(h)=\hat{\mathbf{Y}}(h)\,\hat{\mathbf{V}}(h) \tag{2.6}$$

where $\hat{\mathrm{I}}_{(\mathrm{i})}(h)$ is RMS value of *h*[th] harmonic current in *i*[th] node ($i=1,\dots,n$), $\hat{\mathrm{V}}_{(\mathrm{i})}(h)$ is RMS value of *h*[th] harmonic voltage in *i*[th] node ($i=1,\dots,n$), $\hat{\mathbf{I}}(h)$ is column vector of RMS values of *h*[th] harmonic currents and $\hat{\mathbf{V}}(h)$ is column vector of RMS values of *h*[th] harmonic voltages.

At this point, a description of the system for analyzing the propagation of higher harmonics is defined. In terms of power quality, higher harmonics are evaluated for higher harmonic voltages, due to the fact that they contain information about the interaction of the network and nonlinear loads, as opposed to higher harmonic currents that contain only information about the nonlinear load, not the network. In tasks aimed at propagating and limiting the propagation of higher harmonics, higher harmonic currents are usually used as input values and higher harmonic voltages as output values. The values of higher harmonic currents for a specific type of nonlinear load can be obtained by measurement on an already operated device or by estimation depending on the type of technology.

To solve problems defined in this way, a matrix equation with an impedance short-circuit matrix according to (2.7) is used.

$$\hat{\mathbf{V}}(h) = \hat{\mathbf{Z}}(h)\,\hat{\mathbf{I}}(h) \tag{2.7}$$

Where $\hat{\mathbf{Z}}(h)$ is a short circuit impedance matrix for $h^{\text{th}}$ harmonic describing the analyzed network. This matrix can be obtained by inversion of the corresponding admittance matrix according to (2.8).

$$\hat{\mathbf{Z}}(h) = \hat{\mathbf{Y}}(h)^{-\mathbf{1}} \tag{2.8}$$

Using the above mathematical basis, it is possible to analyze the propagation of higher harmonics according to the following procedure:

1. Collection of input parameters - this is the topology of the network and the parameters of its elements and currents of higher harmonics of nonlinear loads.
2. Conversion of all parameters to a uniform reference voltage level, eventually complete introduction of per-units.
3. Construction of a general admittance matrix based on network topology (2.3) - (2.5).
4. Calculation of admittance matrices for partial higher harmonic frequencies.
5. Inversion of the calculated admittance matrices to obtain short-circuit impedance matrices for partial higher harmonic frequencies (2.8).
6. Calculation of higher harmonic voltages for all nodes and higher harmonics (2.7).
7. Evaluation of results and comparison of results with allowed limits.
8. Proposal of measures to limit the propagation of higher harmonics (parameters changes, the addition of compensation devices, etc.) and recalculation.

## 2.5.2 Example of calculation of higher harmonic propagation

Based on the description of the procedure in the previous section 2.5.1, the calculation of the propagation of higher harmonics will be demonstrated by an example. The example is designed for an industrial distribution system, which is supplied from two nodes of the transmission system (represented by short-circuit equivalents ES1 and ES2). In the studied system, two nonlinear loads are connected, manifesting on a significant scale (represented by current sources of higher harmonics VH1 and VH2). To illustrate the implementation of the filter compensation device, this device is also inserted into the studied system.

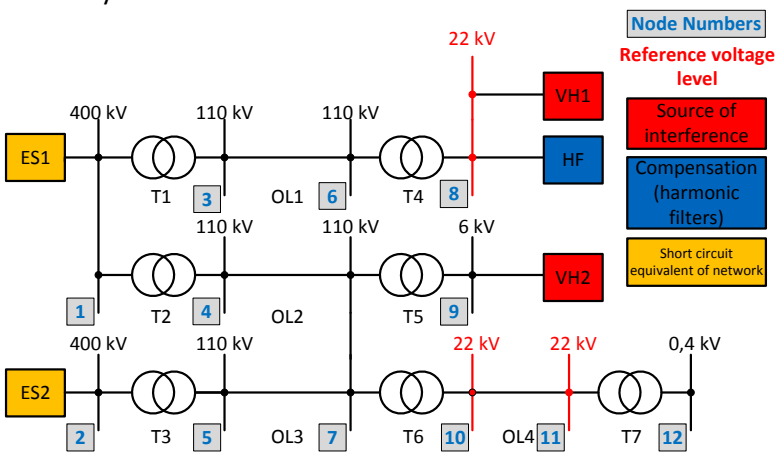


*Figure 2.6: Industrial distribution system for demonstrating the calculation of the propagation of higher harmonics.*

The parameters required to calculate the propagation of higher harmonic disturbances in the industrial distribution system specified in Figure 2.6 are summarized in Table 2.3 (node parameters), Table 2.4 (branch parameters), and Table 2.5 (higher harmonic current values). This demonstration

example is performed in a simplified variant, which means that the parasitic transverse impedances ($R_{k0}$, $C_{k0}$, $R_{m0}$, and $R_{km}$) are neglected. However, it is not recommended to neglect these admittances during a thorough analysis. For example, the parasitic capacitances of overhead lines and especially cables can cause significant resonances in the system.

| Node no. | R [Ω] | L [mH] | C [μF] | $U_n$ [kV] |
|---|---|---|---|---|
| 1 | 0,0 | 0,077 | 0,00 | 400 |
| 2 | 0,0 | 0,128 | 0,00 | 400 |
| 3 | 0,0 | 0,000 | 0,00 | 110 |
| 4 | 18,4 | 4,000 | 0,00 | 110 |
| 5 | 15,0 | 4,500 | 0,00 | 110 |
| 6 | 0,0 | 0,000 | 0,00 | 110 |
| 7 | 25,0 | 5,000 | 0,00 | 110 |
| 8 | 10,0 | 0,000 | 0,00 | 22 |
| 9 | 23,0 | 2,600 | 0,00 | 6 |
| 10 | 0,0 | 0,000 | 0,00 | 22 |
| 11 | 0,0 | 0,000 | 0,00 | 22 |
| 12 | 0,0 | 0,000 | 0,00 | 0,4 |
| Note: Values of R, L a C are recalculated to 22 kV level. | | | | |

*Table 2.3: Nodal parameters for the industrial distribution system according to Figure 2.6.*

| From node | To node | $R_{k0}$ | $C_{k0}$ | $R_{m0}$ | $C_{m0}$ | $R_{km}$ [mΩ] | $L_{km}$ [mH] |
|---|---|---|---|---|---|---|---|
| 1 | 3 | Neglected | | | | 2,37 | 0,44 |
| 1 | 4 | | | | | 2,37 | 0,44 |
| 2 | 5 | | | | | 3,87 | 0,68 |
| 6 | 8 | | | | | 3,78 | 2,31 |
| 7 | 9 | | | | | 10,59 | 4,81 |
| 7 | 10 | | | | | 23,23 | 7,39 |
| 11 | 12 | | | | | 165,60 | 2,04 |
| 3 | 6 | | | | | 0,00 | 0,97 |
| 4 | 7 | | | | | 0,00 | 1,02 |
| 5 | 7 | | | | | 0,00 | 2,55 |
| 10 | 11 | | | | | 0,00 | 11,15 |
| Note 1: Parameters $R_{k0}$, $C_{k0}$, $R_{m0}$ and $R_{km}$ are neglected in the example.<br>Note 2: Values of $R_{km}$ and $L_{km}$ are recalculated to 22 kV level. | | | | | | | |

*Table 2.4: Branches parameters for the industrial distribution system according to Figure 2.6.*

| | | Node number / Higher harmonic current [A] | | | | | | | | | | | |
|---|---|---|---|---|---|---|---|---|---|---|---|---|---|
| | | 1 | 2 | 3 | 4 | 5 | 6 | 7 | 8 | 9 | 10 | 11 | 12 |
| Frequency [Hz] | 100 | 0 | 0 | 0 | 0 | 0 | 0 | 0 | 120 | 0 | 0 | 0 | 0 |
| | 150 | 0 | 0 | 0 | 0 | 0 | 0 | 0 | 150 | 6 | 0 | 0 | 0 |
| | 200 | 0 | 0 | 0 | 0 | 0 | 0 | 0 | 70 | 0 | 0 | 0 | 0 |
| | 250 | 0 | 0 | 0 | 0 | 0 | 0 | 0 | 86 | 60 | 0 | 0 | 0 |
| | 300 | 0 | 0 | 0 | 0 | 0 | 0 | 0 | 40 | 0 | 0 | 0 | 0 |
| | 350 | 0 | 0 | 0 | 0 | 0 | 0 | 0 | 30 | 49 | 0 | 0 | 0 |
| Note: Values are recalculated to 22 kV level. | | | | | | | | | | | | | |

*Table 2.5: Higher harmonics current values for the industrial distribution system according to Figure 2.6.*

For example, the case where a filter-compensation device (FCD) is connected to the studied system (to nodes 8 and 9) is included in the example. The parameters of the individual filters are summarized in Table 2.6.

| Node no. | $I_h$ [A] | h [-] | $Q_{comp}$ [MVAr] | Type | $U_n$ [kV] |
|---|---|---|---|---|---|
| 8 | 120 | 2 | 15 | 3 | 22 |
| 8 | 150 | 3 | 20 | 1 | 22 |
| 8 | 70 | 4 | 10 | 1 | 22 |
| 8 | 86 | 5 | 12 | 2 | 22 |
| 9 | 60 | 5 | 7 | 1 | 22 |
| 9 | 49 | 7 | 5 | 2 | 22 |

*Table 2.6: Parameters of filter-compensation device for the industrial distribution system according to Figure 2.6.*

The filter type parameter in Table 2.6 indicates the three basic most commonly used higher harmonic filters (second-order filter (1), dumped second order filter (2), and C-type filter (3)).

The calculation using the procedure according to section 2.5.1 was performed for the 2nd - 7th harmonic. Of course, the calculation can also be performed for other frequencies, but only a limited range was chosen to maintain the clarity of the illustrated example. The results of the calculations are summarized in Figure 2.7, where the results for each harmonic are individually visualized. The red bars indicate the values for the higher harmonic voltage of a given frequency and at a given node for a system with interference sources VH1 and VH2 and without the use of a filter-compensation device. The blue bars show the results for the case where filter-compensation devices were included in the system, which brought a significant reduction in the propagation of higher harmonics.

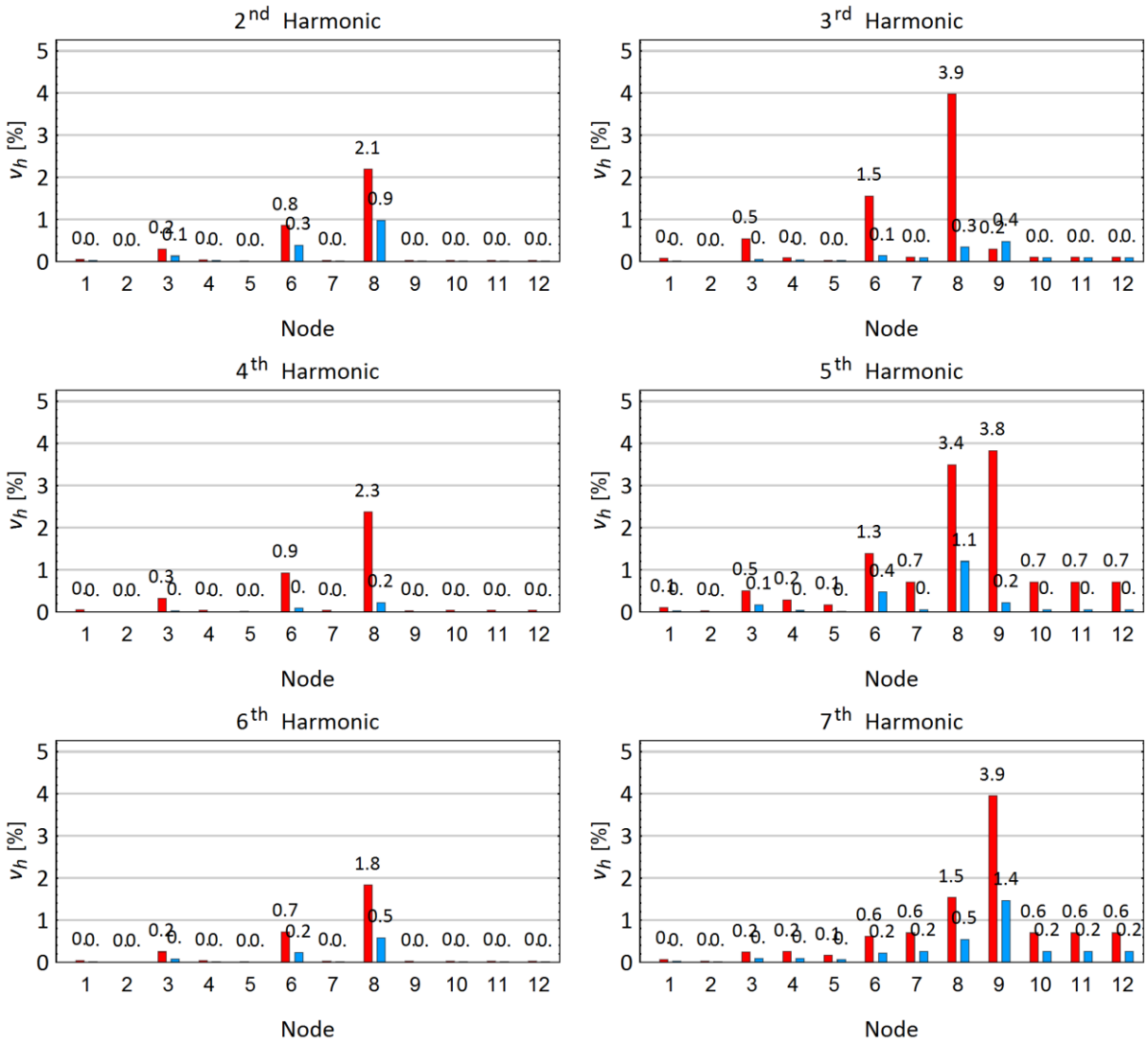


*Figure 2.7: Results of higher harmonic propagation calculations, red bars represent network in basic connection (without FCD), blue bars represent network using FCD.*

### 2.5.3 Flicker effect propagation

The issue of calculations of the propagation of the flicker effect is also important for planning the development of the electricity system with the connection of new types of consumption and sources of electricity. One of three approaches can be used to calculate the propagation of the flicker effect [31]:

1. Methods focused on the analysis of the propagation of the flicker effect in the time domain - the whole network is modeled in the time domain. The source of interference is precisely defined (consumption/generation waveforms). After completion of the simulation, the values of the flicker effect are obtained by applying the algorithm for a standardized flicker meter to the calculated voltage waveforms in individual nodes. This is an accurate method, but computationally demanding, especially for longer periods of time.
2. Methods based on the use of transmission coefficients of the flicker effect - based on the experience in the given type of network, the transmission coefficients of the flicker effect (LV-MV, MV-HV, MV-LV, etc.) are determined. This is a very simple method, but this method is not suitable for networks with more complex topologies.

3. Methods based on the analysis of short-circuit contributions in the nodes of the system - the method is based on the dependence of the flicker effect on the short-circuit power at the connection of the interference source (short-circuit power expresses the imaginary "hardness" of the network). The flicker effect in other nodes is determined based on the ratio of the short-circuit contribution of the analyzed node and the node in which the source of interference is located. This method works reliably even for large networks.

The third described method is the most advantageous for large distribution system topologies. According to the publication [31], this method achieves the most accurate results in comparison with the measured values. The implementation of this method has many common steps with other network calculations (calculation of short-circuit ratios, calculation of higher harmonic propagation). The basis of this method is the knowledge of the impedance short-circuit matrix, which can be obtained by a similar procedure as in the case of propagation of higher harmonics, with the difference that in this case fundamental harmonic is substituted for *h* (*h = 1*). The first step is therefore to construct an admittance matrix for the fundamental harmonic (2.3), which consists of diagonal elements (2.4) and non-diagonal elements (2.5). The impedance short-circuit matrix is then obtained by inverting the assembled admittance matrix (2.8). Subsequently, we work with individual elements of the admittance matrix. The inverse values of the diagonal elements correspond to the short-circuit powers in the respective nodes (the statement applies to the calculation in the established proportional units). Non-diagonal elements indicate a link for the propagation of the flicker effect between two nodes in the sense that for the $i^{th}$ node (node where the source of interference is located) and for the $j^{th}$ node (node in which the transmitted value of the flicker effect is searched) (2.9).

$$P_{\mathrm{lt}_{\mathbf{j}}} = \frac{\left|\hat{Z}_{\mathbf{i},\mathbf{j}}\right|}{\left|\hat{Z}_{\mathbf{i},\mathbf{i}}\right|} P_{\mathrm{lt}_{\mathbf{i}}} \tag{2.9}$$

According to equation (2.9), it is possible to determine the values of the long-term (or short-term) perception of the flicker effect ($P_{lt}$) in all nodes of the system, assuming knowledge of the $P_{lt}$ in the node where the insertion of the interference source is considered. The described procedure can be summarized in the following steps:

1. Collection of input parameters - this is the topology of the network and the parameters of its elements and the values of $P_{lt}$ and $P_{st}$ in the node where the insertion of a potential source of interference is considered.
2. Conversion of all parameters to a uniform reference voltage level, or complete introduction of per-units.
3. Construction of a general admittance matrix based on network topology (2.3) - (2.5).
4. Calculation of admittance matrix for fundamental harmonic.
5. Inverse the calculated admittance matrix to obtain a short-circuit impedance matrix (2.7).
6. Addition of the calculation of the values of the $P_{st}$ ($P_{lt}$) in the other nodes of the system (2.9).
7. Evaluation of results and comparison of results with allowed limits.
8. Proposal of measures to limit the spread of the flicker effect (change of system connection, strengthening of the system, etc.) and recalculation.

Based on the description of the procedure in the previous section 2.5.3, we will show the calculation of the propagation of the flicker effect on an example. The example is designed for an industrial distribution system supplied from a node of the 400 kV transmission system illustrated in Figure 2.8. From this node of the transmission system, two branches of the 110 kV distribution system are supplied from node 2. The first branch (connection of nodes 2, 3, and 4) represents an industrial distribution system with a large source of interference in node 4 (used for calculation case A). The

second branch (connection of node 2, 5, 6, 7) represents the remaining part of the distribution system with a small source of interference in node 7 (used for calculation case B).

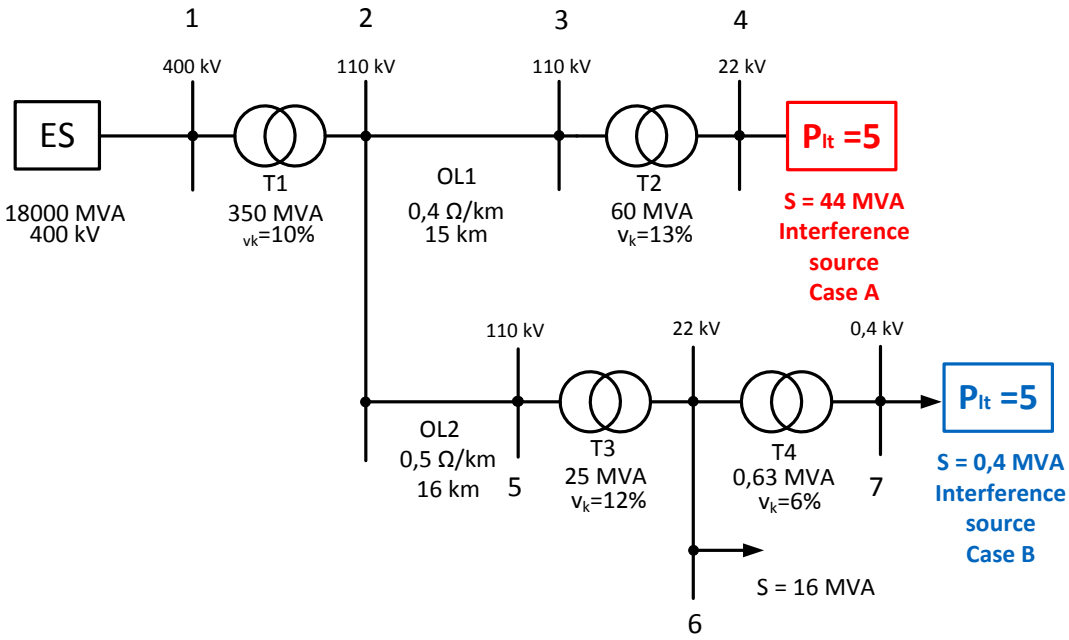


*Figure 2.8: Industrial distribution system for demonstrating the calculation of the propagation of the flicker effect.*

The calculation of the propagation of the flicker effect was realized in two cases to illustrate the principles of the spread of the flicker effect. The first case (according to Figure 2.8 case A) is focused on the case when a large source of interference is included in node 4. The interference rate is defined by the $P_{lt}$ = 5. The second case (according to Figure 2.8 case B) is focused on in the case where a small source of interference is included in node No. 7. The interference rate is again defined by the $P_{lt}$ = 5. The values shown in Figure 2.8 for individual elements were used as input parameters for the calculation.

The results for case A are shown in Figure 2.9. The results show that the flicker effect gradually decreases towards higher voltage levels. They also show that towards the lower voltages there is only a minimal attenuation of the flicker effect and its propagation to a large extent.

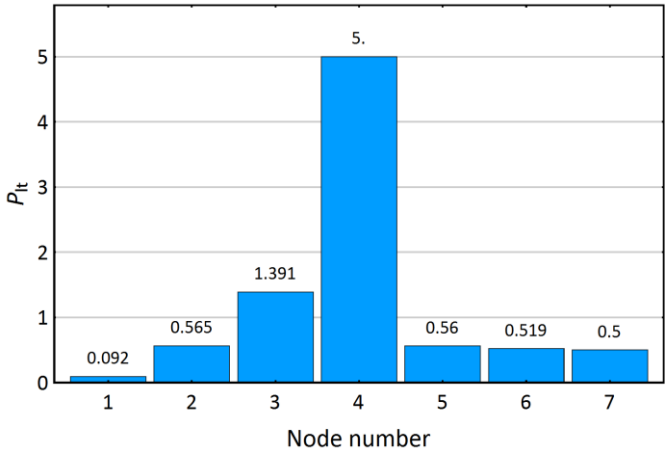


*Figure 2.9: Case A - large source of interference in node no. 4.*

The results for case B are shown in Figure 2.10. In this case, only propagation towards higher voltage levels is possible. Due to the fact that the source of interference is only at the low voltage level

and it is a source of interference that consumes little power from the network, the spread of the flicker effect to higher voltage levels is very small.

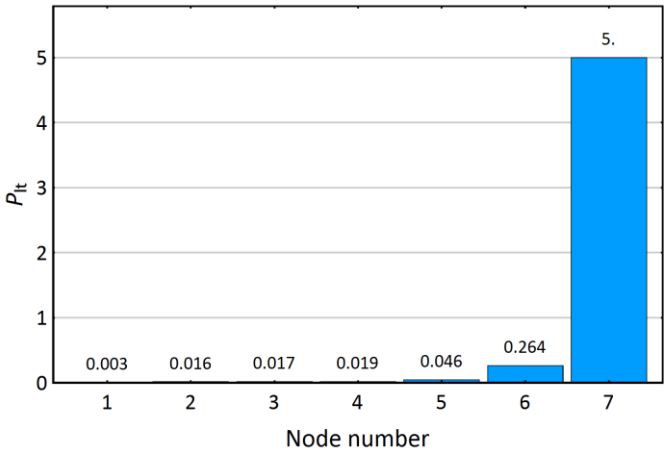


*Figure 2.10: Case B- small source of interference in node no. 7.*

Based on the results of the example described above, more attention must be paid to larger sources of interference that are connected at higher voltage levels. Its interfering effects are manifested in large areas, in contrast to small sources of interference at low voltage levels, which are manifested only locally.

### 2.5.4 Influence of the load character on flicker effect propagation

The propagation of the flicker effect within the electricity system is to some extent also influenced by the nature of the loads connected to the given area. Asynchronous motors, synchronous motors, and drives with static converters can have an effect. These types of loads should be taken into account in the computational model when requiring a more accurate estimate of the propagation of the flicker effect. A more detailed look at this issue will be outlined in Chapter 4.

# 3 Electric arc furnaces

Electric arc furnaces are a very important technology for steel production with more than 120 years of history. In the total world steel production of 1869 million tons, the EAF accounted for 27.7% [11] in 2019, in the case of the EU, in 2019 the total steel production was 158.8 million tons and the EAF production share was 40.9%.

The technology of electric arc furnaces is used exclusively in so-called mini-mills. Mini-mills can be defined as a smaller metallurgical (annual steel production from 200000 to 400000 tons of steel per year, in exceptional cases up to 3 million tons of steel per year) using electric arc furnace technology, followed by continuous steel casting equipment and then a rolling mill for the production of a wide range of long products [32].

Mini-mills use as input material primarily steel scrap in combination with iron (HBI -hot briquetted iron, DRI - direct reduced iron, pig iron), which is used solely to achieve the required chemical composition of steel. The undeniable advantage of the mini-mill is its simplicity compared to traditional steel-mills, which brings additional economic benefits. Mini-mills have much more widespread possibilities of locating construction and thus the possibility of establishing themselves on the market in certain segments of metallurgical products. These advantageous properties have been the driving force behind the development of mini-mills since the 1960s [32], [33].

The technology of electric arc furnaces used in mini-mills has undergone great development and the following parameters are typical for current equipment - batch weight up to 350 t, energy consumption from 345 kWh / t, melting time from 40 minutes, and consumption of graphite electrodes from 1.1 kg / t [12].

Mini-smelters can in many cases negatively affect power quality for two reasons:

- Disruptive nature of the electric arc furnace.
- Their construction is also taking place outside areas with established industrial areas where sufficient infrastructure is available.

The aim of this chapter will be to approach the technology of electric arc furnaces, from the basic description of the technology and its components and the specifics in the field of power engineering - power quality.

## 3.1 Basic description of EAF technology

A combination of an electric arc furnace (scrap melting and basic metallurgical processes) and a ladle furnace (other metallurgical processes) is usually used in the mini-mills. The ladle furnace already works with the liquid melt and electric arc heating is used exclusively to maintain the required melt temperature. Much lower output is sufficient for a ladle furnace than for an electric arc furnace. The basic description of the electric arc furnace is illustrated in Figure 3.1 on the basis of [12].

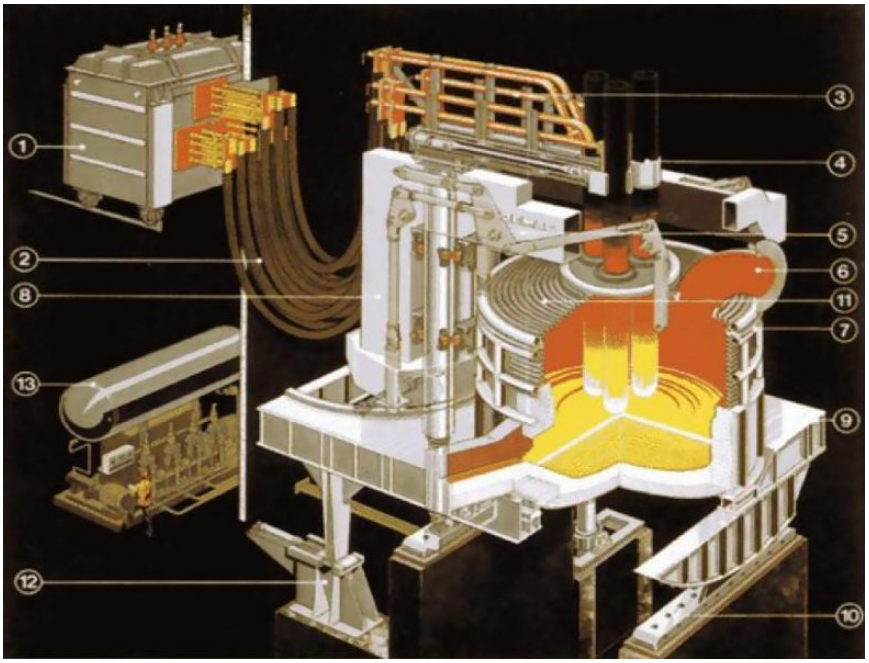


*Figure 3.1: Basic description of electric arc furnace technology [12].*

The following explanatory notes apply to Figure 3.1 [12]:

1. Furnace transformer
2. Flexible cable connection (part of short current path)
3. Part of short current path with electrode arms
4. Electrodes clamping
5. Electrodes arms
6. Cooled off-gas duct
7. Cooled panels
8. Structure
9. Basculating structure
10. Rack
11. Cooled roof
12. Basculating device
13. Hydraulic group

The ladle furnace station is much simpler compared to the electric arc furnace station. The ladle furnace does not tilt, the ladle is handled as a whole. I.e. the melt from the electric arc furnace is poured into an empty ladle. The ladle is then moved by crane to the ladle furnace station. After completion of the ladle metallurgy processes, the ladle with the melt is again moved by a crane to the continuous steel casting station.

From the point of view of power quality, the description of the electrical part of the electric arc furnace is more important, on which the following subchapter 3.2 focuses.

## 3.2 Electric part of EAF

In terms of power quality in industrial distribution systems, the most important technology is electric arc furnaces. Figure 3.2 illustrates a typical configuration for connecting mini-mills (power section of an electric arc furnace and ladle furnace) to an industrial distribution system. The picture also contains a legend describing the individual components, which are described in more detail in the following text.

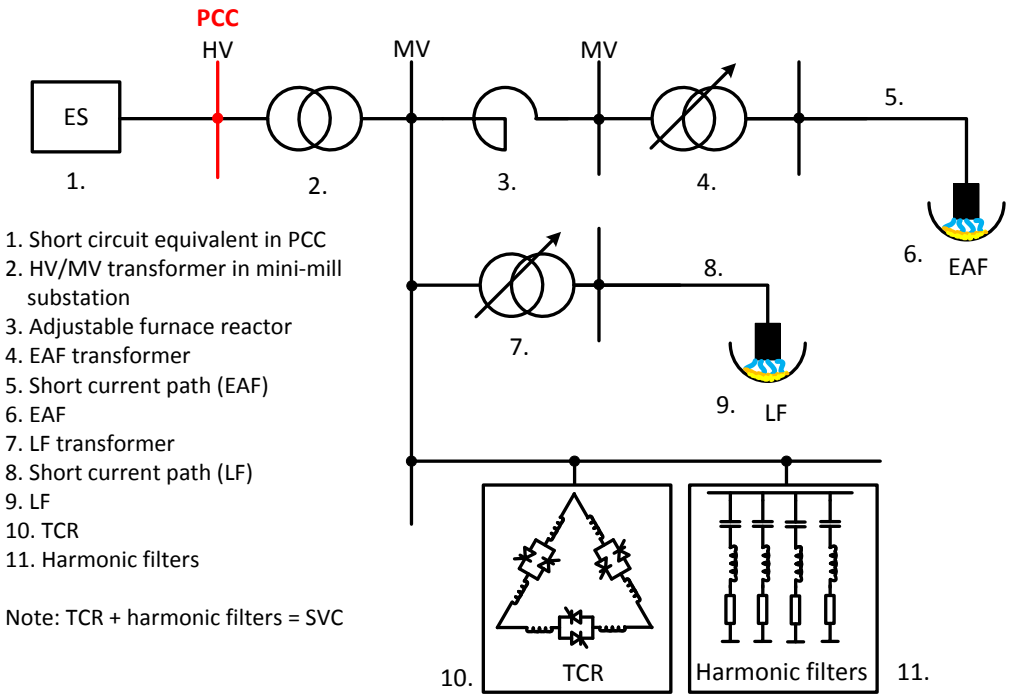


*Figure 3.2: Power sections of electric arc furnace and ladle furnace (mini-mill).*

**The short-circuit equivalent of the system** describes the short-circuit conditions at the point of common coupling (PCC). The value of the short-circuit power is affected by the configuration of the superior industrial distribution system and the transmission system. Sufficient values of the short-circuit power at this point are key to minimizing the interfering effects of the EAF.

**The transformer of the steelworks input substation** is used to transform the voltage, usually from the HV level to the MV level. Typically, this is a three-winding transformer YNyn0/(d). The primary winding is usually connected to a star with a grounded node. The secondary winding is typically connected to a star with a node grounded through a resistor. The tertiary winding is typically connected in a triangle. This transformer is equipped as standard with a tap-changer, which is designed to adapt to the current voltage of the superior system at the connection point.

**The adjustable furnace reactor** serves to limit the short-circuit current of the electric arc furnace and to ensure stable burning of electric arcs. Short-circuits inside the furnace between the electrodes and the charge are common in the initial phase of melting, and the system must therefore be dimensioned so that there is no risk of damaging the equipment in these conditions. With the use of a furnace reactor, this is achieved by the aforementioned short-circuit power limitation. Due to its design, the inclusion of a furnace reactor is usually possible in certain taps (for example 0, 20, 40, 60, 80, and 100% reactance), which allows adaptation to the actual conditions.

**The furnace transformer** of the electric arc furnace and ladle furnace is used to transform the voltage from the MV voltage level to the voltage level in the range from tens to hundreds of V

(depending on the power and type of furnace). The primary winding is usually connected to a star with an ungrounded node. The secondary winding is usually connected in a triangle. Furnace transformers are usually equipped with an on-load tap changer (OLTC), which allows the process to be adapted to the current production phase and conditions. Operation at lower taps is characterized by lower arc voltage (so-called short arcs) and large currents, ie generally lower power. This mode is typical for the initial phase of melting when the purpose is to eliminate the dynamic effects and wear of the furnace and electrode linings (a large proportion of heat shared by radiation). Operation at higher taps is characterized by higher arc voltage (so-called long bends) and higher power delivered to the charge. This mode is typical for the phases of the production process in the liquid metal phase and the presence of slag. The electric arc is thus shrouded in slag, resp. in the foamed slag and thus there is an efficient transfer of energy to the charge, without excessive wear of the furnace linings. The taps of the furnace transformer are usually switched based on a command from the control system, on the basis of the selected melting program, or at the intervention of the operator.

**The short current path** is used to output power from the secondary side of the furnace transformer to the charge. The short current path consists of a terminal for flexible cables at the output of the furnace transformer, flexible water-cooled cables (connecting the terminal and electrode arms, flexible for reasons of electrode positioning during melting and for handling the furnace lid and electrodes during insertion), electrode arms (steel structures with copper cladding and cooling system, or steel structures with a tubular system of conductive paths with a cooling system - used to hold electrodes and allow their movement in the vertical axis) and graphite electrodes (resistance to high temperatures inside the furnace). The short current path is a specific matter for several reasons: it is loaded with currents in the tens of kA, it is exposed to high temperatures and strong dynamic effects, and it requires minimum active losses (various configurations, such as bifilar design, etc.).

**Filtration-compensation stations** are used to compensate for reactive power consumption, limit higher harmonics, symmetrize consumption and limit voltage fluctuations. Most often it is a combination of a thyristor decompensation converter (TCR - thyristor controlled reactor) and passive filters of higher harmonics (filtration of higher harmonics and a source of compensatory reactive power).

**In addition to the furnace sections, the electrical part of the mini-mills consists of other sections** to ensure the operation of the steel plant (flue gas extraction and cleaning, cooling system, compressed air and technical gas management, manipulators, cranes and other drives, continuous casting technology, and many other supporting technologies). Said power supply sections are neglected in the case of power quality analysis because their rated power is and the level of emitted interference is minimal compared to an electric arc furnace.

## 3.3 EAF characteristics

The operating characteristics of the electric arc furnace are an important area needed for the correct design of the electric parts of the electric arc furnace. The characteristics are influenced by the input parameters, which include the nature of the supply system (nominal voltage and short-circuit power in the PCC) and the required furnace parameters (electrical power of the furnace, more precise purpose of use of the furnace). The furnace reactor (choice of a suitable tap based on the short-circuit power in the PCC) is mainly used to adapt to the character of the supply system. The OLTC of the furnace transformer is used for rough regulation of the furnace power during different phases of the production process (melting vs. refining). The impedance or resistance of the arc is regulated using an electrode position control system. Significant limitations that must be considered include the power factor and the power limitations of the individual components. For electric arc furnaces, operation at a maximum power factor of 0.85 is recommended. For better power factor values, the stability of the electric arc is problematic, which leads to frequent arc interruptions and subsequent undesirable

dynamic phenomena, which, among other complications, bring a fundamental deterioration of power quality (higher level of interference).

The basic working characteristics can be compiled on the basis of a simplified model according to the diagram illustrated in Figure 3.3. This model includes the following simplifying assumptions:

- Neglecting the transverse branches of transformers and chokes
- Simplified 1 phase circuit
- The electric arc is represented by a variable resistance
- Neglecting the impedance of the connecting lines within the power supply section
- Neglecting the effects of the ladle furnace (the performance of the ladle furnace is low compared to an electric arc furnace and the ladle furnace is always in operation for only a short time to maintain the melt temperature)
- Neglect of the influences of the power sections of other supporting technologies Reactive power compensation is not considered in the scheme, as it will result in an "increase in surge short-circuit power in the PCC"

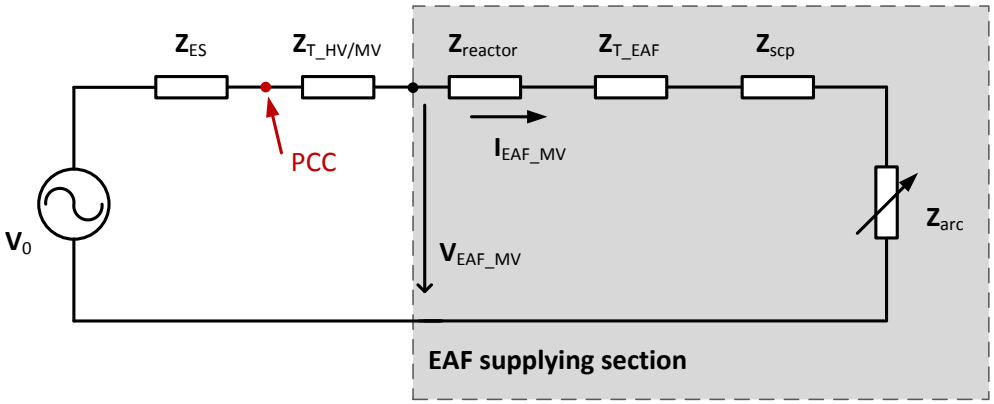


*Figure 3.3: Simplified power diagram of an electric arc furnace for determining the characteristics of the furnace.*

The characteristics of an electric arc furnace are usually compiled for the entire supply section of the furnace, as indicated in Figure 3.3. Thus, it can be simply said that the characteristics are compiled on the basis of the quantities $\mathbf{V}_{EAF\_VN}$ and $\mathbf{I}_{EAF\_VN}$, in accordance with the notation in Figure 3.3.

The following sections will demonstrate the process of compiling theoretical performance characteristics, which will then be compared with data from real operations.

### 3.3.1 Theoretical EAF characteristics

Two basic types of characteristics are used in electric arc furnaces. The first type are the so-called circle diagrams, which show the dependence of the active and reactive power taken by the supply section of the electric arc furnace. The second type are diagrams of the dependence of active and reactive power on the EAF current. To compile these characteristics, it is, therefore, necessary to know the following parameters of the supply section: active power, reactive power, RMS current. The current of the supply section $\hat{I}_{\mathrm{EAF\_MV}}$ can be expressed on the basis of (3.1).

$$\hat{I}_{\mathrm{EAF\_MV}} = \frac{\hat{V}_0}{\hat{Z}_{\mathrm{ES}} + \hat{Z}_{\mathrm{T\_HV/MV}} + \hat{Z}_{\mathrm{reactor}} + \hat{Z}_{\mathrm{T\_EAF}} + \hat{Z}_{\mathrm{scp}} + R_{\mathrm{arc}}} \tag{3.1}$$

where $\hat{V}_0$ is phase voltage at PCC (under no load condition), $\hat{Z}_{\mathrm{ES}}$ is equivalent network impedance in PCC (based on short circuit power in PCC), $\hat{Z}_{\mathrm{T\_HV/MV}}$ is transformer of the steelworks input substation impedance, $\hat{Z}_{\mathrm{reactor}}$ is furnace reactor impedance, $\hat{Z}_{\mathrm{T\_EAF}}$ is EAF transformer impedance, $\hat{Z}_{\mathrm{scp}}$ is short current path impedance and $R_{\mathrm{arc}}$ is resistance of electric arc – variable parameter. An important note is that it is considered to convert all impedances, voltages and currents to one voltage level (MV system), which must take into account the current set taps of the input substation transformer, furnace reactor and furnace transformer.

The voltage $\mathbf{V}_{\mathrm{EAF\_MV}}$ can be expressed on the basis of (3.2).

$$\hat{V}_{\mathrm{EAF\_MV}} = \hat{V}_0 * \frac{\hat{Z}_{\mathrm{reactor}} + \hat{Z}_{\mathrm{T\_EAF}} + \hat{Z}_{\mathrm{scp}} + R_{\mathrm{arc}}}{\hat{Z}_{\mathrm{ES}} + \hat{Z}_{\mathrm{T\_HV/MV}} + \hat{Z}_{\mathrm{reactor}} + \hat{Z}_{\mathrm{T\_EAF}} + \hat{Z}_{\mathrm{scp}} + R_{\mathrm{arc}}} \tag{3.2}$$

The impedance of the short-circuit equivalent of the power supply industrial distribution system with neglect of the real component can be expressed according to (3.3).

$$\hat{Z}_{\mathrm{ES}} = j * \frac{V_{\mathrm{ns}}^2}{S_{\mathrm{ks}}} * \left( \frac{V_{\mathrm{nT\_HV/MV\_sec}}}{V_{\mathrm{nT\_HV/MV\_prim_i}}} \right)^2 \tag{3.3}$$

where $V_{\mathrm{ns}}$ is nominal phase-phase voltage in PCC, $S_{\mathrm{ks}}$ is equivalent short circuit in PCC, $V_{\mathrm{nT\_HV/MV\_prim_i}}$ is nominal voltage of primary winding (HV) of transformer of the steelworks input substation for i[th] tap position, $V_{\mathrm{nT\_HV/MV\_sec}}$ is the nominal voltage of secondary winding (MV) of the transformer of the steelworks input substation.

The impedance of the transformer of the steelworks input substation with the neglect of the real component can be expressed according to (3.4).

$$\hat{Z}_{\mathrm{T\_HV/MV}} = j * z_{\mathrm{k\_T\_HV/MV}} * \frac{V_{\mathrm{nT\_HV/MV\_sec}}^2}{S_{\mathrm{nT\_HV/MV}}} \tag{3.4}$$

where $z_{\mathrm{k\_T\_HV/MV}}$ is relative short circuit impedance of transformer of the steelworks input substation and $S_{\mathrm{nT\_HV/MV}}$ is the nominal of this transformer.

The impedance of the furnace reactor with neglect of the real component can be expressed according to (3.5).

$$\hat{Z}_{\mathrm{reactor}} = j * X_{\mathrm{reactor\_j}} \tag{3.5}$$

where $X_{\mathrm{reactor\_j}}$ is the furnace reactor impedance for j[th] tap position.

The impedance of the furnace transformer can be expressed according to (3.6).

$$\hat{Z}_{\mathrm{T\_EAF}} = \left( r_{\mathrm{k\_T\_EAF\_k}} + j * x_{\mathrm{k\_T\_EAF\_k}} \right) * \frac{V_{\mathrm{nT\_EAF\_prim}}^2}{S_{\mathrm{nT\_EAF}}} \tag{3.6}$$

where $r_{\mathrm{k\_T\_EAF\_k}}$ is resistance component and $x_{\mathrm{k\_T\_EAF\_k}}$ is reactance component of the relative short circuit impedance of furnace transformer for k[th] tap position, $S_{\mathrm{nT\_EAF}}$ is nominal power of furnace transformer and $V_{\mathrm{nT\_EAF\_prim}}^2$ is the nominal voltage of primary winding (MV) of furnace transformer.

The impedance of the short current path can be expressed according to (3.7).

$$\hat{Z}_{\mathrm{scp}} = \left( R_{\mathrm{scp}} + j * X_{\mathrm{scp}} \right) * \left( \frac{V_{\mathrm{nT\_EAF\_prim}}}{V_{\mathrm{nT\_EAF\_sec\_k}}} \right)^2 \tag{3.7}$$

where $R_{\mathrm{scp}}$ is short current path resistance, $X_{\mathrm{scp}}$ is short current path reactance and $V_{\mathrm{nT\_EAF\_sec\_k}}$ is the nominal voltage of secondary winging of furnace transformer for k[th] tap position.

The variable value of the active resistance of the arc $R_{\mathrm{arc}}$ can theoretically be in the range 0 to infinity. In practice, its value is controlled by the electrodes positioning control system to a set value to achieve the required power and power factor of the furnace.

Based on the calculated values (3.1) to (3.7) it is possible to express the relations for 3-phase active (3.8) and reactive (3.9) power.

$$P_{\mathrm{EAF\_MV}} = \mathrm{Re}\{3 * \hat{V}_{\mathrm{EAF\_MV}} * \hat{I}^{*}_{\mathrm{EAF\_MV}}\} \tag{3.5}$$

$$Q_{\mathrm{EAF\_MV}} = \mathrm{Im}\{3 * \hat{V}_{\mathrm{EAF\_MV}} * \hat{I}^{*}_{\mathrm{EAF\_MV}}\} \tag{3.5}$$

Based on the parameters in Appendix A, it is possible to compile the theoretical characteristics of an electric arc furnace according to the above procedure. Due to a large number of combinations of transformer tap settings and furnace reactor tap positions, the given examples consider a fixed transformer tap of the input substation (-7 tap) and a furnace reactor included with maximum reactance. For the furnace transformer, several taps were chosen for clarity.

Figure 3.4 illustrates an example of circle diagrams of an electric arc furnace for selected taps of a furnace transformer with the representation of other quantities.

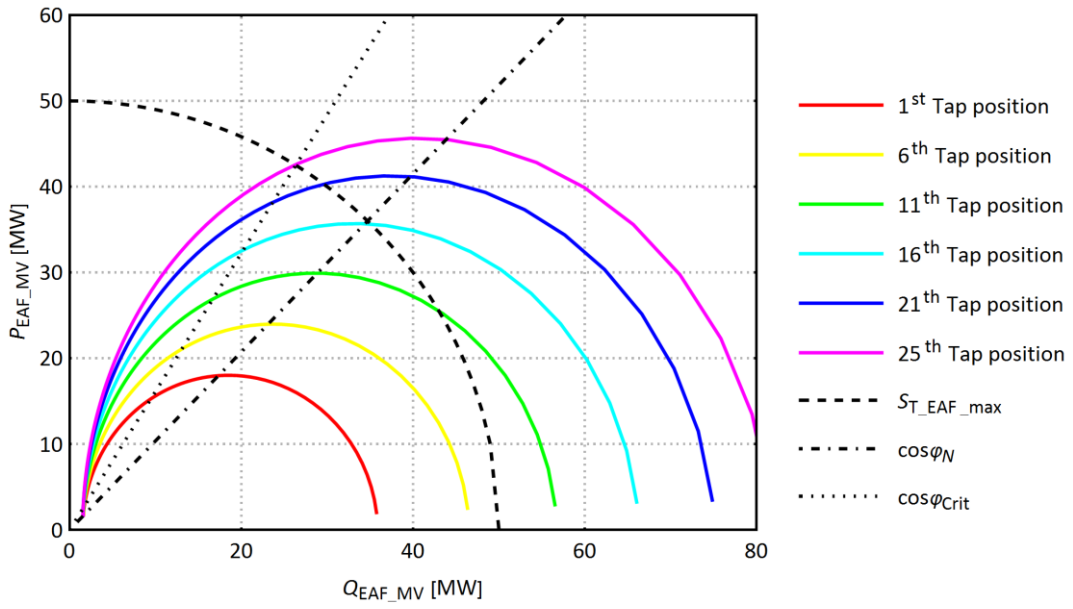


*Figure 3.4: Sample circle diagram of an electric arc furnace for selected tap positions of a furnace transformer.*

Figure 3.4 also shows significant limitations. The first limitation is the rated power of the furnace transformer $S_{T\_EAF\_max}$. However, furnace transformers are standardly designed for short-term overloads that may arise due to the nature of the equipment. Another limitation is the cos$\varphi_{Krit}$, which is the critical value (0.85) of the power factor to maintain a stable arc burn. It is therefore undesirable for the operating point to be in the area above this line. Figure 3.4 also shows a line corresponding to the nominal power factor of the furnace.

Figure 3.5 illustrates an example of P (I) and Q (I) characteristics of an electric arc furnace for selected tap positions of a furnace transformer.

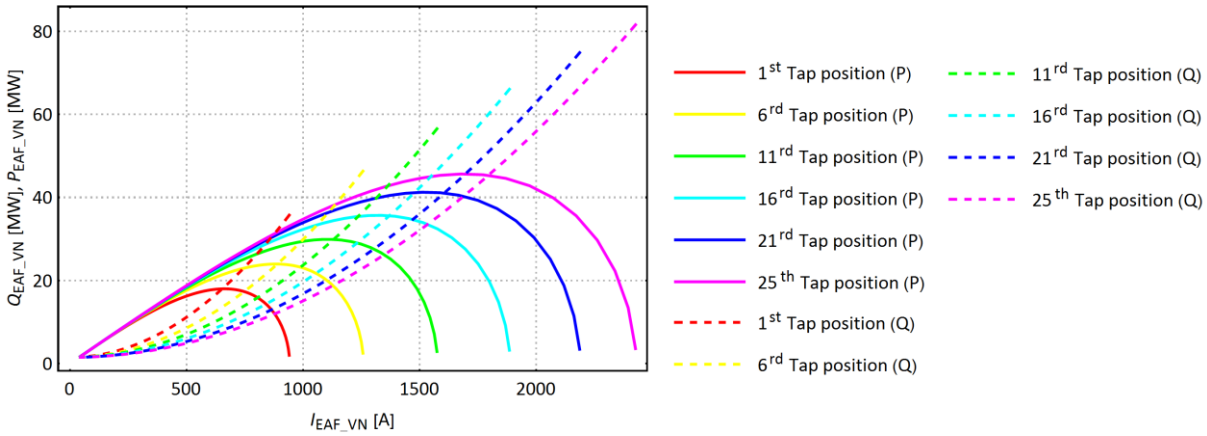


*Figure 3.5: Sample P (I) and Q (I) characteristics of an electric arc furnace for selected tap positions of a furnace transformer.*

### 3.3.2 Real EAF characteristics

Theoretical operation characteristics of the electric arc furnace provide an idealized view of the issue. At the beginning of subchapter 3.3 are simplified assumptions that were used to create characteristics. The actual characteristics can be compiled on the basis of measured data from the operation of the electric arc furnace. Inaccuracies can be expected from the actual characteristics due to the following factors:

- Measurement inaccuracy
- Asymmetrical loading of the furnace, especially in the initial phase of melting
- Influence of the ladle furnace
- Others

This section aims to point out the difference between the measured data and the theoretical characteristics. For the purposes of this comparison, three data sets were selected, obtained by measurements on a section of an electric arc furnace. One data set represents a 64 s long record, with the RMS values of the measured parameters being evaluated every 20 ms. These datasets were compared with theoretical characteristics, which were compiled on the basis of the parameters contained in Annex A. The comparison of characteristics is made in two variants. The first variant compares characteristics and data phase by phase separately. The second variant compares the characteristics and data for the total three-phase outputs.

The first data set was measured during the start of the melting of the batch of the first scrap basket. This is the most critical phase in terms of power quality. Figure 3.6 illustrates a comparison of the characteristics for each phase for the first data set.

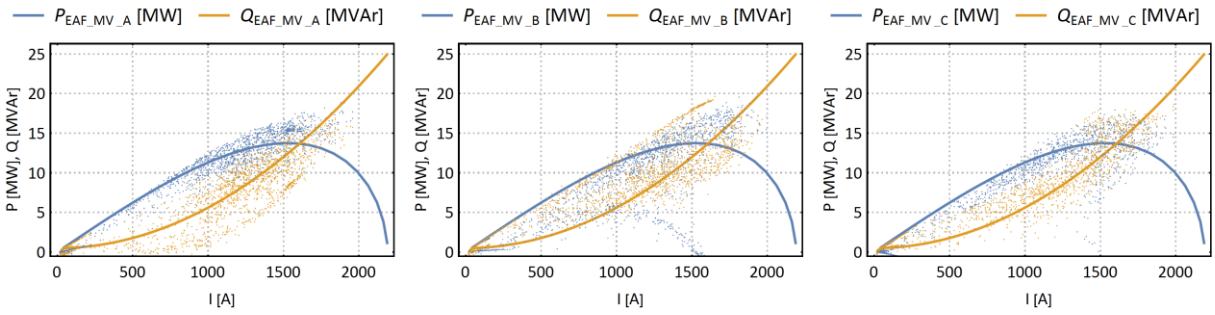


*Figure 3.6: Comparison of theoretical characteristics and real data from the EAF operation (initial phase of meltdown).*

Figure 3.6 shows a significant variance of the measured values as well as significant deviations from the theoretical characteristics, which are characteristic of the initial melting phase. In this case, the characteristic for three-phase outputs, which is illustrated in Figure 3.7, has a better explanatory value. Figure 3.7 shows smaller deviations from the theoretical characteristics, but from the measured data, there are also indications of curves for another (lower) tap position of the furnace transformer. This is a standard procedure during melting when a lower tap position is used at the beginning of the process (ignition and stabilization of electric arc combustion) to reduce unwanted dynamic effects.

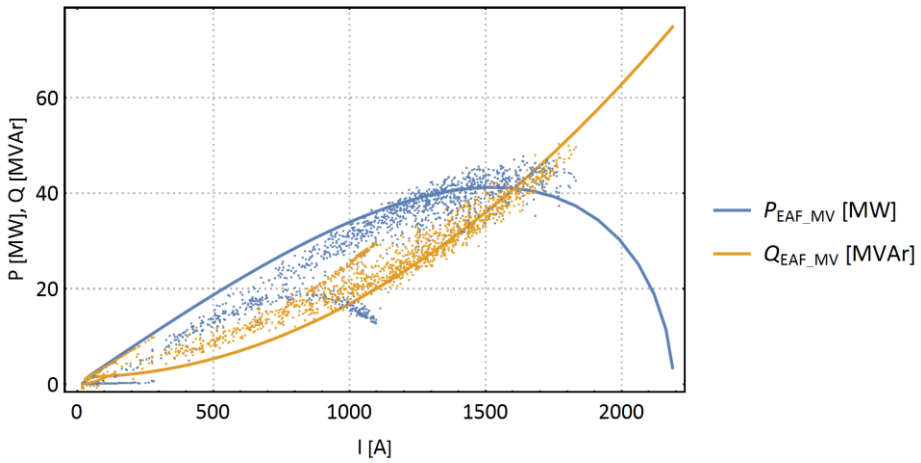


*Figure 3.7: Comparison of theoretical characteristics and real data from the EAF operation (initial phase of meltdown) - three-phase.*

The second data set was measured during the melting of the batch of the first scrap basket after the worst phase had disappeared. Compared to the previous dataset, the operation is more stable. Figure 3.8 illustrates a comparison of the characteristics for each phase for the second data set.

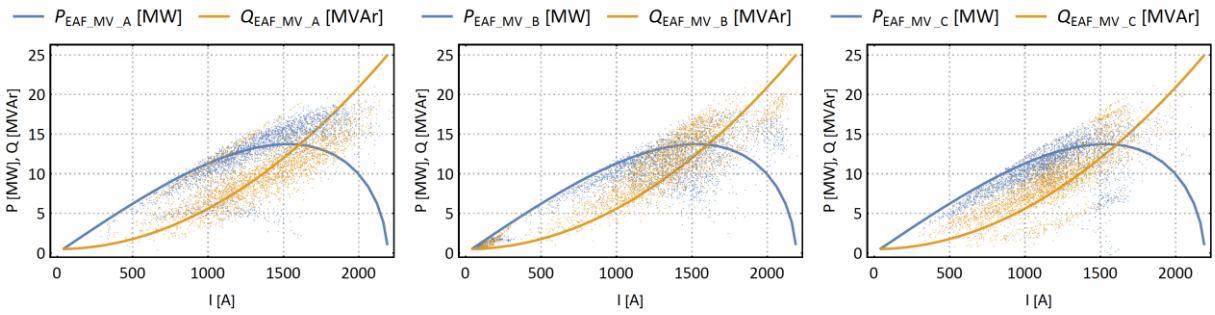


*Figure 3.8: Comparison of theoretical characteristics and real data from the EAF operation (meltdown).*

Figure 3.8 still shows a significant variance of the measured values as well as significant deviations from the theoretical characteristics. The characteristic for three-phase outputs, which is illustrated in Figure 3.9, also has a better informative value in this case. Figure 3.9 shows smaller deviations from the theoretical characteristics.

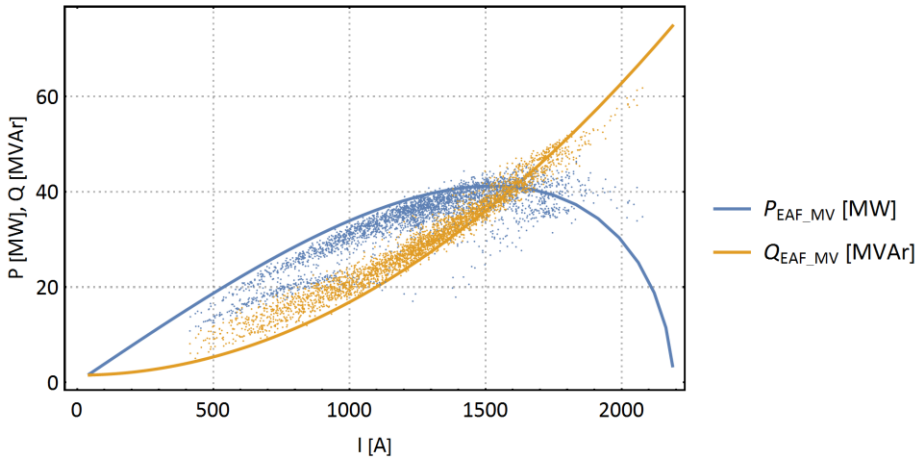


*Figure 3.9: Comparison of theoretical characteristics and real data from the EAF operation (meltdown) three-phase.*

The third data set was measured during refining in the liquid melt phase. Compared to the previous data set, the operation is already stable. Figure 3.10 illustrates a comparison of the characteristics for each phase for the third data set. Figure 3.10 shows a good similarity between the theoretical characteristics and the measured values.

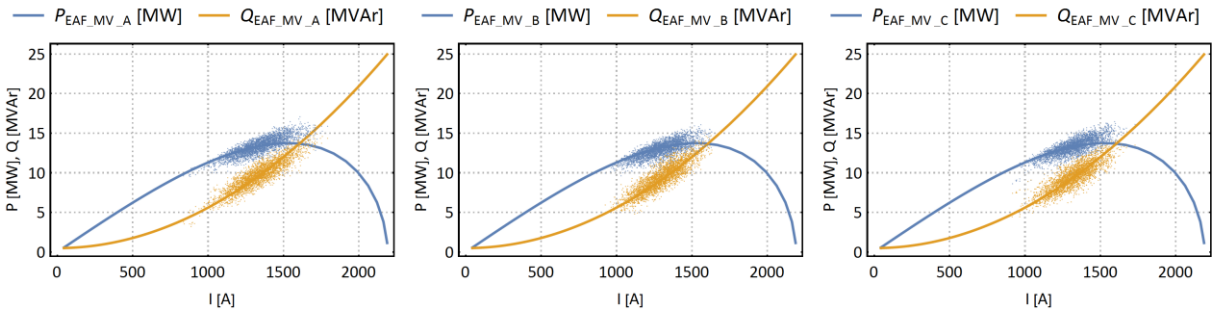


*Figure 3.10: Comparison of theoretical characteristics and real data from the EAF operation (refining).*

For the characteristics of the three-phase outputs illustrated in Figure 3.11, the similarity is even better. In the refining phase, there are no such significant changes in active and reactive power and asymmetries as in the case of the meltdown process.

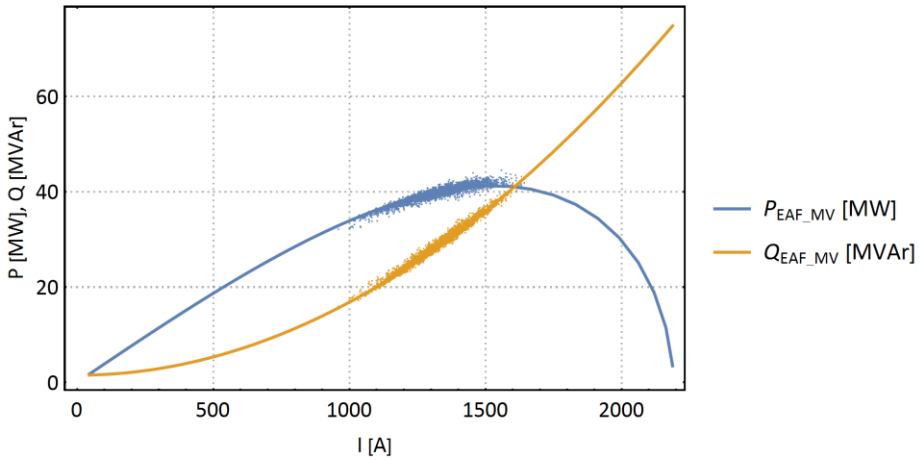


*Figure 3.11: Comparison of theoretical characteristics and real data from the EAF operation (refining) three-phase.*

## 3.4 Specifics of EAF in terms of power quality

The operation of an electric arc furnace in terms of power quality in industrial distribution systems has many specifics. This subchapter will aim to point out the specifics resulting from the operating characteristics of the electric arc furnace and other specifics.

### 3.4.1 Specifics resulting from EAF performance characteristics

To demonstrate the specific nature of the electric arc furnace, Figure 3.12 illustrates the theoretical characteristics created using the procedure described in section 3.1.1 and the parameters of Annex A. In addition to the dependences of active and reactive power on the magnitude of the consumed current of the furnace section, the graphs also show the dependences of efficiency, power factor, and apparent power. Efficiency and power factor are dimensionless quantities, powers are converted to per-units. The graph also shows the nominal power factor of the furnace (0.72) which determines the theoretical operating point.

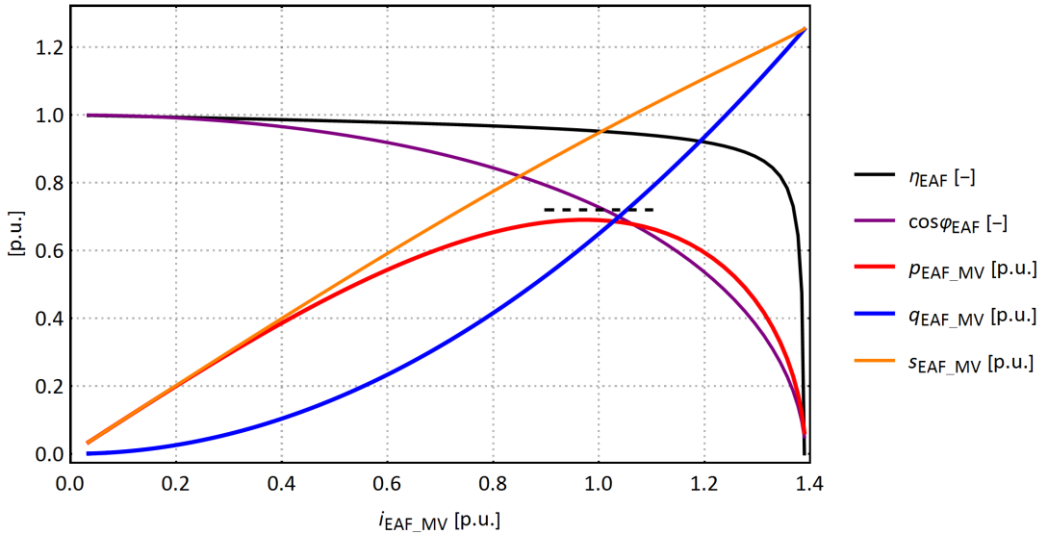


*Figure 3.12: Theoretical operation characteristics of EAF to demonstrate the specific character of EAF.*

In the real operation of the electric arc furnace, however, there are frequent changes in the power consumed due to the nature of the process. This fact is also confirmed by a comparison of data and theoretical characteristics in subchapter 3.3.

Figure 3.13 illustrates the same operating characteristics as Figure 3.12, with Figure 3.13 marking the area to which the operating point and other fluctuations fall. This is a system, for which reactive power compensation is not considered. **A power change band with a width of 0.08 per-units (the band around the operating point) will cause the current to fluctuate in the band of 0.44 per-units!** Such a wide range of currents adversely affects the voltage - there is a significant and at the same time undesirable voltage fluctuation, which causes a flicker effect.

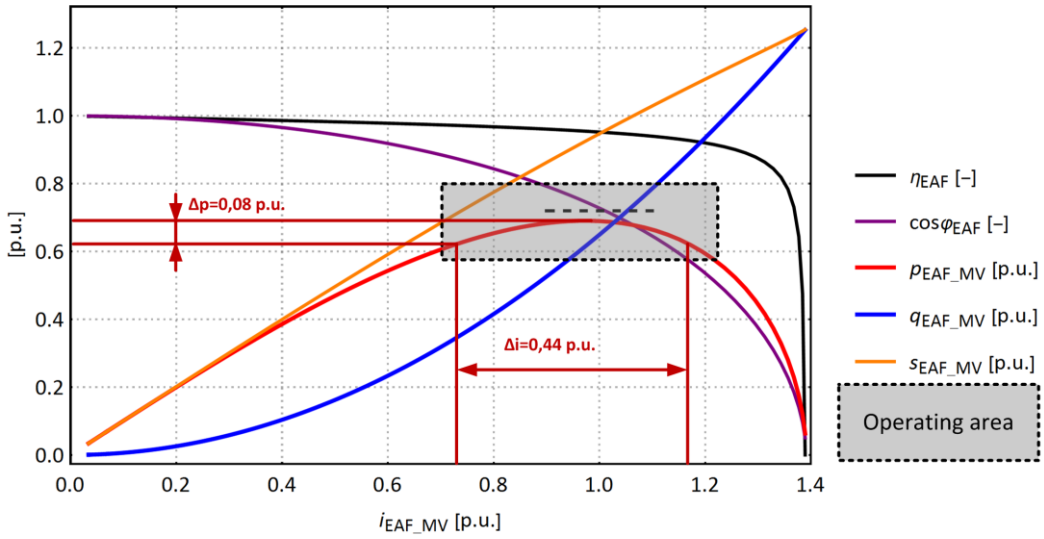


*Figure 3.13: Theoretical operation characteristics of EAF to demonstrate the specific character of EAF with a marked working area.*

In the case of reactive power compensation, the situation is much more favorable. The following simplifying assumptions apply to explain the benefits of reactive power compensation:

- The dependence of the operating characteristic of the active power remains unchanged, which can be ensured by using a different tap position of the furnace transformer and the tap position of the furnace reactor.
- The compensating device can fully compensate even the maximum reactive power consumption of the power section of the electric arc furnace.
- With ideal compensation, the power section will behave according to the characteristics valid for apparent power.

Figure 3.14 illustrates the operating characteristics of EAF with reactive power compensation under the abovementioned simplifying assumptions.

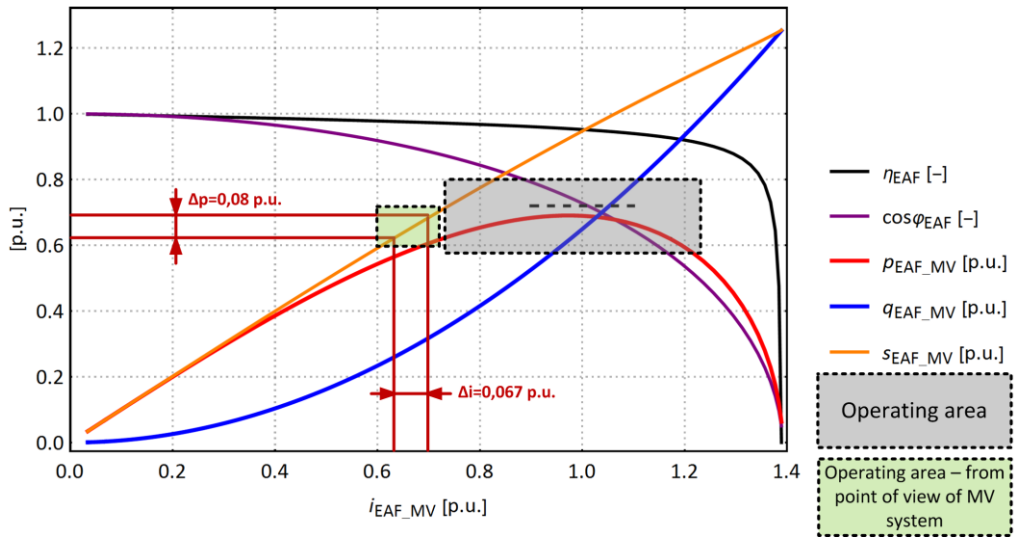


*Figure 3.14: Theoretical operation characteristics of EAF to demonstrate the specific character of EAF including reactive power compensation with a marked working area.*

It can be seen from Figure 3.14 that EAF will behave the same as in the previous case. However, in the case of a power supply section with already compensated reactive power consumption, the

operating characteristics will be different. Assuming ideal reactive power compensation, the behavior of the section will be characterized by a dependence curve for apparent power. **At the same bandwidth of the furnace power changes of 0.08 per-units (band around the operating point), the furnace causes fluctuations in the current in the band of only 0.067 per-units (6.6 times the narrower band).** For this reason, reactive power compensation is one of the most effective measures to reduce the interfering effects of EAF.

# 4 Basic methods for power quality improvement

Problems with power quality in distribution systems typically arise in two model situations.

The first situation occurs when there is a significant development of the distribution area, which brings the connection of new customers. However, the current distribution network does not manage to react quickly enough to these changes and the operation of part of the distribution system in the given areas is beginning to approach its technical limits. During this process, there are more and more justified complaints about the quality of electricity in the area. Problems with voltage magnitude and exceeding the allowable limits for higher harmonics and flicker effect are most common. It is interesting that despite the indicated problems, it is not possible to unequivocally identify the source of the interference and take related measures. This problem is typically the domain of low voltage (LV) distribution networks where there is a development (connection of new customers) to medium to long feeders. An effective solution to this type of problem is to thicken the distribution system by building a new distribution transformer station (DTS) in the problem area, thus eliminating long LV feeders. A less demanding measure is the reconductoring of LV feeders using conductors with a larger cross-section, which may not always bring sufficient improvement.

The second model situation occurs when a device or customer is connected to the distribution system, which is directly a source of unwanted interference, which results in the deterioration of power quality. In this situation, these are more often customers connected at the HV level and the MV level. Appropriate measures to eliminate disruptive measures can be taken both on the side of the distribution system and the side of the customer. The customer should behave in such a way that his interference-generating equipment generates interference only within the permitted limits, and at the same time, the distribution system operator should create the conditions for this. Measures for these situations can be of several types, individual types of measures will be presented in the following subchapters 4.1 to 4.3. This chapter will deal with measures without the use of additional compensation devices.

## 4.1 Modification of basic system components and system configuration

When implementing new projects of equipment with potential interference, it is very important in the preparatory phase to assess its interference and to propose such measures that its interference falls within the range of permissible tolerances. In the case of EAFs, the basic parameters of the technology are specified in the initial phase of project preparation. The most basic parameters include the type of technology (according to the required type of product) and the annual production capacity, which results in the parameters of the melting mass for one melting round and the furnace rated power. From the point of view of the power quality, it is then necessary to assess the possibilities in the considered construction site. The parameters of the industrial distribution system in the given area play an important role, especially the parameter of short-circuit power at the point of connection (PCC) of the new technology. Using certain methods, as well as experience from similar projects, it is possible to assess the proposed solution in terms of the flicker effect and in terms of other power quality parameters. The obtained results give an initial idea, on the basis of which we proceed. It is possible to modify the design of the electrical part of the EAF to meet the permitted interference limits. In particular, the choice of the input transformer, furnace reactor, furnace transformer and the short current path is usually reconsidered. From the point of view of the flicker effect, the short-circuit power parameter plays a crucial role in this case. On the other hand, it is also important for the distribution system operator to analyze the effects of potential interference in order to minimize interference to other customers in the distribution area. For this purpose, it is possible to ensure the highest possible value of the short-circuit power in the PCC and at the same time to isolate the problematic consumption from other customers to the highest possible extent. These goals can be achieved by

choosing a suitable configuration of the transmission and distribution system. The following sections will demonstrate the effect of short-circuit power in the PCC and the effect of isolating interfering consumption from other customers in the distribution system.

### 4.1.1 Influence of short - circuit power in PCC

The method according to IEC TR 61000-3-7:2008: "Electromagnetic compatibility (EMC) - Part 3-7: Limits - Assessment of emission limits for the connection of fluctuating installations to MV, HV and EHV power systems" [34] is generally used to estimate the effect of the flicker effect when connecting a new electric arc furnace. The method is primarily used before the electric arc furnace operation. The method defines the short-term rate of perception of the flicker effect (valid for the 95% percentile) according to (4.1).

$$P_{\mathrm{st95\%}} = K_{\mathrm{st}} * \frac{S_{\mathrm{ksEAF}}}{S_{\mathrm{ksPCC}}} \tag{4.1}$$

where $P_{\mathrm{st95\%}}$ is short-term rate of perception of the flicker effect, $S_{\mathrm{ksPCC}}$ is short-circuit power in PCC, $S_{\mathrm{ksEAF}}$ is short-circuit power of EAF - defined by estimated short-circuit power on "electrodes" of the furnace and $K_{\mathrm{st}}$ is the characteristic emissivity coefficient (servility factor) of the flicker effect of the EAF.

The short-circuit power in the PCC is influenced by the configuration and utilization of the superior electrical system - the transmission system and in connection with the industrial distribution system. Its value can be increased by modifying the system configuration, upgrading the system, or using connections at higher voltage levels. This is often a difficult and time-consuming process.

The short-circuit power of EAF is based on:

a) Short circuit power in PCC
b) Parameters of the transformer of the steelworks input substation, furnace reactor, furnace transformer, and short current path.

With regard to the expected values of the short-circuit power in the PCC, it is possible to modify the partial components of the supply section of the electric arc furnace in order to achieve the required value $P_{\mathrm{st95\%}}$. Modification of these parameters brings relatively wide possibilities, but in certain critical cases, this measure ceases to be technically and economically effective. In the case of a realized electric arc furnace, the value of $S_{\mathrm{ksEAF}}$ can be verified by measurement, the so-called electrode immersion test (immersion of electrodes in the melt - short circuit formation).

The characteristic emissivity coefficient of the flicker effect is based on empirical experience from other implementations of other projects. Individual technology suppliers have a database of implemented projects and take advantage of this knowledge during implementation. The value of $K_{\mathrm{st}}$ can be estimated on the basis of a comparison of real measurements from the operation of the device with similar parameters that work in similar conditions. Standard [34] gives typical $K_{\mathrm{st}}$ values in the range from 52 to 135 for a low voltage distribution system with a nominal voltage of 230 V. For AC-supplied furnaces, standard [34] rather recommends $K_{\mathrm{st}}$ values in the range from 64 to 75. The specific value strongly depends on furnace type and parameters (standard furnace vs. UHP furnace).

To illustrate, it is possible to show an example of a calculation or sensitivity analysis based on (4.1). The example considers an EAF with a characteristic emissivity coefficient of the flicker effect $K_{\mathrm{st}} = 65$. $S_{\mathrm{ksPCC}}$ and $S_{\mathrm{ksEAF}}$ are considered as variables. $S_{\mathrm{ksPCC}}$ is considered in the range from 1000 to 3000 MVA which theoretically corresponds to an industrial HV distribution system. $S_{\mathrm{ksEAF}}$ is considered to be in the range of 30 to 100 MVA. Figure 4.1 illustrates function $P_{\mathrm{st95\%}} = f(S_{\mathrm{ksPCC}}, S_{\mathrm{ksEAF}})$; $K_{\mathrm{st}} = 65$.

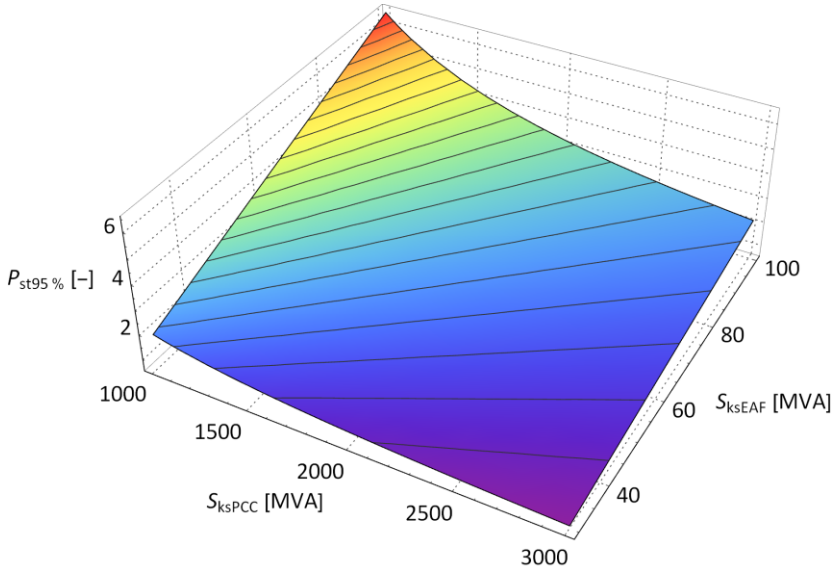


*Figure 4.1: Demonstration of the dependence of the estimated value $P_{st95\%}$ on the short-circuit power in the PCC and on the EAF short-circuit power.*

During the EAF design process, the input parameters are collected and the target value $P_{\mathrm{st95\%}}$ is set based on the current possibilities and the requirement. Figure 4.2 shows the area in the graph for which the criterion $P_{\mathrm{st95\%}} < 1.5$ is met.

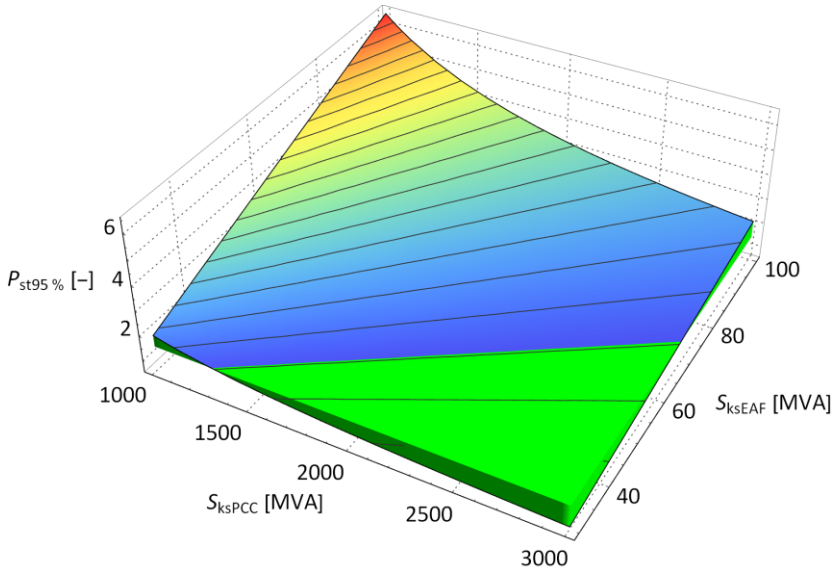


*Figure 4.2: Demonstration of the dependence of the estimated value of $P_{st95\%}$ on the short-circuit power in the PCC and on the EAF short-circuit power with the indication of the $P_{st95\%}$ level 1.5 (green color).*

Another illustration (2D) can be used to illustrate the dependencies contained in Figures 4.1 and 4.2. The dependence illustrated in Figure 4.3 shows the linear dependence of $P_{\mathrm{st95\%}}$ on $S_{\mathrm{ksEAF}}$.

The dependence illustrated in Figure 4.4 demonstrates the hyperbolic dependence of $P_{\mathrm{st95\%}}$ on $S_{\mathrm{ksPCC}}$.

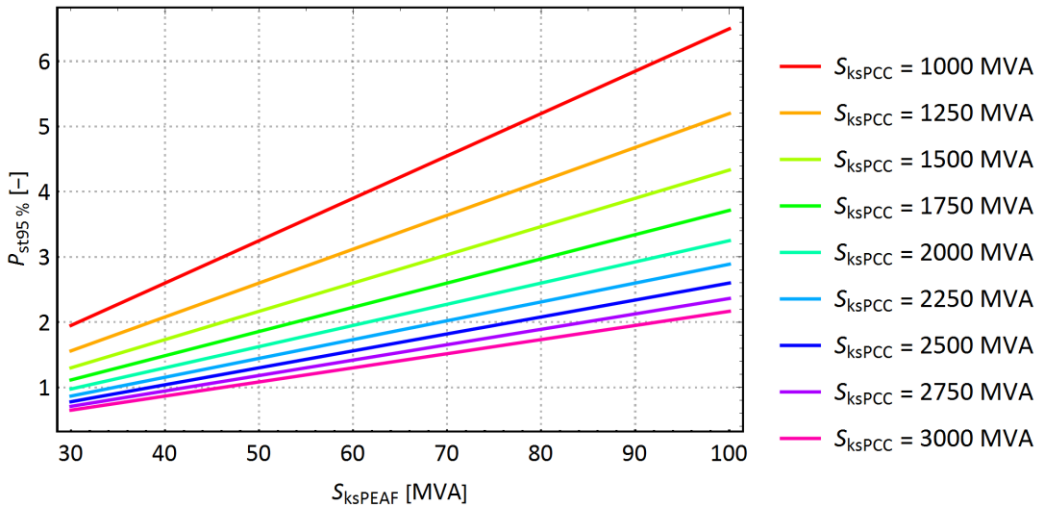


*Figure 4.3: Example of $P_{st95\%}$ dependence on $S_{ksEAF}$ for different values of $S_{ksPCC}$.*

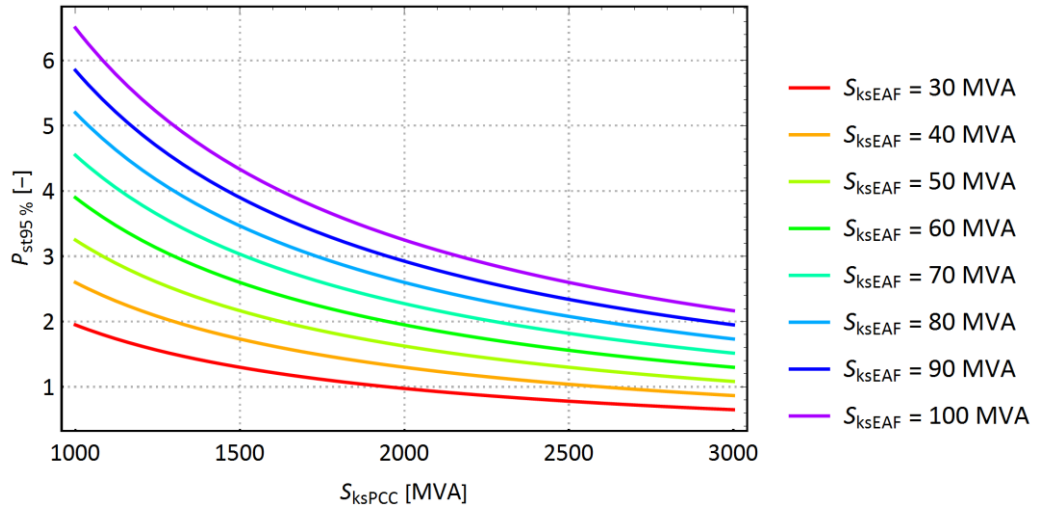


*Figure 4.4: Example of $P_{st95\%}$ dependence on $S_{ksPCC}$ for different values of $S_{ksEAF}$.*

The limit value $P_{\mathrm{st95\%}}$ can also be set at a higher level, provided that a compensation device is used. The aim is to achieve a sufficiently low value of $P_{\mathrm{st95\%}}$ in the sense of current legislative regulations and standards.

In terms of using the method described above according to the standard [34], the IEEE standard [35] also applies. The method is widely used in practice and is presented in many works. An example is [36], [37].

### 4.1.2 Influence of isolation of interfering consumption

As mentioned several times in this work, the configuration of the superior distribution system and transmission system has a major impact on the propagation of interference - flicker effect. The concept of organizing the so-called industrial distribution system is based on the idea of separating large sources of interference from the remaining customers as much as possible. Large industrial areas

often contain many technological units, which have a significant effect on the resulting degree of interference in the system. In the case of powering the remaining customers (small customers - households, etc.) from the same part of the distribution area, there is a significant risk that they will be more exposed to deteriorating power quality parameters. If we divide these two groups of customers into two distribution areas (through the network configuration), these areas will have a common node at a higher voltage level (at the level of the transmission system). This modification will significantly reduce customer interference outside the industrial distribution system. Figure 4.5 illustrates the idea of dividing the distribution system into an industrial distribution system and a distribution system supplying other customers in the area.

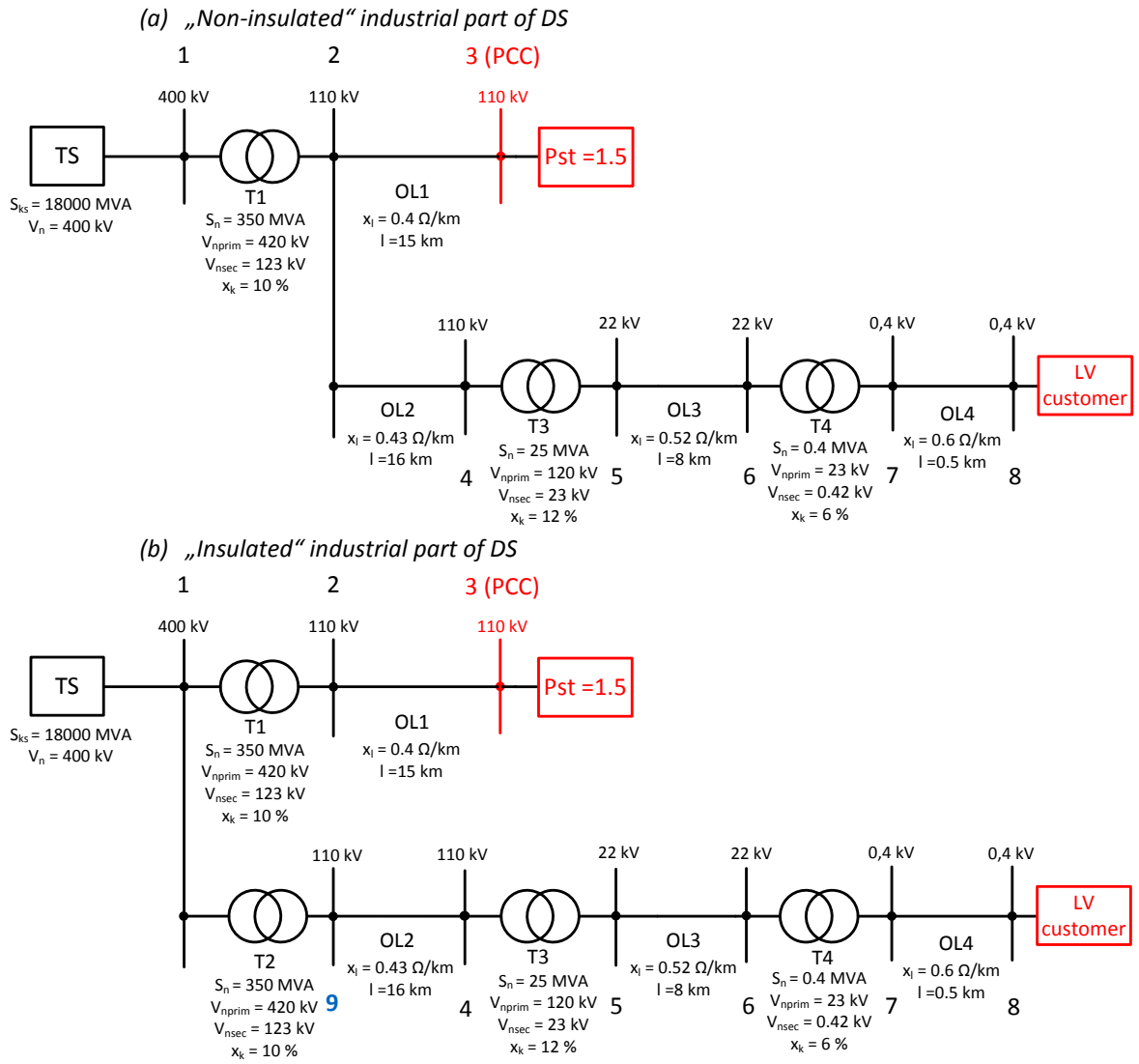


*Figure 4.5: The idea of creating an industrial distribution system.*

Based on Figure 4.5 and the input parameters it contains, based on the procedure described in Chapter 2, it is possible to simply estimate the propagation of the flicker effect for case (a) - "non-isolated" source of interference and for case (b) - "isolated" source of interference with the concept of a defined industrial distribution system. The following simplifying assumptions have been adopted to solve this example:

- Use of a single-phase equivalent circuit
- Only small illustrative parts of the distribution system are considered
- The active component of equivalent element impedance is neglected
- 5 levels of active load share are selected (based on the node consumption)

When analyzing a real problem - case studies, it is more appropriate to avoid these simplifying assumptions, but for an illustrative example demonstrating the basic principle, these simplifying assumptions may be acceptable.

The results of the calculation of the propagation of the flicker effect are summarized in Table 4.1. The table also contains the input power parameters in individual nodes and the percentage of active loads, the parameters of the network elements are summarized in the diagrams in Figure 4.5.

| Location | "Non insulated" industrial part of DS | | | | | | "Insulated" industrial part of DS | | | | | |
|---|---|---|---|---|---|---|---|---|---|---|---|---|
| | Load [MVA] | Percentage of active load | | | | | Load [MVA] | Percentage of active load | | | | |
| | | 0% | 25% | 50% | 75% | 100% | | 0% | 25% | 50% | 75% | 100% |
| | | Pst [-] | | | | | | Pst [-] | | | | |
| Node 1 | 0 | 0,103 | 0,102 | 0,101 | 0,100 | 0,100 | 0 | 0,103 | 0,103 | 0,102 | 0,102 | 0,102 |
| Node 2 | 150 | 0,688 | 0,682 | 0,676 | 0,670 | 0,664 | 30 | 0,688 | 0,687 | 0,686 | 0,685 | 0,684 |
| Node 3 | 50 | 1,500 | 1,500 | 1,500 | 1,500 | 1,500 | 50 | 1,500 | 1,500 | 1,500 | 1,500 | 1,500 |
| Node 4 | 21 | 0,688 | 0,679 | 0,671 | 0,662 | 0,654 | 21 | 0,103 | 0,101 | 0,099 | 0,097 | 0,096 |
| Node 5 | 8,5 | 0,688 | 0,671 | 0,654 | 0,638 | 0,622 | 8,5 | 0,103 | 0,100 | 0,097 | 0,094 | 0,091 |
| Node 6 | 1,2 | 0,688 | 0,669 | 0,651 | 0,633 | 0,616 | 1,2 | 0,103 | 0,100 | 0,096 | 0,093 | 0,090 |
| Node 7 | 0,17 | 0,688 | 0,669 | 0,651 | 0,633 | 0,616 | 0,17 | 0,103 | 0,100 | 0,096 | 0,093 | 0,090 |
| Node 8 | 0,005 | 0,688 | 0,669 | 0,651 | 0,633 | 0,616 | 0,005 | 0,103 | 0,100 | 0,096 | 0,093 | 0,090 |
| Node 9 | NA | NA | NA | NA | NA | NA | 120 | 0,103 | 0,102 | 0,100 | 0,099 | 0,097 |
| **Legend** | Input value | | | | | | | | | | | |
| | Output value | | | | | | | | | | | |
| | Base case | | | | | | | | | | | |
| | Probable state | | | | | | | | | | | |
| | Theoretical state | | | | | | | | | | | |

*Table 4.1: Comparison of flicker effect propagation for network configurations according to Figure 4.5.*

Figure 4.6 shows a graphical comparison of the results of the analyzed variants.

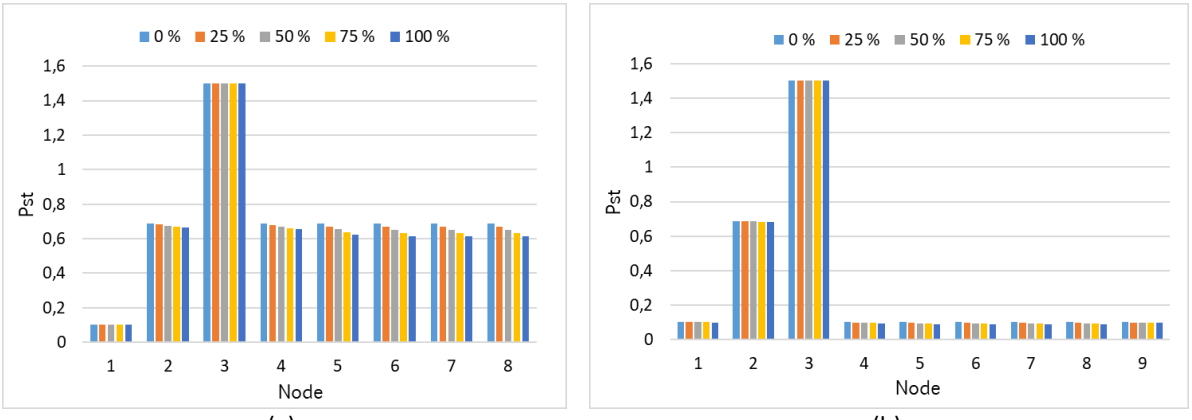


*Figure 4.6: Graphical representation of the results of the calculation of the propagation of the flicker effect for non-insulated (a) vs. isolated (b) problematic consumption.*

The results of the illustrative example show that in the case where problematic consumptions (industrial consumptions causing interference) have a common supply point at the HV voltage level, there is a significant propagation of interference to other customers in the distribution system (at LV, MV and HV voltage levels). If problematic consumption is allocated to the "isolated" industrial distribution system and the common supply point of both groups of customers is at the voltage level of EHV, interference is transmitted to customers outside the industrial distribution system only to a minimal to a negligible extent.

As an example:

- In the first case, with the source of interference in node 3 ($P_{st}$ = 1.5), small customers at the LV level also received interference at the level of $P_{st}$ = 0.688 (node 8 - Base case).
- In the second case, with the source of interference in node 3 ($P_{st}$ = 1.5), small customers at the LV level received interference at the level of $P_{st}$ = 0.103 (node 8 - Base case), which is a significant difference compared to the first case.

The advantage of the described measure is that this measure does not have to be specifically focused only on arc furnaces, but generally also works for other types of sources of interference. An important note is the effect of active loads, which can to some extent reduce the spread of the flicker propagation in the distribution system.

### 4.1.3 Specific influence of loads - asynchronous motors

In addition to the factors mentioned so far, the propagation of the flicker effect in the distribution system is also influenced by the nature of the loads connected to the distribution system. Typically, these are asynchronous motors, which are characterized by their short-circuit contribution, which can be justified on the basis of the energy stored in the inertial masses of the motors that are in operation.

In addition to the technology of EAFs, many supporting technologies and secondary metallurgical production (rolling mills) are in operation within the industrial distribution systems supplying mini-mills, the consumption of which consists mainly of various types of electric drives. Within electric drives, these are most often asynchronous motors, due to the availability of frequency converters. Due to the large proportion of asynchronous motors, it is appropriate to consider its effect on the system in studies aimed at propagating the flicker effect.

It is possible to use the standard to include the short-circuit contribution of an asynchronous motor [38]. The cited standard determines the magnitude of the replacement impedance of an asynchronous motor according to (4.2).

$$Z_{\mathrm{M}} = \frac{1}{i_{\mathrm{z}}} * \frac{V_{\mathrm{nM}}}{\sqrt{3} * I_{\mathrm{nM}}} = \frac{1}{i_{\mathrm{z}}} * \frac{V_{\mathrm{nM}}^2}{S_{\mathrm{nM}}} \tag{4.2}$$

Where $Z_{\mathrm{M}}$ is short-circuit equivalent impedance of the asynchronous motor, $i_{\mathrm{z}}$ is relative inrush current of the asynchronous motor (ratio of starting current and current at rated speed), $V_{\mathrm{nM}}$ and $I_{\mathrm{nM}}$ are nominal voltage and current of the asynchronous motor and $S_{\mathrm{nM}}$ is nominal apparent power of the asynchronous motor.

The standard [38] states the following ratios of reactance and resistance, different for different types of asynchronous motors:

- $\frac{R_{\mathrm{M}}}{X_{\mathrm{M}}} = 0{,}1;\ \ X_{\mathrm{M}} = 0{,}995 * Z_{\mathrm{M}}$ for MV motors with power greater than 1MW / pole pair
- $\frac{R_{\mathrm{M}}}{X_{\mathrm{M}}} = 0{,}15;\ \ X_{\mathrm{M}} = 0{,}989 * Z_{\mathrm{M}}$ for MV motors with power less than 1MW / pole pair
- $\frac{R_{\mathrm{M}}}{X_{\mathrm{M}}} = 0{,}42;\ \ X_{\mathrm{M}} = 0{,}922 * Z_{\mathrm{M}}$ for group of LV motors

Standard [38] also indicates approximately applicable values of $i_{\mathrm{z}} = 5$ for asynchronous motors and $i_{\mathrm{z}} = 3$ for motors with static converters.

The influence of asynchronous motors within the industrial distribution system can be illustrated on a simplified example in a total of 4 example cases. The basic division of cases is based on the different involvement of the industrial distribution system. Figure 4.7 illustrates the connection of

system A, where the interfering consumption (source of the flicker effect), consumption with asynchronous motors, and other customers have a common supply point just after the transformation between the transmission and distribution system.

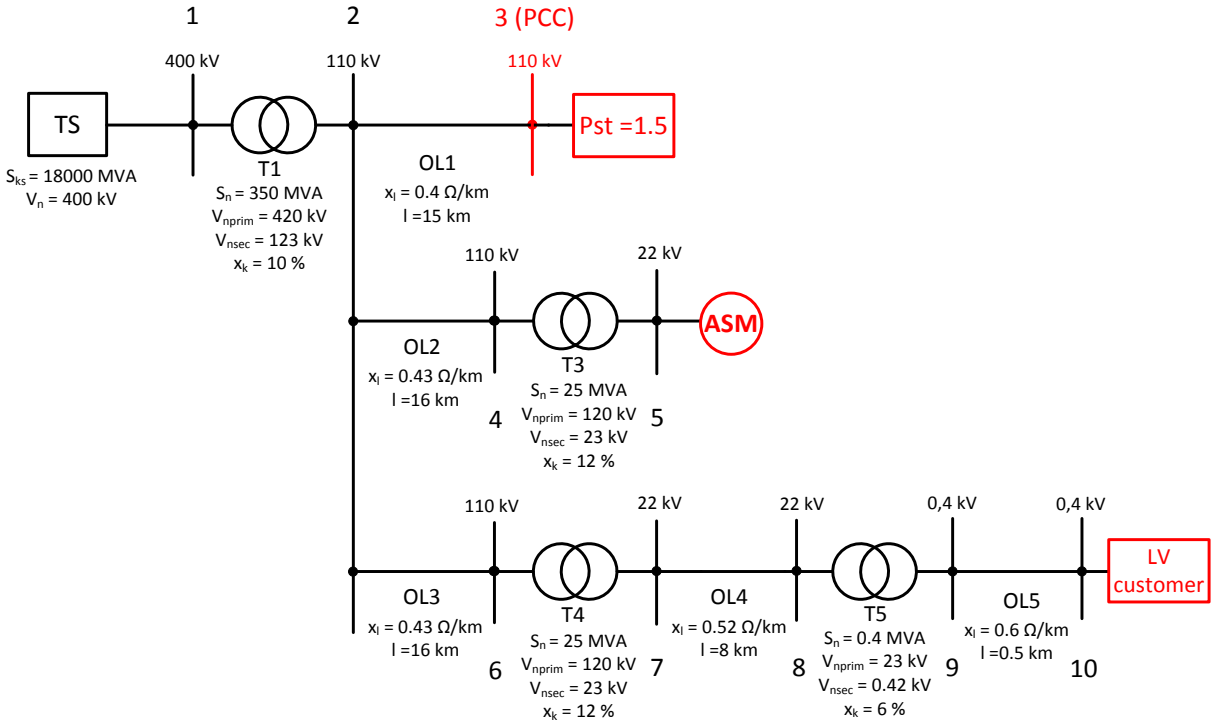


*Figure 4.7: Illustration scheme of system A for demonstration of the influence of short-circuit contributions of asynchronous motors on the propagation of the flicker effect.*

Figure 4.8 illustrates the connection of system B, where the interfering consumption (source of flicker effect) and the lines supplying another power station (supplying other consumptions and a group of asynchronous motors and drives) have a common supply point just after the transformation between transmission and distribution system. Consumption with asynchronous motors with other customers has a common supply point in the HV station supplied by the said line.

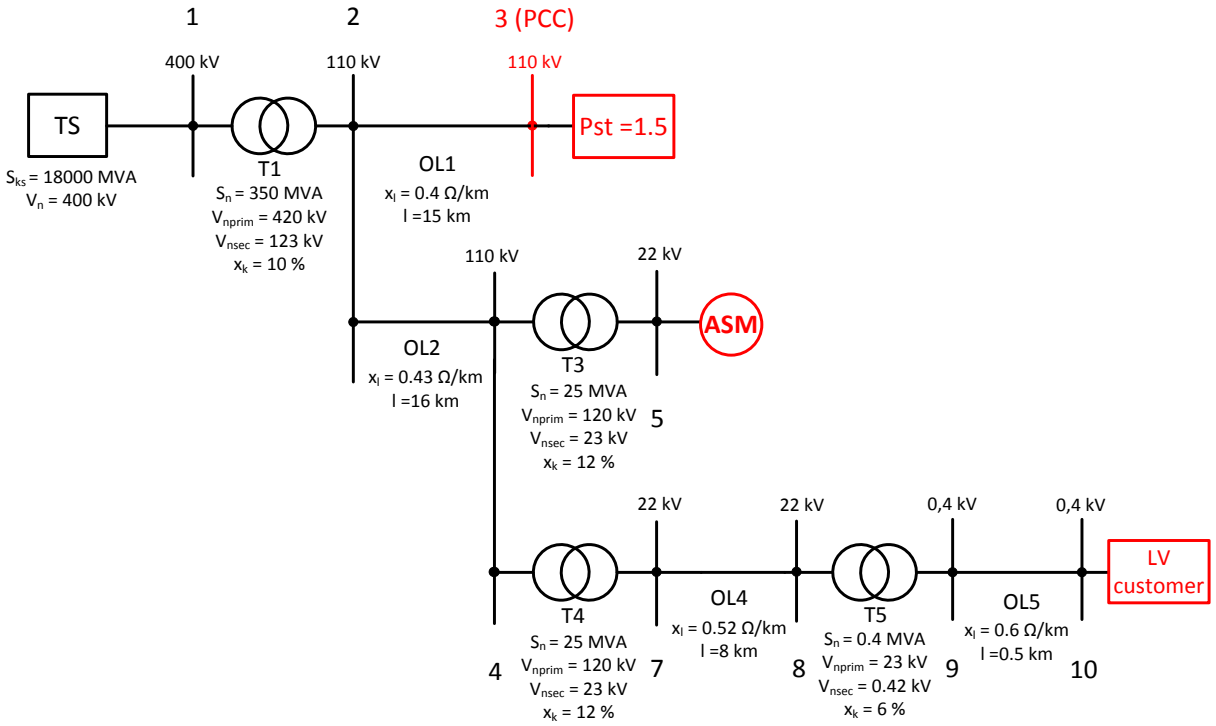


*Figure 4.8: Illustration scheme of system B for demonstration of the influence of short-circuit contributions of asynchronous motors on the propagation of the flicker effect.*

The following simplifying assumptions were adopted for the demonstrative calculations:

- For drives included in node 5, the active component of the spare impedance is neglected
- Drives are considered as a group of appliances defined by rated power, rated voltage and relative value of inrush current
- The electric drives connected to node 5 are divided into two categories. The first category represents asynchronous motors ($i_z = 5$), the second category represents drives with static converters ($i_z = 3$).
- The total power of electric drives (including asynchronous motors) connected to node 5 is 20 MW, the proportion of drives with a static converter is 50%.
- In the calculations, consumption in individual nodes is considered.
- For the connection of systems A and B, the calculation is realized for the case with asynchronous motors / drives and for the case without them (a total of 4 cases).
- The influence of other loads is not considered to illustrate the influence of asynchronous motors

By applying the procedure for determining the propagation of the flicker effect (described in Chapter 2) it is possible to obtain an evaluation of an illustrative example of the influence of asynchronous motors / drives with static converters on the propagation of the flicker effect in systems with connections A and B, which is summarized in Table 4.2.

| Location | Network connection A | | | | Network connection B | | | |
|---|---|---|---|---|---|---|---|---|
| | Load [MVA] | Pst without ASM[-] | Pst with ASM[-] | Pst % change | Load [MVA] | Pst without ASM[-] | Pst with ASM[-] | Pst % change |
| Node 1 | 0 | 0,103 | 0,102 | -1,13% | 0 | 0,103 | 0,103 | -0,37% |
| Node 2 | 150 | 0,688 | 0,680 | -1,13% | 150 | 0,688 | 0,686 | -0,37% |
| Node 3 | 50 | **1,500** | **1,500** | 0,00% | 50 | **1,500** | **1,500** | 0,00% |
| Node 4 | 0 | 0,688 | 0,663 | -3,61% | 21 | 0,688 | 0,680 | -1,19% |
| **Node 5** | **20** | **0,688** | **0,467** | **-32,10%** | **20** | **0,688** | **0,615** | **-10,57%** |
| Node 6 | 21 | 0,688 | 0,680 | -1,13% | NA | NA | NA | NA |
| Node 7 | 8,5 | 0,688 | 0,680 | -1,13% | 8,5 | 0,688 | 0,680 | -1,19% |
| Node 8 | 1,2 | 0,688 | 0,680 | -1,13% | 1,2 | 0,688 | 0,680 | -1,19% |
| Node 9 | 0,17 | 0,688 | 0,680 | -1,13% | 0,17 | 0,688 | 0,680 | -1,19% |
| Node 10 | 0,005 | 0,688 | 0,680 | -1,13% | 0,005 | 0,688 | 0,680 | -1,19% |

| Legend | |
|---|---|
| | Input value |
| | Output value |
| | Node with ASMs/drives |

*Table 4.2: Evaluation of an illustrative example of the influence of asynchronous motors / drives with static converters on the propagation of the flicker effect in systems with connection A and B.*

The results summarized in Table 4.2 show that asynchronous motors / drives with static converters to some extent limit the propagation of the flicker effect (in the order of percentage units). In the case of connection A, the limitation is smaller than in case B. This is due to the fact that the short-circuit contribution to node 2 (connection of an interfering source via line V1) from node 1 is significantly higher than the short-circuit contribution from node 5 (respectively 4). Node 2 is the common power point in case A. In the case of connection B, the flicker effect will be significantly reduced, which is the result of the greater weight of the short-circuit contribution from node 5 (respectively 4) to node 6 in comparison with connection A.

These results confirm the hypothesis that asynchronous motors and drives with static converters have a certain small effect on the propagation of the flicker effect. However, this effect cannot be confused with a targeted measure to reduce the flicker effect, but it is more appropriate to take it into account in planning studies of new facilities (EAF - flicker verification study), which can provide an estimate of future flicker values closer to real conditions after the commissioning of the EAF.

The above example serves as a simplified demonstration. In a more detailed study, it is necessary to consider the relevance of simplifying assumptions and to perform a more detailed analysis of the types of appliances connected to the analyzed system.

## 4.2 Modification of EAF technological processes

On the part of the EAF operator, it is possible to mitigate its adverse effects on the distribution system by modifying and tuning the steel production process. These modifications are often implemented mainly due to other advantages, which consist mainly in a better operating economy and higher productivity of the equipment.

The first important factor is the modification of the input material. Steel scrap must be selected according to the needs of metallurgical processes. To minimize adverse dynamic effects, the input material needs to be free of water, which causes adverse dynamic effects when reacting with a high-temperature metal. For steel scrap, it is also very important that it is fed into the furnace correctly. For optimal operation of the furnace, this means that liquid metal is required to form at the bottom of the furnace as soon as possible, which leads to more stable burning of electric arcs and less wear of the furnace linings and electrodes. To ensure this condition, it is first necessary to insert homogenized steel scrap of smaller dimensions (shredded scrap) and then to add larger inhomogeneous pieces. [39]

An important factor is also the control of the melting process. Again, the electrode position controller is often very important for optimal furnace operation and minimizing the negative effects on the distribution system. The electrode position controller is integrated into the EAF main control system. This system contributes to optimized operation throughout the process [40]. Before the start of the production cycle (melting), information on the required quality of steel is entered into the system (qualities differ in chemical composition). Based on this specification, the required composition of the input material of the charge (type of scrap, the proportion of pig iron, etc.) is determined. The actual amounts of the individual components are entered into the control system, which then evaluates them and recommends a suitable melting program. As part of the evaluation, the overall energy balance of the process is evaluated. The energy entering the process is considered to be electrical energy, chemical energy (partial chemical reactions between the charge material, injected oxygen, natural gas, anthracite and other additives). This energy is used to melt the charge and reach the required melt temperature, to the heat loss contained in the flue gas, to the heat contained in the slag, to the losses caused by furnace cooling, and to radiation losses [41]. During the process, the control system measures the energy required to reach the desired melt temperature. Within the melting program, a lower tap position on the furnace transformer is set for the initial melting phase (the most critical phase in terms of voltage fluctuations). This setting limits the maximum power of the furnace, while after overcoming the critical phase, it automatically switches to higher tap positions of the furnace transformer and thus increases the electrical power supplied to the furnace.

Another important factor is the use of oxygen and gas burners, which are another source of energy, which contributes to shortening the melting time [42] [43] [44]. Oxygen and gas burners are especially important in the initial phase of melting when they accelerate the phase of liquid metal formation at the bottom of the furnace. They, therefore, help to quickly bridge the critical phase of the process in terms of furnace interference. An example of oxygen and gas burners is illustrated in Figure 4.9 [42]. The addition of oxygen during melting (liquid metal phase - heating to the required temperature) is also realized using another technology - ultrasonic oxygen injection. Oxygen is ultrasonically injected into the furnace space, where it overcomes the slag layer and thus reaches directly to the melt, where it chemically reacts with iron and other chemical elements. The positive effect of oxygen burners is manifested in terms of reducing voltage fluctuations, especially by the formation of foamed slag [45]. With the help of special control system modules and the addition of suitable additives, foamed slag is formed [46]. The electric arcs are therefore shrouded in a layer of foamed slag, which significantly improves the stability of the electric arcs (reduction of dynamic effects) and the efficiency of the furnace.

*Figure 4.9: [42] Oxygen and gas burners (Primetals - EAF RCB Injection Technology) in operation [42].*

# 5 Use of compensation devices to improve the power quality

## 5.1 Classification of compensation devices

At present, in practice, we encounter a wide range of devices causing problems with power quality. It is a device with a wide power range, different operating characteristics, connection points in the distribution system, and different levels of network interference. The following text deals with the division of compensation devices according to various criteria, with respect to the purpose of use.

### 5.1.1 Classification under control options

The control options of the compensation device indicate the usability of the device. These are mainly parameters of response time and fineness of regulation (stepped or continuous). Compensation devices can therefore be divided into:

- **Static** - these are fixed capacitor banks, detuned filter capacitor banks, resonant harmonic filters.
- **Mechanically switched** - they enable stepwise switching of compensation stages (again capacitor banks, detuned filter capacitor banks, resonant harmonic filters) by means of contactors
- **Semiconductor switched** - also allow step switching, but instead of contactors semiconductor switches are used (on-off states only), which significantly improves the compensation dynamics
- **Semiconductor controlled** - allow continuous control of compensating power and dynamics surpass other devices. They can be implemented using phase-controlled thyristors, or pulse-width modulation using transistors.

Additionally, it should be noted that in practice, the division into static compensation systems and rotary compensation systems is also used. Static compensation systems use a suitably arranged capacitor system as a source of compensation power. Rotary compensation systems use a rotary synchronous compensator (synchronous machine in a suitably controlled excitation system) as a source of compensating power. In applications focused on the quality of electricity in industrial distribution systems, static compensation systems are used exclusively.

### 5.1.2 Classification according to voltage level

A wide range of power compensation devices (from kVAr units to tens of MVAr) results in connecting compensation devices to different voltage levels. The compensation is usually connected to the same voltage level as the problematic appliance. Compensation devices can therefore be divided into:

- **Compensation devices connected to LV** - these are compensations for smaller outputs, maximum hundreds of kVAr. This is most often the compensation of small industrial buildings and office buildings.
- **Compensation devices connected to MV** - these are compensations of medium outputs, from MVAr units up to tens of MVAr. They are used in larger industrial units (arc furnaces, rolling mills, mining machines), or as railway system compensation.
- **Compensation devices connected to HV** - these are compensations for high outputs, which are used for large industrial complexes (aluminum plants) and applications in the transmission system.

### 5.1.3 Classification according to functionalities

The primary function of compensating devices is reactive power compensation, which can be supplemented by other functions contributing to the improvement of power quality and the prevention of interfering loads. In connection with the short-circuit conditions at the connection point and the degree of interference of the connected device, it is necessary to specify the required functions of the compensation device. The basic functions are as follows:

- **Reactive power compensation** - the only function of the compensation device is the correction of the power factor at the PCC to the permissible values set by the relevant legislation. Compensation can be realized in two ways, namely compensation at constant active power and constant apparent power. In many applications, the use of compensation capacitor banks is sufficient.
- **THD reduction** - due to the connection of nonlinear types of loads, the voltage is deformed by higher harmonic frequencies. In terms of power quality, limits are set for the voltages of individual higher harmonic voltages and limits are set for total harmonic distortion (THD - Total Harmonic Distortion). In order to achieve an improvement, it is, therefore, necessary to filter higher harmonics by means of detuned filter capacitor banks, or passive resonant harmonic filters.
- **Asymmetry reduction** - the parameter of power supply asymmetry is also included in the requirements for the power quality. This problem can also cause problems of increasing active losses and overloading the neutral conductor (LV system). For these purposes, however, it is necessary to be able to switch or continuously control the compensating power independently in each phase.
- **Flicker effect mitigation** - again one of the requirements for the power quality. These are the undesirable effects of voltage fluctuations with a frequency from Hz to 35 Hz, which causes unpleasant visual sensations. In order to limit the flicker effect, it is, therefore, necessary to prevent changes in the power consumption with the specified frequency. This function, therefore, requires fast response and the possibility of continuous control of the compensation device.

### 5.1.4 Compensation devices benchmark

Table 5.1 summarizes a comprehensive overview of the properties of individual types of compensation devices. For comparison, the most important properties were selected from the design point of view and from the point of view of improving power quality.

Table 5.1 highlights a group of semiconductor-controlled compensating devices that represent the most suitable solution for industrial distribution systems, especially for electric arc furnaces. The remaining unhighlighted types of compensation devices are more suitable as local compensation, for example in electric drives and the like (in applications where there are no high requirements for the dynamics of the response of the compensation device).

| Compensation type | Specification | Control | Dynamic properties | THD reduction | Asymmetry reduction | Flicker effect mitigation |
|---|---|---|---|---|---|---|
| Static | Capacitor banks | NA | NA | No | No | Slightly |
| | Detuned filter capacitor banks | | NA | Partially | No | Slightly |
| | Harmonic filters | | NA | Yes | No | Slightly |
| Mechanically switched | Capacitor banks | Stepped | seconds | No | Theoretically | Slightly |
| | Detuned filter capacitor banks | | seconds | Slightly | Theoretically | Slightly |
| | Harmonic filters | | seconds | Yes | Theoretically | Slightly |
| Semiconductor switched | Capacitor banks | Stepped | n*20 ms | No | Yes | Slightly |
| | Detuned filter capacitor banks | | n*20 ms | Slightly | Yes | Slightly |
| | Harmonic filters | | n*20 ms | Yes | Yes | Slightly |
| Semiconductor controlled | TCR + capacitor banks | Continuous | 10 ms | No | Yes | Yes |
| | TCR + detuned filter capacitor banks | | 10 ms | Slightly | Yes | Yes |
| | TCR + harmonic filters | | 10 ms | Yes | Yes | Yes |
| | Active filter | | Based on modulation frequency | Yes | Yes | Yes |

*Table 5.1: Overview of the types and functionalities of compensation devices.*

Equally important parameters of compensation devices include the operating costs of compensation devices, which are mainly made up of costs for active losses. The design of compensation devices plays an important role in terms of voltage level. As illustrated in Table 5.2, compensating devices connected at the low voltage level show higher losses than devices connected at the high voltage level. Active losses also depend on the complexity of the equipment. In the case of decompensation converters, it is necessary to take into account the additional losses of the decompensation element. For active filters and thyristor-controlled compensating devices, the losses are increased by switching losses. With thyristor-controlled compensation devices, switching takes place in every half-period; with active filters, the losses are based on the PWM modulation frequency, which can range from hundreds of Hz to kHz. Due to the above factors, the choice of a suitable compensation device technology needs to be carefully considered based on the functional requirements for each specific application.

| Compensation type | Specification | Dynamic properties | Decompensation reactor losses | Capacitors losses | Detuning reactors losses |
|---|---|---|---|---|---|
| Static | Capacitor banks | - | - | 0,4 W/KVAr[1] | - |
| | Detuned filter capacitor banks | - | - | 3 - 8 W/KVAr[1] | |
| | Harmonic filters | - | - | 3 - 8 W/KVAr[1] | |
| Mechanically switched | Capacitor banks | seconds | - | 0,4 W/KVAr[1] | - |
| | Detuned filter capacitor banks | seconds | - | 3 - 8 W/KVAr[1] | |
| | Harmonic filters | seconds | - | 3 - 8 W/KVAr[1] | |
| Semiconductor switched | Capacitor banks | n*20 ms | - | 0,4 W/KVAr[1] | - |
| | Detuned filter capacitor banks | n*20 ms | - | 3 - 8 W/KVAr[1] | |
| | Harmonic filters | n*20 ms | - | 3 - 8 W/KVAr[1] | |
| Semiconductor controlled | TCR + capacitor banks | 10 ms | 2 kW/MVAr[3] | 0,2 W/kVAr[2] | - |
| | TCR + detuned filter capacitor banks | 10 ms | 2 kW/MVAr[3] | 0,2 W/kVAr[2] | 2 kW/MVAr[3] |
| | TCR + harmonic filters | 10 ms | 2 kW/MVAr[3] | 0,2 W/kVAr[2] | 2 kW/MVAr[3] |
| | Active filter | Based on modulation frequency | - | 0,2 W/kVAr[2] | - |

1) Assuming LV compensation devices.
2) Assuming MV capacitors.
3) Assuming MV reactors (varying based on quality factor of reactance)

*Table 5.2*: *Overview of active losses of various types of compensation devices.*

## 5.2 Influence of compensating devices on the flicker effect mitigation

Compensating devices have a significant effect on reducing the flicker effect. The previous chapter, more precisely section 4.1.1, describes the procedure for planning the allowable values of the flicker effect for an electric arc furnace for the specified conditions of short-circuit power in PCC and rated power EAF. The limit value $P_{\mathrm{st95\%}}$ can be set at a higher level (depending on the $S_{ks}$ in the PCC power of the EAF) provided that a compensation device is used. The aim is to achieve a sufficiently low value of $P_{\mathrm{st95\%}}$ in the sense of current legislative regulations and standards. The use of a compensating device is necessary in the vast majority of cases.

For the case of using the compensation device, equation (4.1) is extended by the coefficient of limiting the flicker effect due to the use of the compensation device $k_{\mathrm{comp}}$ according to (5.1).

$$P_{\mathrm{st95\%}} = K_{\mathrm{st}} * \frac{S_{\mathrm{ksEAF}}}{S_{\mathrm{ksPCC}}} * k_{\mathrm{comp}} \tag{5.1}$$

The coefficient of reduction of the flicker effect due to the use of the compensation device

$$R_{comp} = \frac{P_{\mathrm{st\_comp\_off}}}{P_{\mathrm{st\_comp\_on}}} = \frac{1}{k_{\mathrm{comp}}} \tag{5.2}$$

Where $R_{comp}$ is the coefficient of reduction of the flicker effect due to the use of the compensation device, $P_{\mathrm{st\_comp\_off}}$ is the value of the short-term perception of the flicker effect with the compensation device switched off and $P_{\mathrm{st\_comp\_on}}$ is the value of the short-term perception of the

flicker effect with the compensation device switched on. The coefficient $R_{comp}$ will be the subject of the following chapters of this work.

Figure 5.1 illustrates the relationship between the rated furnace power and the short-circuit power in the PCC for different planned values of $P_{\mathrm{st95\%}}$ for the case without the use of a compensation device. For example, for the planned value $P_{\mathrm{st95\%}} = 1$, in the case of a short-circuit power in the PCC 2000 MVA, it is possible to connect an EAF with a nominal power of barely 30 MVA.

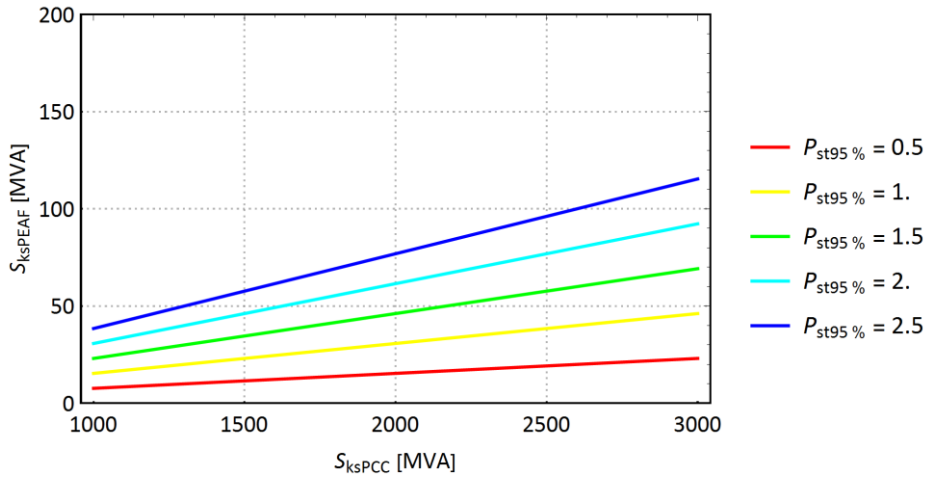


*Figure 5.1: Relationship between rated furnace power and short-circuit power in PCC for different planned values $P_{st95\%}$ for the case without the use of compensation device.*

In the case of using a compensation device with a reduction factor of the flicker effect $R_{comp} = 1.6$, according to the dependence illustrated in Figure 5.2, it is possible to connect an EAF with a power of 50 MVA for the planned value $P_{\mathrm{st95\%}} = 1$.

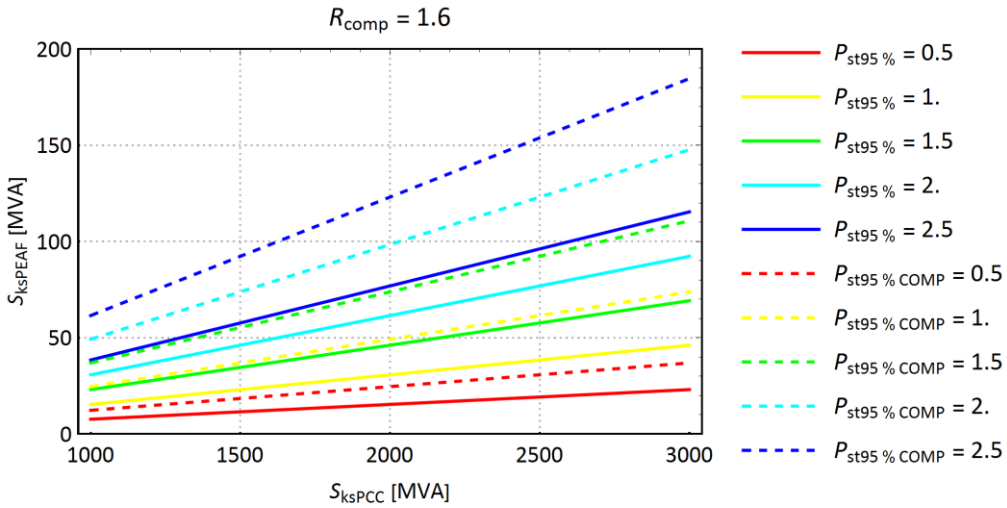


*Figure 5.2: Illustration of the influence of the compensation device, according to equation (5.1)*

The reduction factor of the flicker effect $R_{comp}$ differs according to the type of compensating device, the dynamic properties and the nominal power of the compensating device play an important role. The greater the dynamics of the compensation device, the greater the coefficient $R_{comp}$. The coefficient $R_{comp}$ is to a certain extent dependent on the techniques used in the control system of the compensation device, which this work will focus on in the practical part.

## 5.3 Compensation devices for industrial distribution systems

Due to the available technologies, rotary compensators were most often used in the morning period of compensating devices. The use of compensation devices was also mainly in applications in the transmission system. Technological development in the field of HV capacitors and power electronics brought about the rapid development of FACTS technologies (Flexible AC Transmission Systems). The growing representation of large nonlinear loads and the definition of industrial distribution systems have gradually resulted in the idea of using FACTS technologies in the field of power quality.

FACTS devices are divided into parallel, serial and hybrid (combined systems) in terms of the basic functional arrangement. The most frequently used systems include parallel systems (even in the area of Power Quality), where a specific device is connected in parallel to a selected node of the system. This type of system affects the node parameters in a given node. Serial systems are used to influence the parameters of the branch connecting two nodes in the electrical system. Their most common applications can be found in transmission systems for the transmission of power over long distances, or the control of required power flows between two nodes. In the field of power quality, this type of system is hardly used. Hybrid FACST systems consist of a combination of a serial and a parallel system. They have the widest range of functionalities from the group of FACTS devices, both in the area of use in transmission systems and the area of power quality. However, their use is very rare (small pilot projects) due to the complexity and high space and financial demands.

For applications in industrial distribution systems in the field of power quality, we can exclusively talk about parallel FACTS technologies. In practice, the technologies summarized in Table 5.3 are most often used.

| **Technology** | **Description** | | **Basic dynamic properties** | **Dynamic response** |
|---|---|---|---|---|
| MSC (DN) | Mechanically Switched Capacitors | Using Harmonic resonant filters | Discrete switching | Based on circuit breaker technology |
| | Mechanically Switched Capacitors with Dumping Network | Using Harmonics resonant filters with modified design for dumping switching oscillations | | |
| SVC | Thyristor Controlled Reactor + Harmonics resonant filters | Using Harmonic resonant filters in various configurations | Continuous control | 15 ms |
| STATCOM | VSC + DC capacitors | Using Harmonic resonant filters in various configurations + filters for PWM frequency effects | Continuous control | less than 1 ms |

*Table 5.3: An overview of the basic features of FACTS devices used for power quality applications.*

SVC technology is most often used for applications in industrial distribution systems with electric arc furnaces. The use of STATCOM technology has future potential, however, there are still many pitfalls at present. MSC technology has been used more in the past and with the development of power electronics in the field of power quality, new projects are practically no longer emerging.

### 5.3.1 Thyristor based FACTS devices

SVC belongs to the group of FACTS devices, specifically, it is a system connected in parallel to a node of a transmission or distribution system operating on the basis of power thyristors. The original SVC applications began to appear in the late 1970s and early 1980s, especially for applications in the transmission system. The main function of SVC in transmission systems was the dynamic regulation of voltage in selected nodes and the improvement of the possibilities of static and dynamic stability, which enabled an increase in the transmission capacity of the line and the distance of power

transmission at that time. This technology has undergone considerable development and, due to the greater development of power quality issues since the 1990s, this technology has been extended to applications in industrial distribution systems. The main functions of SVC in these applications were reactive power compensation, reduction of voltage fluctuations - flicker effect, reduction of higher harmonic disturbances, and symmetrization of consumption. With this development, SVC is currently a modular system with a number of functions for the transmission system, distribution system, and industrial applications. This work focuses on the use of SVC for industrial distribution systems.

SVC for use in industrial distribution systems consists of a decompensation converter TCR (Thyristor Controlled Reactor), works as a dynamic controlled element and passive filters of higher harmonics, which are used as a fixed source of reactive power and to reduce higher harmonic interference. The construction and properties of the individual parts of the SVC differ according to the type of application (EAF, high power rectifiers - electrolytic processes, mining machines, electric drives, etc.), the required compensating power and the place of installation.

There are two basic design arrangements for the TCR. The first, most commonly used, is a 6-pulse connection, which is sufficient for most applications in various conditions. The second arrangement is a 12-pulse circuit, the advantage of which is less harmonic distortion of the output current as in the case of a 6-pulse circuit with the same rated power. The disadvantage is the higher investment and space requirements. 12-pulse connection finds typical use in cases where there is a requirement for high values of rated power and at the same time, it is a system with low short-circuit power. There is also another important technological aspect of the TCR unit, such as the type of inductance connection. The inductors in the TCR unit can be connected separately - Figure 5.3 (a), or split - Figure 5.3 (b) and (c). Split wiring is most often used for reasons of better protection of thyristor blocks against short-circuit currents and overvoltage phenomena [47]. A comparison of TCR connections is shown in Figure 5.3.

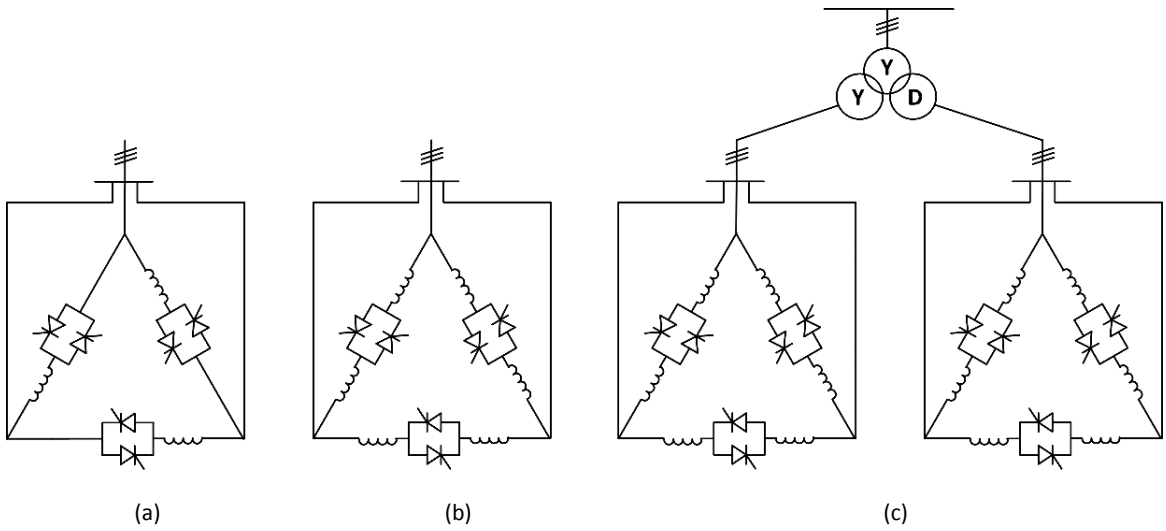


*Figure 5.3:* Basic 6-pulse TCR connection (a), 6-pulse TCR connection with split inductors (b) 12-pulse TCR connection (c).

For industrial SVC applications, 3 basic types of passive harmonic filters are most often used. The first basic type is a second-order filter, which consists of a series resonant circuit of a capacitor and a tuning reactor, where, in addition, the active resistance of the reactor is significantly manifested. The second type is a second-order damped filter, the connection of which differs from the previous type by the connection of a parallel damping resistor to the filter reactor. The third type is the c-type filter, which is used mainly for applications with EAF. The possible connection of individual types of filters is shown in Figure 5.4. Individual types differ in frequency and amplitude characteristics (possibilities of

limiting higher harmonics of their resonant frequency vs. limitation of higher harmonics at other than resonant frequency), active losses and complexity of construction.

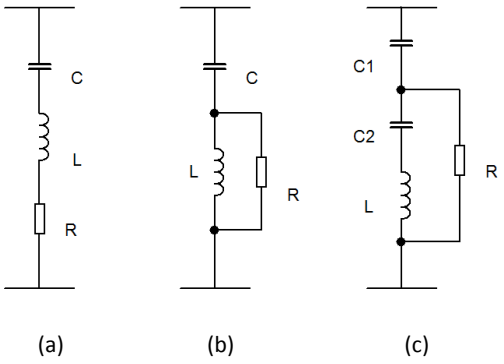


*Figure 5.4: The most commonly used types of passive harmonic filters for industrial SVC, second order filter (a), dumped second order filter (b) and C-type filter (c).*

In the case of the use of SVC in industrial distribution systems with EAFs, SVC is typically connected to the HV level (node common to the supply sections EAF). A typical set consists of a TCR unit and 2 - 4 higher harmonic filters (for 2nd to 5th harmonics). When using SVC for other applications (mining machines, rolling mills and other technologies), higher harmonic filters are designed for the 5th, 7th, 11th and 13th harmonics, which corresponds to the interference typical of semiconductor converters.

SVC is implemented as standard in a three-phase connection. Exceptions are applications in the field of alternating railway systems, where a single-phase SVC design is used.

At the beginning of its development, STATCOM technology also used thyristor semiconductor elements. However, these were switchable GTO (Gate Turn Off) thyristors. However, this is the early development phase of this technology and currently, STATCOM technology uses exclusively IGBT (Insulated Gate Bipolar Transistor) power transistors.

### 5.3.2 Transistor based FACTS devices

The beginnings of STATCOM technology date back to the 1980s, when the technology was originally developed and the first projects were implemented. The first pilot projects were built on the basis of thyristors with forced commutation later on the basis of GTO thyristors [48].

The development of semiconductor component technology for power electronics has led to the advent of IGBT technology, despite the greater robustness of thyristor technology. The topology of STATCOM technology is based on VSC (Voltage Source Converter). To achieve sufficient performance of the inverter as a whole, it was necessary to proceed to its parallel or serial switching due to the limiting parameters of the IGBT elements. In the case of parallel switching, the disadvantage was that the currents in the inverter circuit were relatively large, which brought a number of problems (for example, the requirement for a highly reliable cooling system). In addition, a transformer with a conversion from kV units to tens of kV was needed to connect to the network. The DC part of this circuit was common, as illustrated in Figure 5.5 [49] (the designation D-STATCOM is used for STATCOM technology adapted for use in distribution systems). In the case of series switching elements, there are also considerable risks associated with uneven voltage distribution and overvoltage generation.

The described solution had a number of disadvantageous features. The switching frequency of the inverter's PWM (pulse width modulation) was limited by several factors. The first factor was the

durability and life of semiconductor components, and the second significant factor was switching losses. Restrictions on the switching frequency side also brought certain restrictions on the functionality side of the device. The lower switching frequency resulted in a reduced ability to limit the higher harmonics of the compensated load, and it was often necessary to use additional higher harmonic passive filters for higher orders. This solution is often referred to as hybrid STATCOM, which is a combination of STATCOM and passive resonant filters of higher harmonics. Another undesirable manifestation of a lower switching frequency is the occurrence of interference to a significant extent due to PWM modulation. For this reason, an additional filter was necessary for this type of interference.

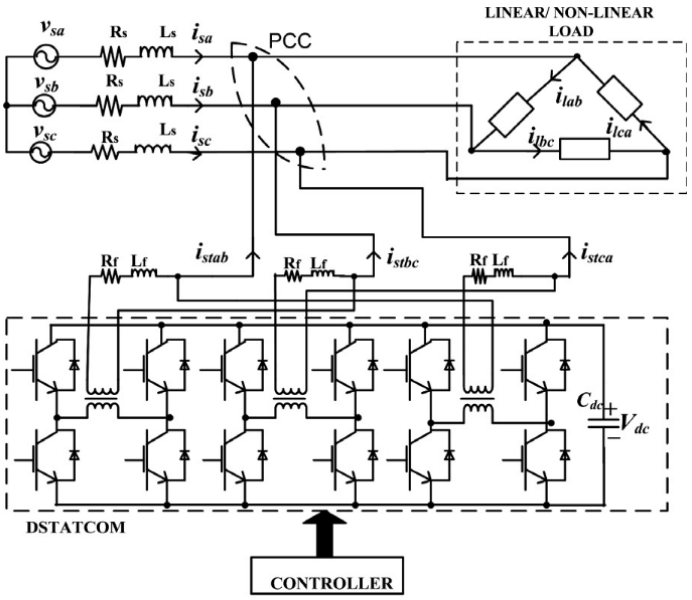


*Figure 5.5: Illustration of D-STATOM connection [49].*

STATCOM technology has long been built in a competitive role against SVC technology. It has long exceeded the capabilities of SVC in terms of functionality, but SVC technology still excels in many other areas. The long-term challenge with STATCOM technology is to achieve better parameters in all respects compared to SVC technology.

The current development of STATCOM technology is moving towards multi-level modular converters. This trend is also being followed by key manufacturers in the market [50] [51]. It is a VSC technology specially adapted for applications with high-rated power. The figure shows the concept of Multilevel Valve Module technology within the Multilevel STATCOM technology from ABB [50]. A similar solution is being promoted by SIEMENS - Multilevel Modular Converter [52].

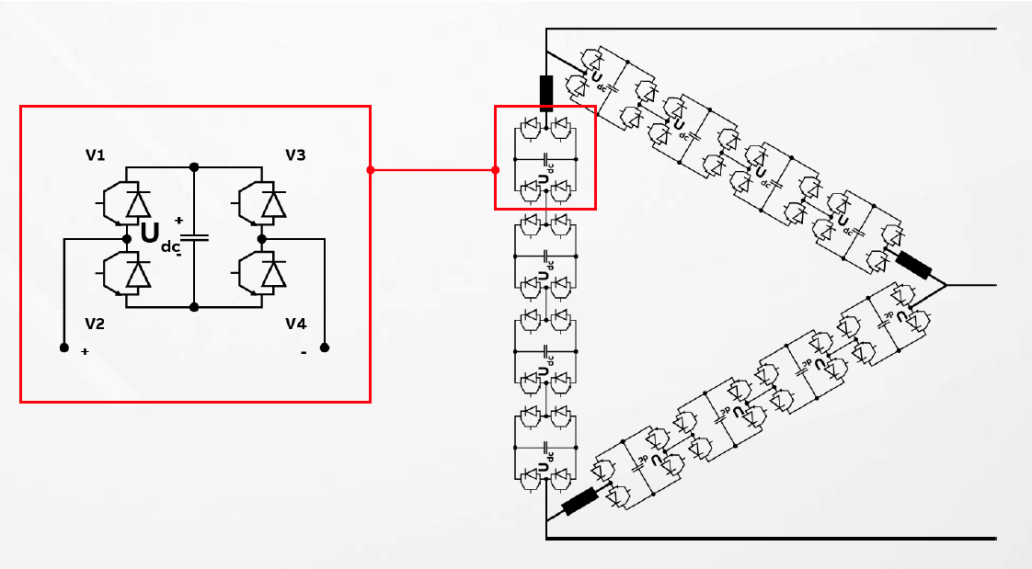


*Figure 5.6: Demonstration of the concept of multilevel modular inverters for STATCOM technology (Multilevel Valve Module from ABB). [50]*

The arrangement of multi-level modular converters is based on sub-modules. One module normally consists of four switching (IGBT) elements and a DC capacitor in the DC circuit (see Figure 5.6). The structure is similar to the structure of the SVC technology decompensation TCR converter. The inverter as a whole consists of 3 branches connected in a triangle. One branch is formed by a series connection of the reactor and the chain of switching modules. An obvious advantage of this configuration is that the DC circuits of the sub-modules are not interconnected, which overcomes the problems with uneven voltage distribution that have occurred with earlier STATCOM technology concepts. Another advantage is that the output signals are very similar in shape to the sinusoidal waveform of the fundamental harmonic frequency due to the multi-level design, as a result of which the requirement for a high switching frequency is no longer necessary. In connection with this feature, the requirements for the HF filter are also reduced. The reduced switching frequency also reduces switching losses and reduces the stress on semiconductor elements. Last but not least, the undeniable advantages include modularity, which allows the implementation of devices for a wide range of uses.

Further development of STATCOM technology is likely to be the implementation of the electricity storage function, although it is more of a transmission system application [53].

## 5.4 Operational aspects of FACTS systems

The operational aspects of the FACTS systems are extremely important in terms of power quality in industrial distribution systems. The operators of industrial enterprises operating facilities that are significant in terms of emitting interference most often act as investors in these technologies. For this group, compensation devices (FACTS systems) represent an investment necessary to ensure the operation of its technology. However, the more advanced functionality of compensation devices does not bring them a direct financial benefit or improvement of product parameters in its business segment.

### 5.4.1 Space requirements

For transmission system applications, STATCOM technology often reports reduced (30 to 40%) space requirements compared to SVC [54]. Compared to industrial applications, transmission system applications have higher output power requirements (resulting in a higher voltage level of the FACTS

technology itself) and requirements for connection to the transmission system. In industrial applications, it is sufficient to connect the FACTS device directly to an existing MV system.

As an example, typical SVC and STATCOM system configurations are shown in Figures 5.7 [55] and 5.8 [51]. The examples show similar space requirements for STATCOM and SVC (for SVC in Figure 5.7, not all holdings are completely covered, as is done for STATCOM in Figure 5.6) in applications for industrial distribution systems. In general, however, trends show that STATCOM technology tends to be less space-consuming than SVC (modular container solutions). For example, the new Multilevel Valve Module technology from ABB states that the space requirement of STATCOM technology is halved compared to SVC technology [50].

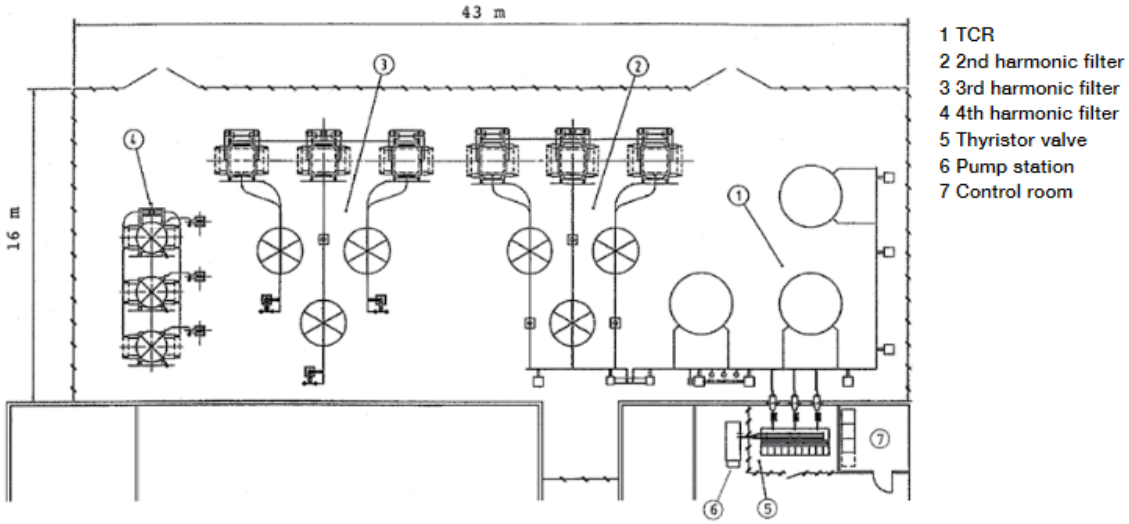


*Figure 5.7: Demonstration of the layout and space requirements of SVC technology – ABB solution - 120 MVAr / 31.5 kV [55].*

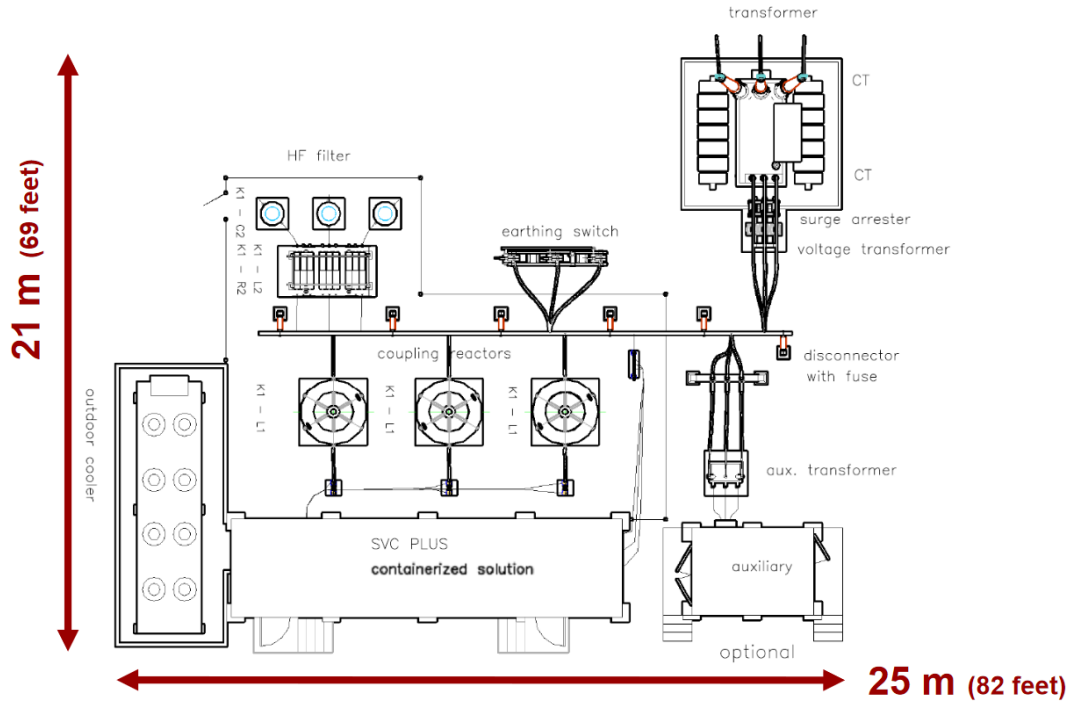


*Figure 5.8: Demonstration of the layout and space requirements of STATCOM technology - solution from SIEMENS (SVC PLUS L 50 MVAR) [51].*

### 5.4.2 Investment intensity

The investment intensity of compensation devices in industrial distribution systems is a frequently discussed topic. For example, for steelworks operators with EAF, it has compensating power mainly from the following points of view:

- Restriction of reactive power consumption from the distribution system and the associated elimination of charges
- Increased productivity of EAF (intensification of production), the benefit is income from increased production.
- Reduction of other EAF disturbances (flicker effect, higher harmonics and voltage asymmetry) - does not bring a direct economic benefit

Based on these considerations, steelworks operators are looking for a compromise solution between investment intensity and functionality. Most operators operate SVC technology, often lacking strong enough arguments to replace this technology with STATCOM technology, and therefore often choose the path of maintenance and gradual renewal of existing SVC technology. STATCOM technology is often opposed by higher investment intensity and higher operating costs (cost of losses), as well as a smaller circle of experienced suppliers, than in the case of SVC technology. For example, the source [50] states a comparable investment intensity for both technologies in the range of 500-100 USD/kVAr (depending on the configuration of the required solution). The same source [50] further states that STATCOM losses are higher than for SVC.

Investments in STATCOM technology are therefore more of a domain of projects where there are increased demands on the advanced functions of compensating equipment or projects of newly emerging industrial areas.

In general, the investment intensity of compensation is highly variable due to many external factors.

# 6 Enhanced possibilities of deploying FACTS systems in industrial distribution systems

With the development of the possibilities of power electronics, FACTS technologies were created and developed mainly in applications for the transmission system. The goal of the FACTS devices was primarily to enable the transmission of energy over long distances using an AC network. In another statement, it was mainly about supporting the stability of voltage and the stability of power transmission. The architecture and control system of these devices were adapted for this purpose. The most commonly used variants are parallel FACTS systems with control system blocks focused on node voltage regulation, support of dynamic stability, slow action, and damping of power oscillations. The functionalities of SVC technology gradually began to find application in industrial distribution systems for solving the problem of power quality (power factor, voltage fluctuations, consumption symmetrization) and increasing productivity. In terms of hardware, there are no significant differences compared to FACTS devices for the transmission system. The main differences are hidden in the control system, where applications for industrial distribution systems use a different philosophy of control with a greater emphasis on dynamics. The work focuses and then suggests certain improvements for this type of system.

## 6.1 Basic FACTS control methods

Parallel FACTS systems in the transmission system behave as an impedance connected to a node with time-varying capacitive or inductive reactance. In the following text, these devices will be referred to as sources of variable reactive power. It can be, for example, a technological unit SVC composed of units TCR (Thyristor Controlled Reactor), TSC (Thyristor Switched Capacitors), MSC (Mechanically Switched Capacitors) and MSR (Mechanically Switched Reactors), or STATCOM and TCR, TSC, MSC and MSR. The structure of such a control system is illustrated in Figure 6.1 [56].

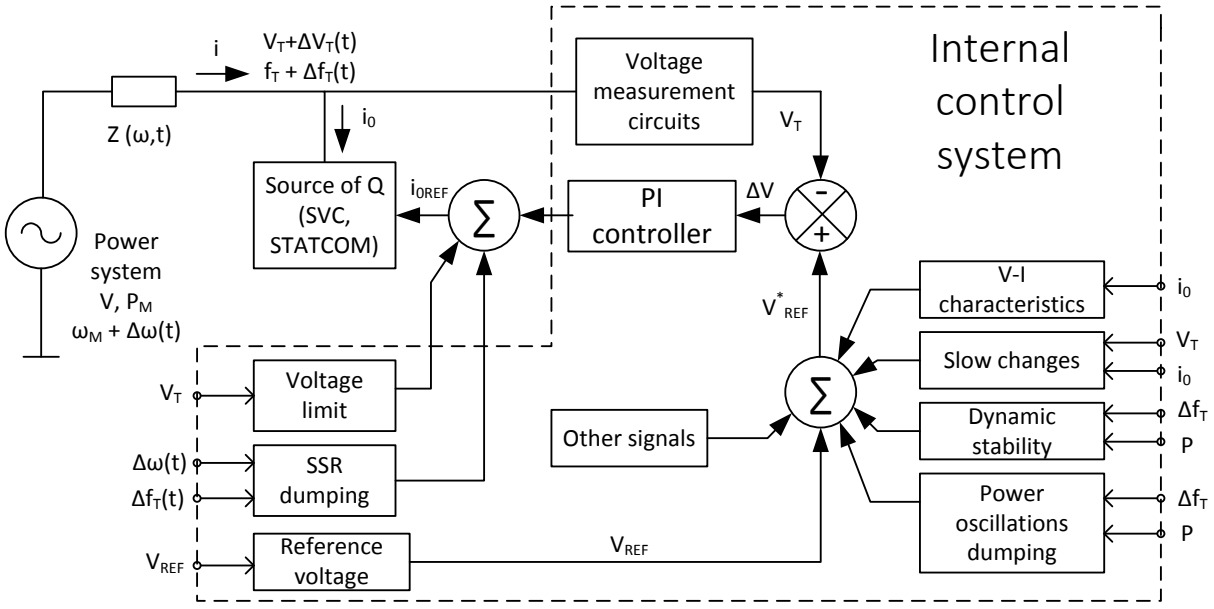


*Figure 6.1: Control system structure of parallel FACTS systems (SVC, STATCOM) [56].*

The dominant part of the control system is a voltage loop with a proportional-integral (PI) feedback controller. The actual value of the voltage $V_T$ is the voltage measured in the connection node of the FACTS system, $i_0$ is the current of the compensation device and current $i$ is the current entering the system node. PI controller controls the reactive power of the FACTS device so that the reference

voltage $V_{\mathrm{REF}}$ is set in the given node. However, the $V_{\mathrm{REF}}$ voltage does not enter the control loop directly, but its signal is summed with the signals of the partial control function blocks. The basic blocks include, in particular, voltage regulation according to volt-ampere characteristics and reactive power reserve regulation. The control system can be extended with a module for improving dynamic stability and a module for damping power oscillations. It is also necessary to add that other blocks, functionally focused more on safety, directly affect the output of the PI controller. These include overvoltage reduction and prevention of subsynchronous resonances.

### 6.1.1 Voltage regulation function

The basic control block of parallel FACTS devices is controlled according to volt-ampere characteristics. The purpose of this control block is to respond to rapid voltage changes. The basic principle of this control block is based on the characteristics illustrated in Figure 6.2 (characteristics valid for SVC).

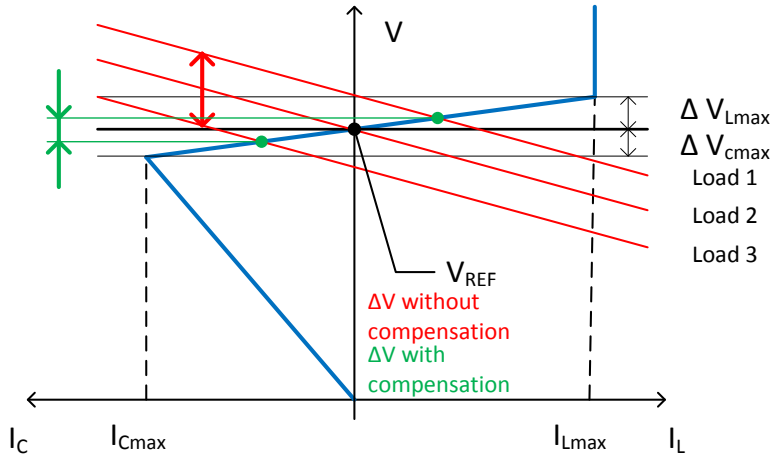


*Figure 6.2: Illustration of V-I characteristics of SVC voltage control [56].*

The blue curves show the settings of the specific allowed operating points of the SVC in the V-I plane. The red curves demonstrate the dependence of the voltage in a node on the reactive power that is injected from that node into the network or is injected into it from the network. As the load of the node changes, the position of these lines changes in displacement, ie. the higher the load, the lower the line. Therefore, "load 1" < "load 2" < "load 3" applies to the designation in Figure 6.2. If the system without SVC is considered, the voltage drop during the transition from "load 1" to "load 3" will be much larger than in the case of a system with SVC, which starts injecting reactive power into the node due to the voltage drop. The implementation of this control block is illustrated in Figure 6.3. A certain value is added to the set value of the reference voltage so that the operating points marked in green in Figure 6.2 are reached. The reference voltage will therefore be modified according to (6.1).

$$V_{\mathrm{REF}}^{*} = V_{\mathrm{REF}} + kI_{\mathrm{Q}} = V_{\mathrm{REF}} + \frac{\Delta V_{\mathrm{Cmax}}}{I_{\mathrm{Cmax}}} I_{\mathrm{Q}} = V_{\mathrm{REF}} + \frac{\Delta V_{\mathrm{Lmax}}}{I_{\mathrm{Lmax}}} I_{\mathrm{Q}} \tag{6.1}$$

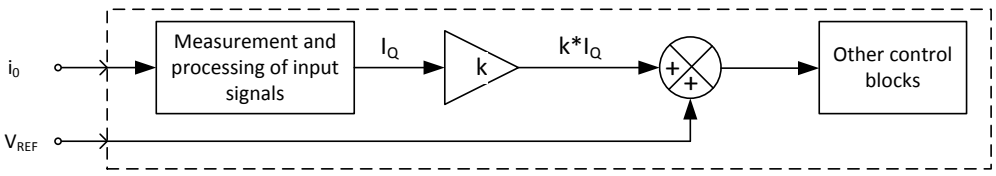


*Figure 6.3: Voltage control block according to V-I characteristics.*

A detailed description of the design of the described characteristics is contained in IEEE Standard 1031 "IEEE Guide for the Functional Specification of Transmission Static Var Compensators" [57].

### 6.1.2 Reactive power reserve control function

Voltage regulation according to V-I characteristics serves mainly for fast control of dynamic parts of FACTS devices. For the purposes of the transmission system, compensation systems (Static Var Systems) are used, consisting of devices with different dynamic properties. An example is an SVC device, which as a system consists of a TCR, TSC, MSR, and MSC. However, mechanically switched elements differ fundamentally from thyristor-switched elements in their dynamic properties. For MV circuit-breakers with SF6 isolation medium, the tripping time is around 60 ms from the issuance of the command, which is longer than for devices using thyristors or transistors. Other limiting factors also apply to mechanically switched devices. The tripping time is 60 ms, but after a certain number of cycles (typically 3), a longer time is needed to save mechanical energy to move the tripping mechanism of the circuit breaker. From the point of view of the control of compensation systems, a control strategy is therefore important, which avoids encountering technical limits for this reason. The desired strategy will enable the required function of the compensation system with the limitation that the number of switchings of mechanically switched elements will be in the order of units (maximum tens) of switchings per day. An important aspect is also the service life of circuit breakers, which is given in the order of tens of thousands of switchings. To take these properties of the mechanically switched elements of the compensation system into account, the control system includes a "slow action" block (Figure 6.1), also called a "Var Reserve".

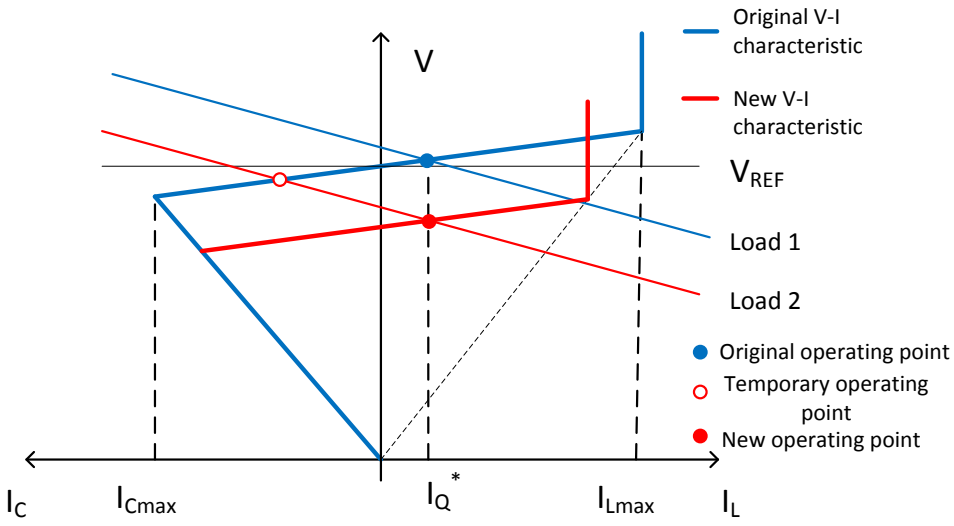


*Figure 6.4: Influence of reactive power reserve control on SVC operating characteristics [56].*

The behavior of this control block is demonstrated in Figure 6.4. The initial state is marked with a blue dot, ie. at a specific load the required reactive current is taken from the network. Subsequently, the load in the node changes in a short time (transition from load 1 to load 2 according to Figure 6.4). Due to the fast regulation according to the V-I characteristics, the output compensation power will change. However, the new operating point of the compensation device is located in the capacity area close to the capacity limit of the compensation system. If there were another rapid change or power oscillations at this point, the dynamically controlled TCR would not be able to make full use of its range and the device would therefore be less efficient. The slow action control block maintains the set value of the compensation current so that the TCR range can be used to the maximum. However, this control block works with a slow response to maintain the dynamic properties of other control circuits. The

control block diagram is illustrated in Figure 6.5. The voltage reference value is thus corrected by the slow integration of the current control deviation of the compensation device.

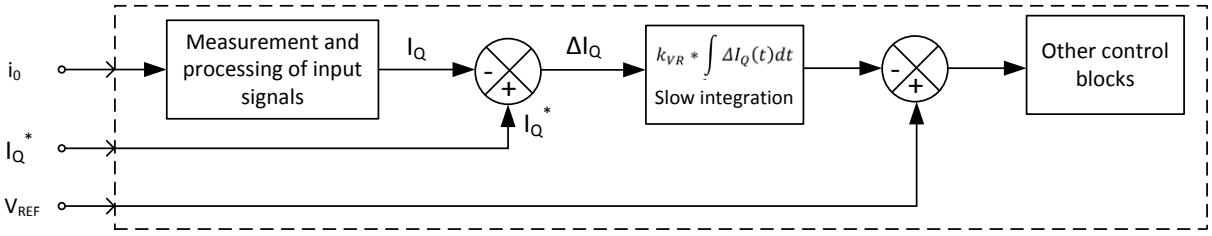


*Figure 6.5: Control diagram of the reactive power dynamic reserve.*

## 6.2 Advanced FACTS control methods for applications in industrial distribution systems

The SVC control system in industrial applications is mainly adapted to compensate for reactive power consumption, symmetrization of consumption, and reduction of voltage fluctuations - flicker effect [58]. This work is focused on this system and especially on the reduction of voltage fluctuations - flicker effect.

The requirements for the SVC system for industrial applications are as follows:

- Reactive power consumption compensation in PCC
- Limitation of higher harmonic voltages
- Power consumption symmetrization
- Limitation of voltage fluctuations - flicker effect mitigation

To ensure the above-mentioned requirements, sufficient dynamics of the SVC system are needed - especially for load balancing and reducing voltage fluctuations. On the contrary, accuracy is also required for reactive power consumption compensation. The limitation of higher harmonics is ensured by passive resonant filters of higher harmonics. The most common solution for these applications is two-loop control (open loop and closed loop) illustrated in Figure 6.6 [59]. A reactive current is typically considered as the control variable. The control diagram in Figure 6.6 is adjusted for industrial applications with EAF and LF, and in other parts of the work, this configuration is considered.

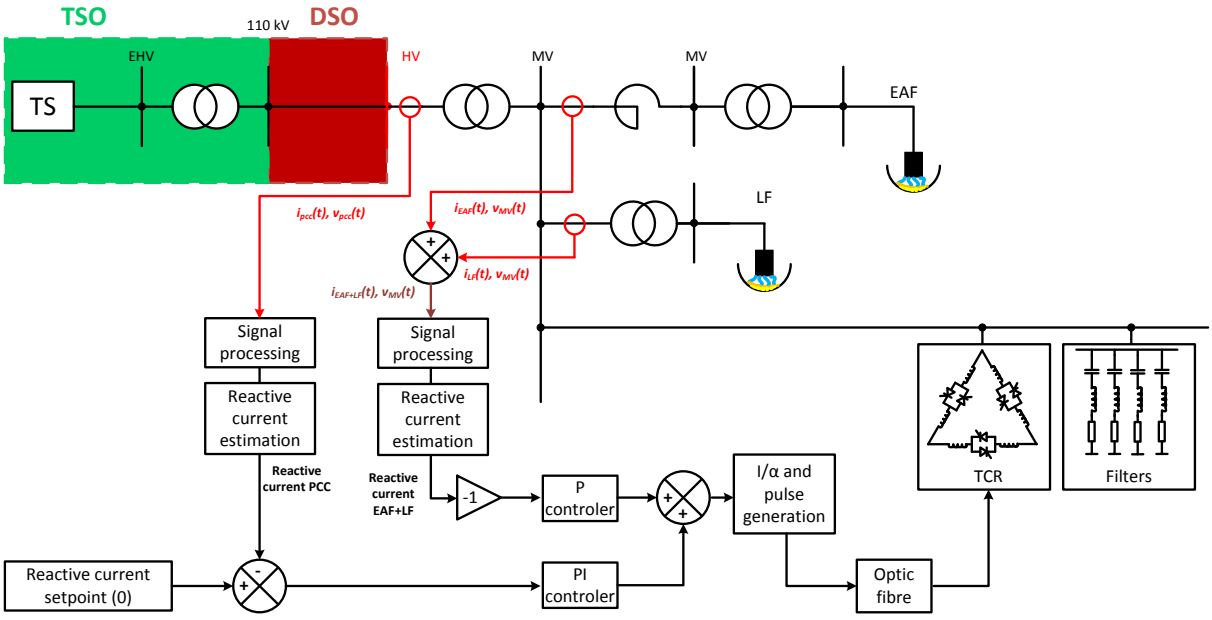


*Figure 6.6: Illustration of SVC control scheme in applications for industrial distribution systems with EAF and LF. [59]*

The open loop is adapted to fast events and its main functionalities are load balancing, response to rapid changes in reactive power, and mitigation of voltage fluctuations - flicker effect. The response of this loop varies between 10 and 30 ms, depending on the settings of the proportional controller and the parameters of the elements in the system. The input value of the control variable is the reactive current of the load (in our case the sum of the reactive current EAF and LF). The measurement of these quantities is carried out at the medium voltage level in order not to limit the dynamics due to the HV / MV transformer. Specific measured quantities are voltages and currents of supply sections EAF and LF in MV substation. The processing of the input signals is very important for the efficient function of this control loop, as these signals are considerably disturbed with respect to the measuring point.

The closed loop is adapted for precise control of reactive power consumption in PCC. The response of this loop varies between 150 and 300 ms, depending on the settings of the PI controller and the parameters of the system and system elements. The input value of the control variable is the reactive current in the PCC. The measurement is performed directly in the PCC, usually at the high voltage level. Here, too, the processing of input signals is an important part.

### 6.2.1 Reactive current estimation

For the SVC control system described above, it is necessary to know the reactive currents of the system equivalent to the triangular connection of the decompensation TCR converter. In the following text, we will show the derivation of two different methods.

The method is based on the derivation of reactive current from the instantaneous voltage and current values. The derivation of the method is based on the definition of the instantaneous reactive power for the $i^{th}$ phase according to (6.2) [59], [60].

$$Q_{\mathrm{i}}(t) = \frac{1}{2}\left[v_{\mathrm{i}}\left(t - \frac{T}{4}\right) i_{\mathrm{i}}(t) - v_{\mathrm{i}}(t) i_{\mathrm{i}}\left(t - \frac{T}{4}\right)\right] \tag{6.2}$$

*T* denotes the period, in this expression corresponds to an angle of 90°. To determine the reactive power waveform, it is also necessary to obtain the voltage and current signals shifted by a quarter of a period (90 °), which can be obtained by mathematically adjusting the voltage and current waveforms defined in (6.3) to (6.8).

$$v_{\mathrm{a}}(t) = V_{\mathrm{peak}} * \sin(\omega t) \tag{6.3}$$

$$v_{\mathrm{b}}(t) = V_{\mathrm{peak}} * \sin\left(\omega t - \frac{2}{3}\pi\right) \tag{6.4}$$

$$v_{\mathrm{c}}(t) = V_{\mathrm{peak}} * \sin\left(\omega t - \frac{4}{3}\pi\right) \tag{6.5}$$

$$i_{\mathrm{a}}(t) = I_{\mathrm{peak}} * \sin(\omega t - \varphi) \tag{6.6}$$

$$i_{\mathrm{b}}(t) = I_{\mathrm{peak}} * \sin\left(\omega t - \frac{2}{3}\pi - \varphi\right) \tag{6.7}$$

$$i_{\mathrm{c}}(t) = I_{\mathrm{peak}} * \sin\left(\omega t - \frac{3}{4}\pi - \varphi\right) \tag{6.8}$$

where $v_{\mathrm{a}}(t), v_{\mathrm{b}}(t), v_{\mathrm{c}}(t)$ are the phase voltages, $i_{\mathrm{a}}(t), i_{\mathrm{b}}(t), i_{\mathrm{c}}(t)$ are the phase currents, $V_{peak}$ is the phase voltage amplitude, $I_{peak}$ is the phase current amplitude, $\omega$ is the angular frequency equal to $2 * \pi * f$, and $\varphi$ is the phase shift between voltage and current. The derivation of the voltage and current waveforms with a phase shift of 90 ° will be shown on the waveforms (6.3) and (6.6). From the definition of the derivation of trigonometric functions holds and the properties of the cos function hold (6.9).

$$\frac{d\,\mathrm{A}.\sin(\omega t-\varphi)}{dt}=\omega A\cos(-\omega t+\varphi) \tag{6.9}$$

By applying (6.9), we obtained the waveform shifted by an angle ¾ π (270 °) with the gain ω compared to the original waveform $\mathrm{a(t)}=\mathrm{A}.\sin(\omega t-\varphi)$. The waveform with a phase shift of 90 ° from the a(t) is obtained according to (6.10).

$$a\left(t-\frac{T}{4}\right)=-\frac{1}{\omega}A\omega\cos(-\omega t+\varphi) \tag{6.10}$$

We apply the formula (6.10) to waveforms (6.3) and (6.6) to determine the phase-shifted voltage and current waveforms (6.11) and (6.12).

$$v_{\mathrm{a}}\left(t-\frac{T}{4}\right)=-V_{\mathrm{peak}}\cos(-\omega t) \tag{6.11}$$

$$i_{\mathrm{a}}\left(t-\frac{T}{4}\right)=-I_{\mathrm{peak}}\cos(-\omega t+\varphi) \tag{6.12}$$

We put the derived waveforms (6.11) and (6.12) into the relation for the reactive power function (6.2) and obtain the relation for phase “a” (6.13).

$$Q_{\mathrm{a}}(t)=\tfrac{1}{2}\left[-i_{\mathrm{a}}(t)V_{\mathrm{peak}}\cos(-\omega t)+v_{\mathrm{a}}(t)I_{\mathrm{peak}}\cos(-\omega t+\varphi)\right] \tag{6.13}$$

The relation (6.13) can be extended using the Werner formulas for trigonometric functions (6.14) to the form (6.15), which can then be simplified into the form (6.16).

$$\sin(\alpha)\cos(\beta)=\frac{1}{2}[\sin(\alpha-\beta)+\sin(\alpha+\beta)] \tag{6.14}$$

$$Q_{\mathrm{a}}(t)=\frac{1}{2}V_{\mathrm{peak}}I_{\mathrm{peak}}\left\{-\frac{1}{2}[\sin(-\varphi)+\sin(2\omega t-\varphi)]+\frac{1}{2}[\sin(\varphi)+\sin(2\omega t-\varphi)]\right\} \tag{6.15}$$

$$Q_{\mathrm{a}}(t)=\frac{1}{2}V_{\mathrm{peak}}I_{\mathrm{peak}}\sin(\varphi) \tag{6.16}$$

The magnitude of the reactive current component $i_{\mathrm{a\_re\_peak}}(t)$ can thus be expressed as follows (6.17), which, after modification, is valid for the other phases (b and c).

$$i_{\mathrm{a\_re\_peak}}(t)=2\frac{Q_{\mathrm{a}}(t)}{v_{\mathrm{a\_peak}}} \tag{6.17}$$

The reactive phase currents determined by the procedure described above need to be transformed into delta wiring for use in SVC applications. Using the Steinmetz principle, the resulting reactive currents in the delta circuit are defined according to (6.18),(6.19) and (6.20).

$$i_{\mathrm{ab\_re\_peak}}(t)=\frac{i_{\mathrm{a\_re\_peak}}(t)+i_{\mathrm{b\_re\_peak}}(t)-i_{\mathrm{c\_re\_peak}}(t)}{\sqrt{3}} \tag{6.18}$$

$$i_{\mathrm{bc\_re\_peak}}(t)=\frac{-i_{\mathrm{a\_re\_peak}}(t)+i_{\mathrm{b\_re\_peak}}(t)+i_{\mathrm{c\_re\_peak}}(t)}{\sqrt{3}} \tag{6.19}$$

$$i_{\mathrm{ca\_re\_peak}}(t)=\frac{i_{\mathrm{a\_re\_peak}}(t)-i_{\mathrm{b\_re\_peak}}(t)+i_{\mathrm{c\_re\_peak}}(t)}{\sqrt{3}} \tag{6.20}$$

## 6.3 Possibilities of improving the SVC control system in industrial distribution systems

Signal processing in the SVC controller has a significant effect on the effectiveness of limiting voltage fluctuations using SVC. Specifically, these are voltage and current input signals from which the actual value of the reactive current is determined, as described above. The most commonly used technique is the low pass filter. This work is focused on the possibility of using other techniques of input signal processing to achieve a more effective reduction of voltage fluctuations - the flicker effect using SVC. Figure 6.7 highlights the blocks affected by the enhancements. This work is focused on the use of the following techniques:

- Low pass filter
- Second Order Generalized Integrator (SOGI)
- Flicker filter (FF)

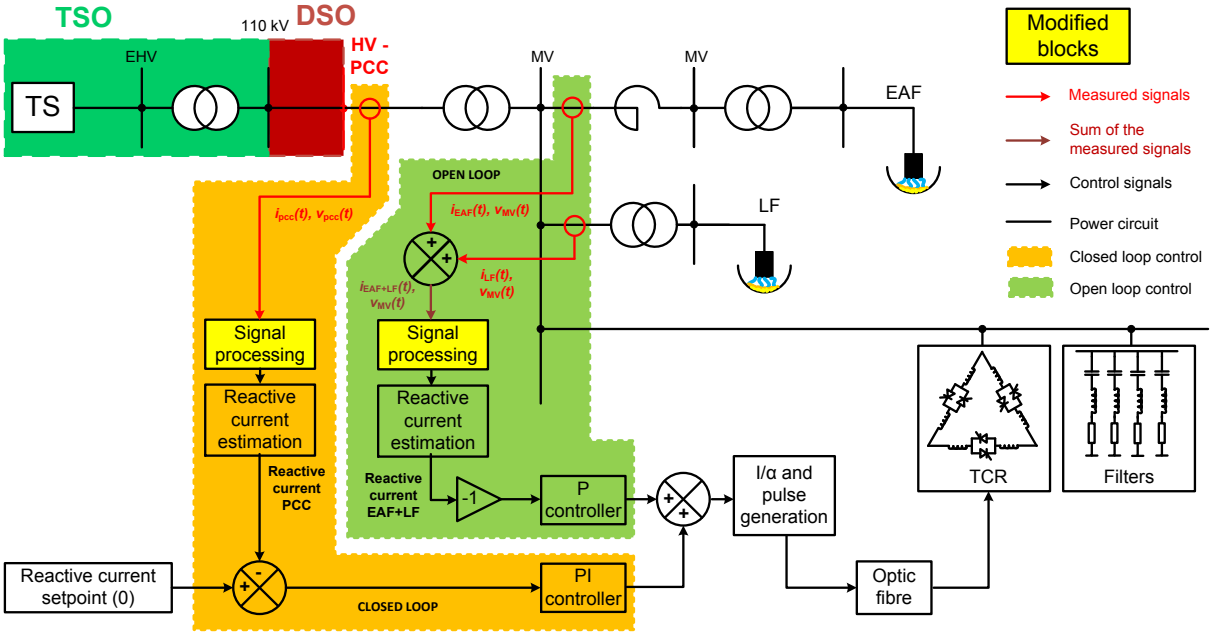


*Figure 6.7: Adjusted SVC control scheme illustration in applications for industrial distribution system with EAF and LF based on [59].*

The signal processing of input signals and voltages has a fundamental influence on the function of the SVC controller from the point of view of flicker effect mitigation. In terms of voltage fluctuations – the flicker effect, based on [61], the frequency band up to 35 Hz is significant. The standard [61] defines the weighing function of a standardized flicker meter according to (6.21).

$$F(s) = \frac{k\omega_1 s}{s^2 + 2\lambda s + \omega_1^2} * \frac{1 + \frac{s}{\omega_2}}{\left(1 + \frac{s}{\omega_3}\right)\left(1 + \frac{s}{\omega_4}\right)} \tag{6.21}$$

where $k$, $\lambda$, $\omega_1$, $\omega_2$, $\omega_3$, $\omega_4$ are constants defined in [61]. These constants differ according to the electrical system (230 V 50 Hz or 120 V 60 Hz). Figure 6.8 shows the frequency amplitude characteristic of the transmission function of the weighting function of the flicker meter, which indicates the frequency band significant in terms of the flicker effect. Significant is the signal processing of the inputs for the weighing function - low pass and high pass filter, which define the frequency band from 0.05 to 35 Hz, also illustrated in Figure 6.8.

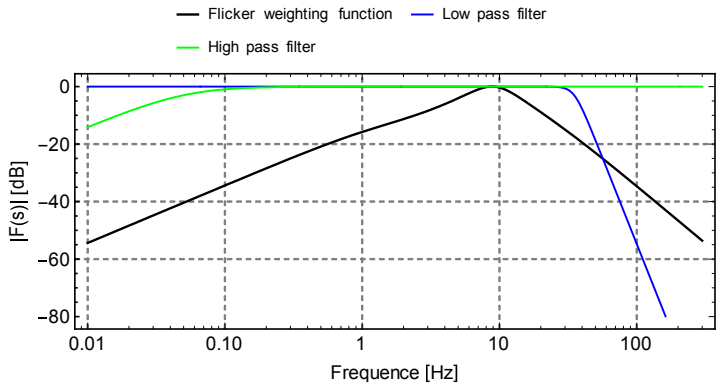


*Figure 6.8: Standardized flicker meter weighting function and pre-filtering using low pass and high pass filters.*

Signal processing based on the use of low pass filters (LPF) is used as a standard for compensation devices. The LPF is used in the synchronous reference frame area, whereby the fundamental harmonic frequency signal is not affected by the LPF because it behaves as a direct current. In our work, we used this and this technique (conventional) for comparison with other techniques. We considered a first-order low pass filter defined by the transfer function according to (6.22).

$$G(s) = \frac{\omega_c}{s + \omega_c} \tag{6.22}$$

### 6.3.1 Improvements using the SOGI technique

A proposed option for improving the SVC control feature is to use the Second Order Generalized Integrator (SOGI) technique in a bandpass configuration. Compared to the conventional use of LPF, SOGI provides advantageous properties in terms of amplitude and phase characteristics, which will be emphasized below. The basic block diagram of SOGI is illustrated in Figure 6.9 [62].

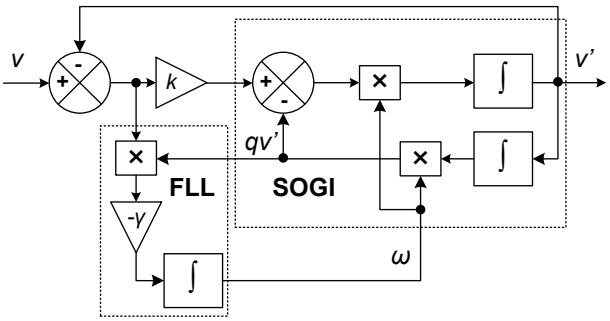


*Figure 6.9: Block diagram of the used SOGI-QSG (SOGI-Quadrature Signal Generator) based FLL [62].*

According to the block diagram in Figure 6.9 $v$ represents the input signal, $k$ represents the damping factor (usually using the value $k = \sqrt{2}$ [62]), $\omega$ represents the resonant frequency (fundamental mains frequency), $v'$ represents the output signal and $qv'$ represents the output signal shifted by 90°. This variant is called SOGI-QSG (Second Order Generalized Integrator - Quadrature Signal Generator). The SOGI-QSG transfer functions are defined according to (6.23) for the output signal $v'$ and according to (6.24) for the shifted signal $qv'$.

$$D(s) = \frac{v'(s)}{v(s)} = \frac{k\omega s}{s^2 + k\omega s + \omega^2} \tag{6.23}$$

$$Q(s) = \frac{qv'(s)}{v(s)} = \frac{k\omega^2}{s^2 + k\omega s + \omega^2} \tag{6.24}$$

The external parameter $\omega$ is a resonant angular frequency provided by the FLL. The integrator with a negative gain $-\gamma$ is used to adapt the SOGI resonant frequency $\omega$ to the grid frequency $\omega_{grid}$. In three-phase systems, two SOGI-QSGs can be used for two orthogonal components of the input voltage vector (in the $\alpha\beta$ reference frame) separately. Using such a DSOGI-FLL the input voltage vector v can be separated into the positive and negative sequence components. The gain $\gamma = 0.16$ guarantees the time constant of the FLL about 13 ms [63], so a fluctuation in $\omega$ would not affect the correct function of the SOGI-QSG. Moreover, the mentioned gain will provide reasonable dynamics in the grid frequency estimation.

### 6.3.2 Improvements using the flicker filter technique

Another way to improve the properties of the SVC controller to reduce the flicker effect is to use the transfer function (6.21) that detects the flicker effect as defined by the flicker meter standard [61]. However, this type of filter substantially attenuates the fundamental frequency signal, leading to imperfect correction of the power factor. For this reason, this type of signal processing can be used only for open loop (diagram in Figure 6.7), which dynamically responds to changes in power consumption, which mainly contribute to the flicker effect. Precise power factor control in the PCC is ensured by a closed loop, where another signal processing technique must be used.

### 6.3.3 Comparison of the proposed improvements with the conventional solution

The different properties of the considered signal processing techniques are visible in the amplitude and phase characteristics of the individual functional blocks. Figure 6.10 shows a comparison of the amplitude characteristics and a comparison of phase characteristics for LPF, SOGI-QSG, and flicker weighting function.

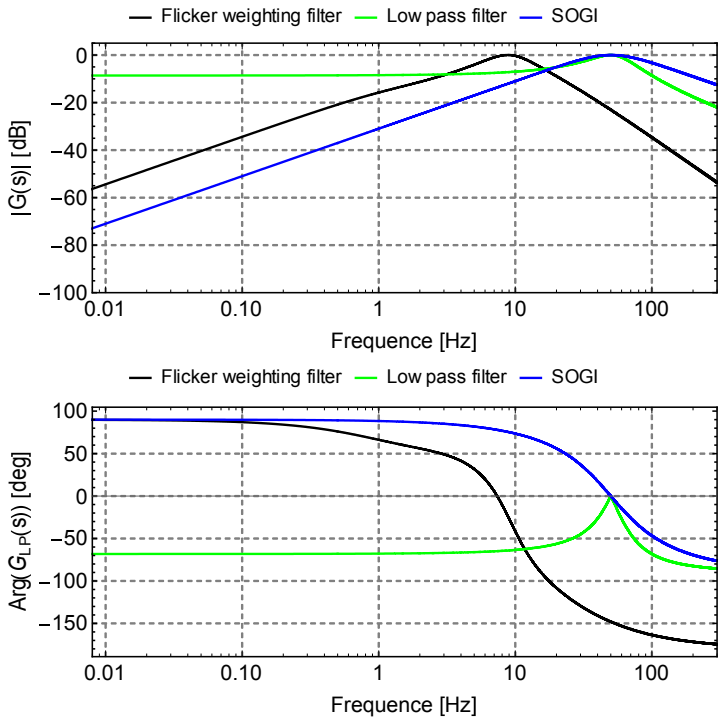


*Figure 6.10: Frequency amplitude and phase characteristics of the used signal processing techniques.*

As mentioned previously, the flicker weighting filter based on the characteristic in Figure 6.10 attenuates the fundamental harmonic frequency, which is a disadvantageous property in terms of power factor correction. The LPF and DOGI-QSG techniques transmit the fundamental harmonic signal without change, but for frequencies significant in terms of the flicker effect, these techniques cause some attenuation for lower frequencies. In the case of LPF, this attenuation is not so significant.

From the point of view of phase characteristics, the disadvantageous property of LPF is manifested, which consists of a considerable difference of the phase shift from the phase shift in the case of the flicker weighting function, which predetermines the size of the flicker effect. A more favorable situation is in the case of SOGI-QSG, where the transfer function (6.23) is analyzed, which was further used in the work.

# 7 Case study of an industrial power system in a problematic area

The aim of the case study is to point out the possibilities of the flicker effect mitigation in an industrial distribution system with EAF. In this case study, a clearly observable gradual reduction of the flicker effect following the measures taken will be demonstrated.

## 7.1 Problematic area description

The industrial area in the selected area is a long-term producer of steel products. The gradual development of this company has led and continues to improve the technological level of the production process in order to maintain competitiveness and emphasis on quality products with higher added value. From the point of view of this work, it is important to focus on the development in the last 30 years from more than 180 years of history. A significant technological breakthrough was the commissioning of a UHP (Ultra High Power) EAF type with a capacity of 60 tons and LF with a capacity of 60 tons, which replaced older EAFs and Siemens-Martin furnaces. This step closed the company's production cycle. The furnace transformer of the UHP furnace has a rated power of 50 MVA and the furnace transformer of the ladle furnace has a rated power of 12 MVA. The stated values indicate considerable demands on the power supply system, which was implemented through the defined 110 kV distribution system lines. At the time of commissioning, the nodal area of the distribution system was supplied from the node of the transmission system with a nominal voltage of 220 kV. Then the power supply system was characterized by unfavorable short-circuit conditions for the operation of such a demanding technology. For this reason, at the same time as the new EAF, the dynamic reactive power compensation SVC was built, with a nominal compensation power of 90 MVAr, equipped with $2^{nd}$ , $3^{rd}$ , $4^{th}$ and $5^{th}$ harmonic filters.

## 7.2 Measures and their benefits

Since the commissioning of the above-mentioned devices, the gradual introduction of various measures and new technologies has been ongoing both in terms of productivity and efficiency of the devices on the one hand and in terms of adverse effects on the supply network. In terms of adverse effects on the supply network, measures leading to improvement can be divided into categories, according to the entity that participates in the measure to the greatest extent as follows:

- Measures on the side of the steelworks operator
- Measures on the side of the transmission system
- Measures on the side of the distribution system

Partial measures on the part of individual entities will be elaborated in the following sections.

### 7.2.1 Measures on the part of the steelworks operator

There is a considerable number of measures on the side of the steelworks operator with a high potential to reduce the disturbing effects of the EAF. In the case of the problematic area described in sub-chapter 7.1, together with the construction of the steelwork's metallurgical technology, the construction of the electrical part of the technology, including 90 MVAr compensation, also took place. At the time of implementation, it was a unique solution, given that in that period the most frequently used static filter-compensation stations were without the function of continuous and dynamic regulation. The implementation of continuously dynamic controllable SVC compensation enabled the operation of modern UHP EAF technology even in conditions with low short-circuit power. Despite the

use of SVC, the issue of the flicker effect in this area has been an important topic. A possible improvement could have occurred if the production process had been improved.

Since the commissioning of the steelworks equipment, various improvements to the production process have taken place today, with the following goals:

- Improving the economic efficiency of production (lower specific electricity consumption, lower consumption of graphite electrodes, lower maintenance costs, etc.)
- Increasing equipment productivity (production intensification)
- Improving product quality
- Other factors (these include the degree of distortion effect on the distribution system - flicker effect)

All these goals are interlinked. The following text will aim to briefly present the implemented measures and their effect.

In order to ensure the production process using EAF in terms of disturbance, in terms of wear of the furnace components and electrode consumption, the quality and character of the input material are of great importance. There has been a gradual improvement in this area. In the beginning, many problems caused by inhomogeneous input material (steel scrap of various sizes, roughness, and homogeneity) were stored in open spaces. Residues of water, snow, and ice in the input material contributed to the formation of undesirable dynamic phenomena during melting when there was contact with molten metal. The induced sharp dynamic phenomena caused undesired sharp scrap slides of material inside the batch, which resulted in frequent short circuits or interruptions of the arcs. These operating conditions have led to increased wear of the furnace bottom and furnace linings, increased consumption of graphite electrodes, increased consumption of specific energy (kWh/t), and worsening of disturbing effects on the distribution system - especially the degree of flicker perception - flicker effect. To avoid the described problems, the storage spaces for input materials were gradually roofed, thus preventing the access of water. Another measure was the creation of a system for the use of homogenized input material. The result of this process is an input material that is sorted by character, large and inhomogeneous pieces of steel scrap no longer occur because a significant amount of scrap comes from the shredder lines, which produce a homogeneous material at the output. These measures have successfully avoided the problems described.

Another technological part, which plays an important role, is the electrode positioning system control. The position of the individual electrodes affects the lengths of the electric arcs, which are one of the parameters defining the impedance of the electric arcs. Through this system, the electrical power of the furnace is directly controlled. This system has to deal with many types of dynamic processes (landslide of materials, short circuits, interruption of arcs, action of electric forces, etc.). During the operation of the technology, it turned out that even with this system there is great potential for improvement. The electrode positioning control system has been modernized to a system based on a hydraulic actuator, which achieves good dynamic properties and, in the case of short-circuit operation, can quickly reduce this undesirable condition using the electrode fast-lift function. However, the most important role is played by the controller itself, which uses the fuzzy-regulation technique after the last modernization. This controller is fully integrated into the control system of the steel production process. This system monitors the amount of energy required for the production process based on the requirements for product quality and the composition of the input material. The electrode positioning system together with the control system brought both an improvement of the steel production process in the EAF both in terms of energy costs and wear of the furnace components, as well as a further reduction of disturbing effects on the distribution system.

Another breakthrough technology that has been implemented is the technology of oxygen and natural gas burners. From the point of view of the field of metallurgy, this technology is important solely to increase productivity - the supplied additional chemical energy shortens the melting time (tap to tap time). It is thus possible to reduce equipment wear, electricity consumption, and electrode consumption. In terms of the power quality, this technology is important in terms of shortening the melting time - especially shortening the initial phase of melting (mainly natural gas burners are used), which is the most critical in terms of disturbance. After overcoming the initial melting phase, oxygen burners are used to a greater extent. Another supporting technology is a system for creating foaming slag using additives. In addition, the foamed slag ensures a smooth burning of electric arcs because the arcs themselves are shrouded in foamed slag.

The implementation of the described technologies to a large extent brought a streamlining of the production process and also alleviation of the power quality issues.

### 7.2.2 Influence of the transmission system

The nature of the transmission system, which supplies the distribution system containing a part of the supplying industrial area, is also of great importance in terms of the power quality. As already demonstrated in Chapter 4, the impact short-circuit power in the PCC has a significant effect, the value of which is fundamentally influenced by the character of the node of the transmission system that supplies the given distribution area. Depending on the configuration and parameters of the transmission system node, the priority is to isolate problematic consumption (industrial areas) from other customers in the given distribution area as much as possible. In the studied problematic area - industrial distribution system with UHP EAF, there were gradually changes in this direction.

At the time of the commissioning of the UHP EAF, the node of the transmission system in the given area was connected to a 220 kV system. This set was to a large extent the problem of low short-circuit power, which could be provided at the PCC point. The result was a significant propagation of disturbances - especially the flicker effect. Despite the use of SVC compensation equipment within the steelworks, the level of the flicker effect was high.

With the coming development of the transmission system in the area, the given node of the transmission system was rebuilt into a 400 kV system. The project included the construction of a new 400 kV line and a 400 kV substation (transmission system node), which is equipped with two 400 kV/110 kV transformers, each with a rated power of 350 MVA. The project was put into proper operation in 2014, which was preceded by a trial operation.

The implementation of the mentioned project brought a significant improvement of short-circuit conditions (an increase of short-circuit power) in the given node, but also in PCC, which significantly reduced the level of flicker effect. Since the commissioning of the UHP EAF, measurements have been carried out regularly, with the participation of the Department of Electric Power Engineering, FEE CTU, the steelworks operator, the transmission system operator, and the distribution system operator to monitor developments. A summary of the results of these measurements is given in Table 7.1.

| **Location of measurements** | Distribution system supplied by 220 kV transmission system | Distribution system supplied by 220 kV transmission system + SVC | Distribution system supplied by 400 kV transmission system + SVC |
|---|---|---|---|
| Nodal substation of distribution system (110 kV) | 7,4-7,5 | 4,2-4,3 | 1,15-2,1 |
| PCC (110 kV) – Input substation of the steelworks | 11,1-11,5 | 6,3-6,5 | 1,87-4,33 |

*Table 7.1: An overview of the long-term perception of the flicker effect - Plt depending on the TS and the use of SVC.*

Table 7.1 shows the development of measured values of the long-term perception of the flicker effect ($P_{lt}$) in the supply node of the transmission system (in the distribution system substation on the 110 kV side) and the PCC (connection of the steel plant or section of the EAF and LF to the 110 kV distribution system). According to the results, the use of SVC reactive power compensation brings a significant improvement. Reconstruction of the transmission system node to a 400 kV system brings even more significant improvements (assuming the use of SVC). The values of the $P_{lt}$ in the PCC vary in a relatively wide interval, which is due to the configuration of operated transformers in the TS/DS substation (one or two transformers in operation) and the configuration of the HV distribution system. The following section "Influence of the distribution system" deals with this issue in more detail.

### 7.2.3 Influence of the distribution system

The influence of the distribution system on the power quality issues in connection with the EAF is also of great importance. In the following text, it will be linked to the previous section 7.2.2 "Influence of the transmission system". The conversion of the transmission system node to a 400 kV system brought new challenges. The new configuration has created a natural need to explore new system operation options in the area. The first question was the influence of the configuration of the transformation between the transmission and distribution system. Here are 3 technically possible configurations:

- Operation of 1 350 MVA transformer
- Operation of 2 350 MVA transformers in parallel
- Operation of 2 350 MVA transformers separately

The second issue was the configuration (utilization of HV lines) of the HV distribution system. In the area, it was possible to use various configurations of 4 overhead HV lines for supplying the steelworks. The requirements for the magnitude of the voltage in the distribution system proved to be a significant limiting factor. The distribution system operator prefers the operating voltage in the substation at the node of transformation from the transmission system at the level of 120 kV to minimize losses in the distribution system. On the other hand, there is a restrictive condition on the part of the steelworks operator that the voltage of the sections supplying the sections (at point PCC) of the electric arc furnace and ladle furnace must not exceed 119 kV. Taking into account the no-load operating state, the Ferranti phenomenon, and transients, this means in practice limiting the voltage in the distribution system to 117 kV. To explore possible configurations, six variants were compiled, which are illustrated in Figure 7.1.

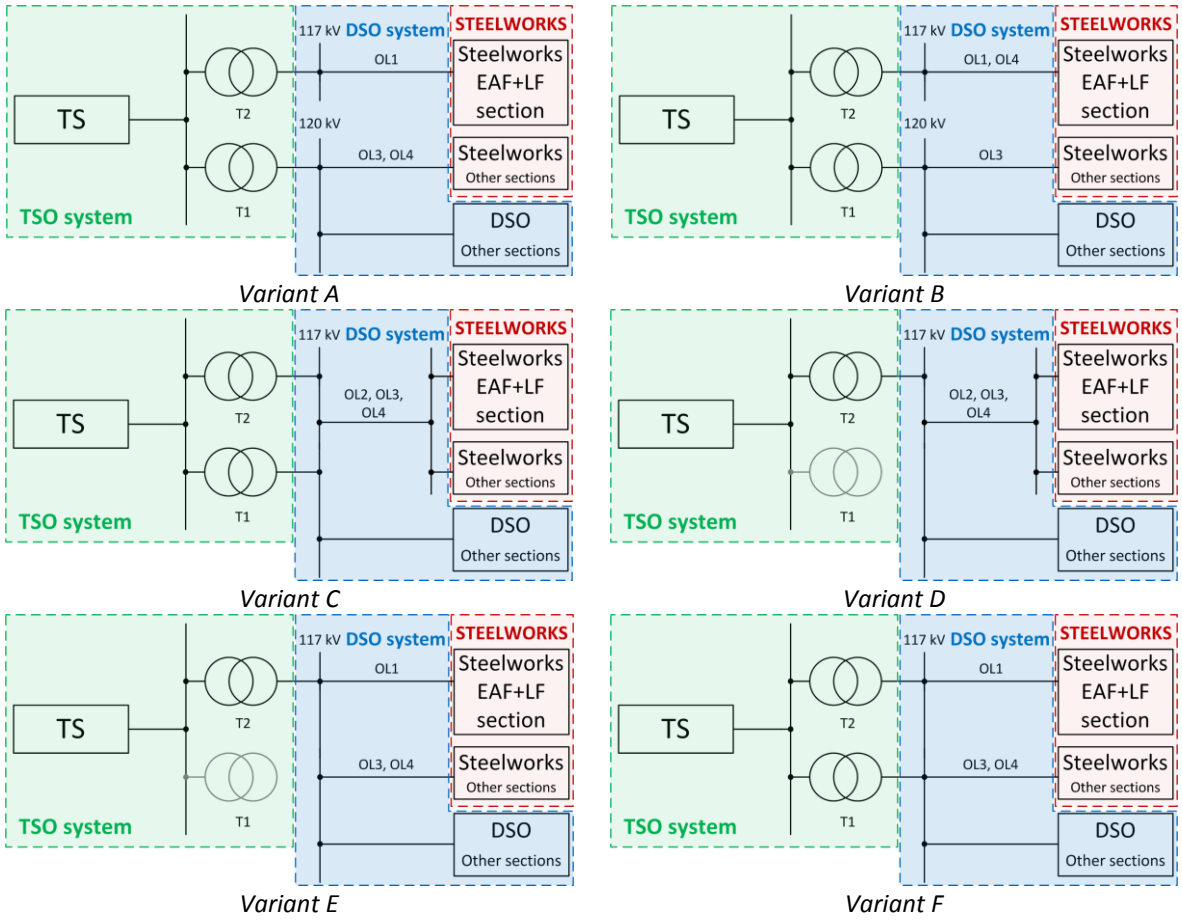


*Figure 7.1: Possible configurations of the distribution system for the steelworks supplying.*

**Variant A** considers the operation of both 400/110 kV transformers in separate operation. For the section of the EAF and LF, the supply of a separate line V1 is considered, with the proviso that the voltage on the secondary side of the 400/110 kV transformer would be limited to 117 kV. The second transformer supplies the remaining part of the HV distribution system as well as other sections of the steelworks, with the voltage on its secondary side being regulated to 120 kV. The advantage of this variant is that the problematic part of the steel plant's consumption is largely isolated from other customers connected to the given distribution area, as well as meeting the conditions for the size of the supply voltage.

**Variant B** is almost identical to variant A, it differs in that two lines V2 and V4 are used to supply the section of the EAF and FL. In addition, this variant is more advantageous in terms of short-circuit power at the PCC point, which is higher compared to variant A due to the use of two lines.

**Variant C** considers the operation of both 400/110 kV transformers in parallel operation. The EAF and LF section, together with the other sections of the steelworks, would be supplied using lines V1, V3 and V4. This variant appears to be advantageous in terms of achieving high short-circuit power in the PCC. The disadvantages of this variant include the reduced operating voltage of 117 kV for the entire HV distribution system in the node area and the fact that the problematic consumption (EAF and LF section) is not separated from each other to the same extent as in variants A and B.

**Variant D** is almost identical to variant C, it differs in that it considers the operation of only one 400/110 kV transformer. This variant is manifested by reduced short-circuit shock power in PCC. Other disadvantages of this variant are the same as for variant C.

**Variant E** considers the operation of one 400/110 kV transformer. The power supply of the EAF and LF section is considered with the use of the V1 line, the power supply of the other sections of the steelworks is considered with the use of the V3 and V4 lines. This variant is manifested by a reduced short-circuit power in the PCC compared to variant D. Other disadvantages of this variant are the same as in variant C.

**Variant F** considers the operation of both 400/110 kV transformers in parallel operation. The line configuration is the same as in the case of variant E. Compared to variant E, this variant is advantageous in increasing the short-circuit power in PCC due to the use of both 400/110 kV transformers. Other disadvantages of this variant are the same as in variant C.

The design of the described variants involved: the transmission system operator, the distribution system operator, the steelworks operator, and the Department of Electric Power Engineering, FEE CTU. Within this cooperation, the following goals were set:

- Verification of the feasibility of measurement - whether the operating modes of the transmission system, distribution system and steelworks allow testing of the specified variants. The inspection was focused on the possibilities of manipulation and possible necessary changes in the setting of the electrical protection system.
- Design of the measurement schedule - the measurement was planned for June 2014 and at the same time, the order of testing of individual variants was designed to minimize the number of complex manipulations.
- Choice of measurements locations - was determined so that it is possible to assess all the effects of individual variants (how other customers connected to the distribution system are affected, how the variants affect disturbance in PCC, in the internal HV distribution of the steelworks, and the HV distribution system on-site in connection with the transmission system).
- Ensuring the operating conditions of the steelworks so that the results are comparable - so that 6 melt cycles (3 times charging scrap during a cycle) in a row take place in 6 hours, with the recording being even longer to reduce the long-term flicker effect affected by the previous variant. This task was complicated due to the fact that the steelworks may have various technological breaks (change of the continuous casting production format, replacement of worn components, etc.).
- Evaluation of results and comparison of individual variants.

The fulfillment of the set goals was preceded by careful preparation, which was a prerequisite for the successful course of this exercise. The processed measurement results give a clear picture of the applicability of individual variants. To understand the differences of individual variants, the outputs from three measuring locations are presented here: PPC - supply section of EAF and LF at HV level, busbar of HV distribution system in place in connection with transmission system (in case of parallel operation of 400/110 kV transformers it is a busbar, which is supplied by the section of the EAF and LF) and in the low voltage distribution system, which represents the other customers of the distribution system in the specified node area.

To search for logical connections in the results, it is relevant to start not only the topology of individual variants but also the short-circuit conditions at the PCC point. For this purpose, the values were supplied by the distribution system operator and at the same time, the calculated values were obtained based on measurements during the experiments. The values are summarized in Table 7.2.

| Variant | Value calculated based on measurements $S_{ks}$ [MVA] | Value calculated based on measurements $I_k$“ [kA] | Value provided by DSO $I_k$“ [kA] |
|---|---|---|---|
| A | 1500 | 7,37 | 7,1 |
| B | 1150 | 5,65 | Not available |
| C | 2800 | 13,76 | 13,3 |
| D | 2200 | 10,81 | 10,7 |
| E | 1700 | 8,35 | 7,1 |
| F | 2100 | 10,32 | 8,6 |

*Table 7.2:* Comparison of short-circuit ratios in PCC for individual variants.

The measurement outputs are visualized in two ways. The first way of visualization is the course of the long-term perception of the flicker effect $P_{lt}$. The second way of visualization is the outputs of the statistical evaluation of the course of the long-term perception of the flicker effect using the 95% percentile.

The results for measurements in PCC are illustrated in Figures 7.2 and 7.3.

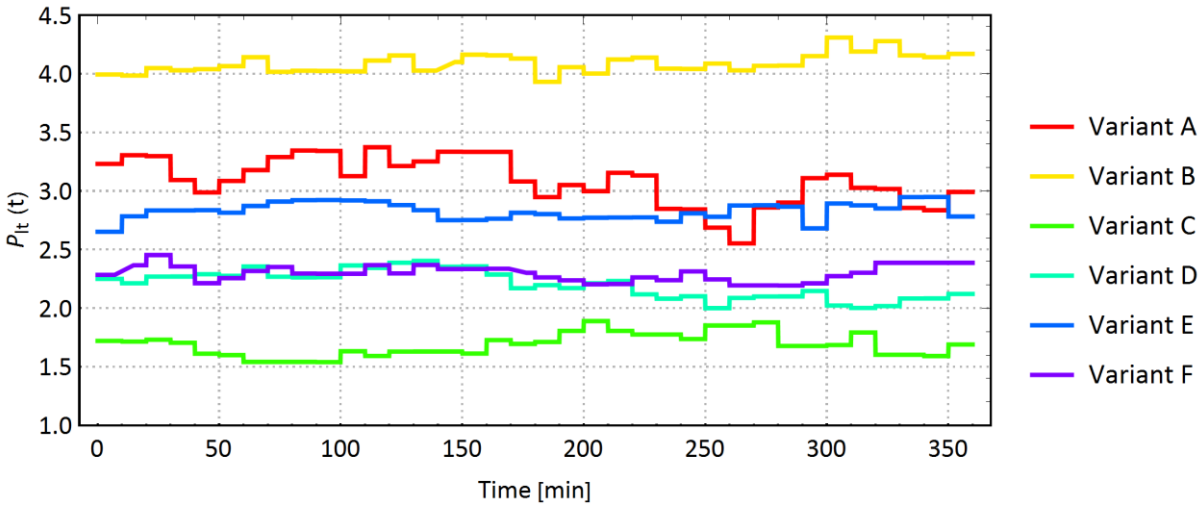


*Figure 7.2: Courses of the $P_{lt}$ for individual variants based on measurements in PCC.*

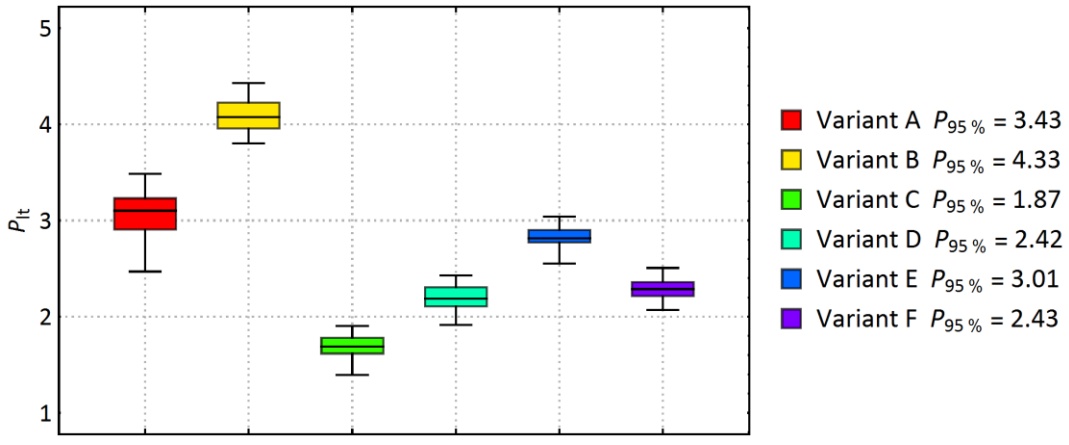


*Figure 7.3: Statistical evaluation of the course of the $P_{lt}$ for individual variants based on measurements in PCC.*

The results correspond to the assumption that the $P_{lt}$ in PCC depends (hyperbolic function) exclusively on the magnitude of the short-circuit power in PCC. This dependence is demonstrated in Figure 7.4. It can also be seen from the figure that by gradually increasing the short-circuit power, the effect of this measure is smaller and smaller.

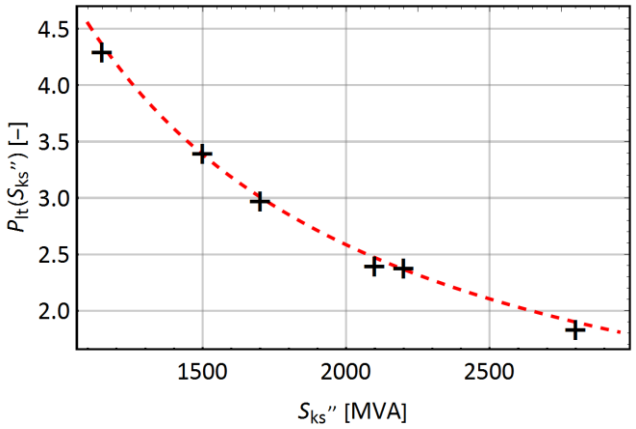


*Figure 7.4: Dependence of the $P_{lt}$ in PCC on the short-circuit power in PCC.*

The results for measurements on the busbar of the HV distribution system substation at the point of its connection with the transmission system (in the case of parallel operation of 400/110 kV transformers it is a busbar from which the electric arc furnace and ladle furnace section is fed) are illustrated in Figures 7.5 and 7.6.

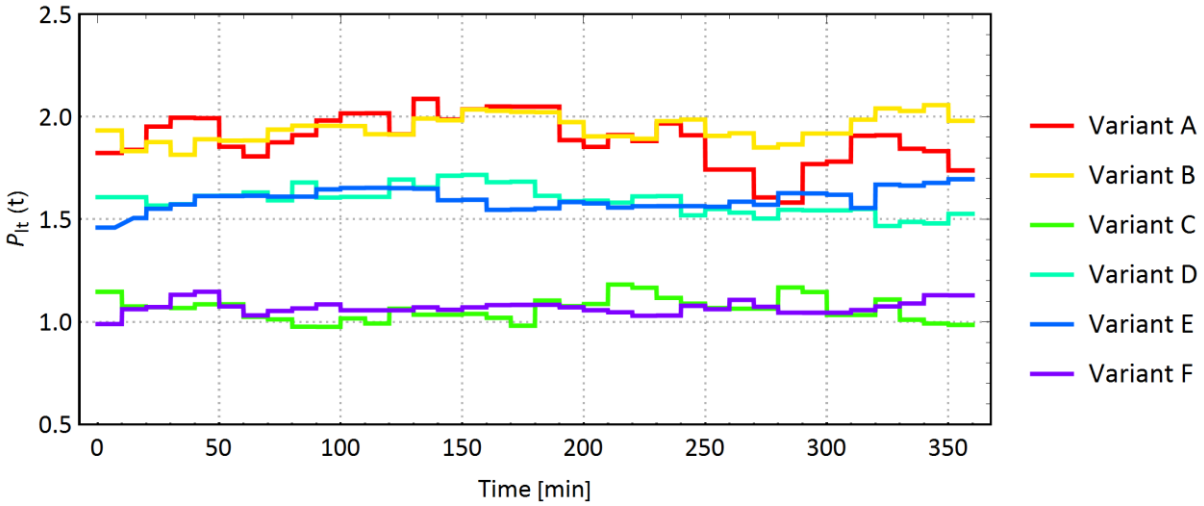


*Figure 7.5: Courses of the $P_{lt}$ for individual variants based on measurements in the substation of the DSO.*

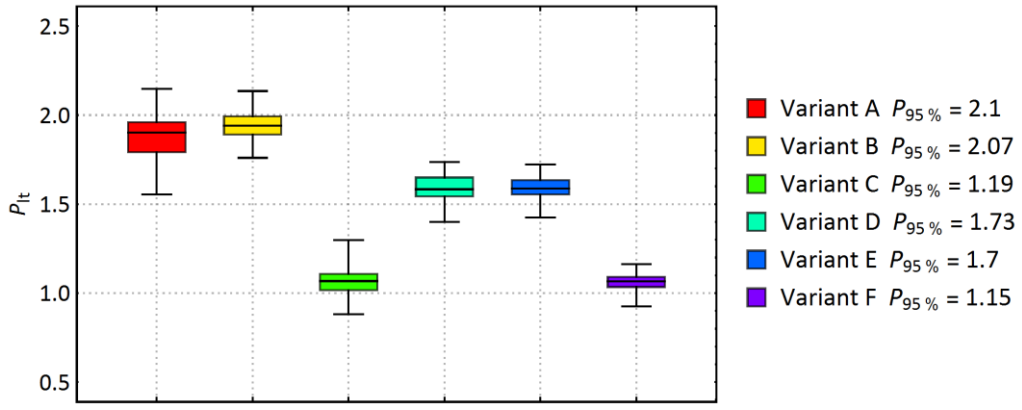


*Figure 7.6: Statistical evaluation of the course of the $P_{lt}$ for individual variants based on measurements in the substation of DSO.*

Even in the case of the results illustrated in Figures 7.5 and 7.6, it would be possible to demonstrate a similar dependence as in the case of Figure 7.4, however, short-circuit conditions were not analyzed for this measuring location.

The results for measurements in a low voltage distribution system that represents other customers of the distribution system in the node area are illustrated in Figures 7.7 and 7.8.

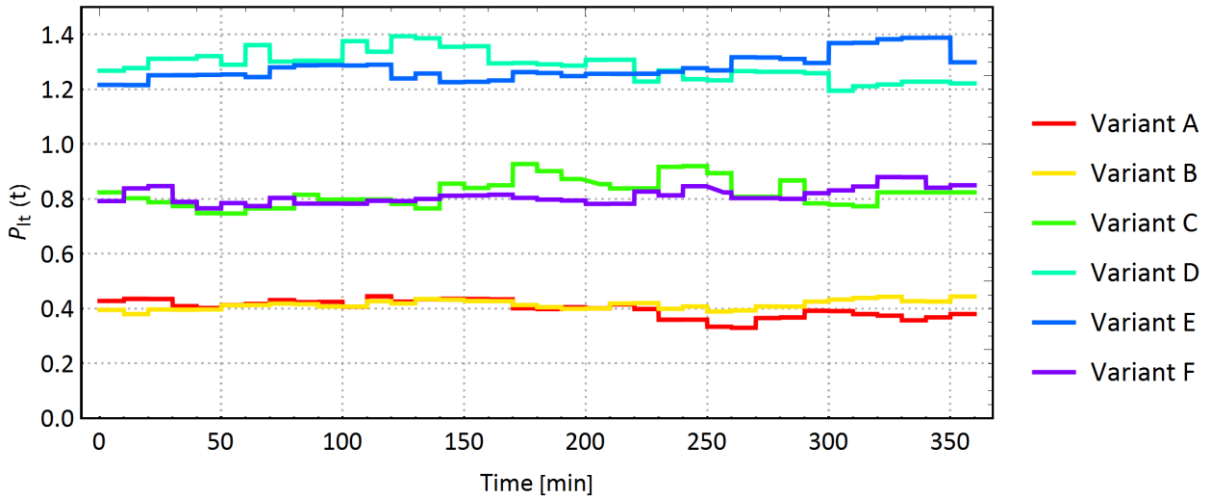


*Figure 7.7: Courses of the $P_{lt}$ for individual variants based on measurements in LV distribution system.*

For this measurement, it is necessary to emphasize that the configuration of the HV distribution system and the fact whether only one 400/110 kV transformer or both are operated in parallel or separately is of great importance.

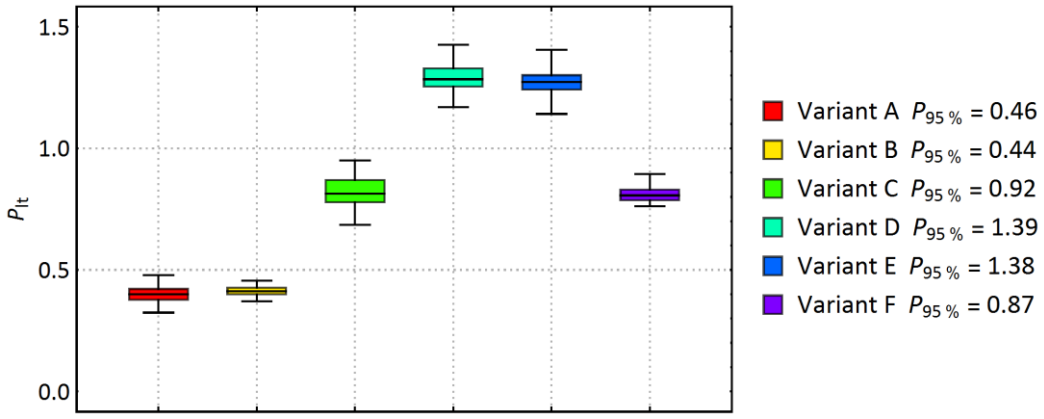


*Figure 7.8: Statistical evaluation of the course of the $P_{lt}$ for individual variants based on measurements in LV distribution system.*

The results presented in Figures 7.7 and 7.8 clearly show that the isolation of problematic consumption (supplying section of the EAF and LF) has a very positive effect on the disturbance levels of other customers in the distribution system. Another crucial factor is the operation of transformers in the 400/110 kV transmission system. From the point of view of the propagation of the flicker effect in the distribution system, it is advantageous to use both transformers at the same time. In this case, in the case of experiments, it was shown that the value of $P_{lt}$ in other parts of the distribution system in the node is less than 1. Here it is necessary to point out that the values obtained by measurements in the LV distribution system may be burdened by other sources of interference.

Based on the results and other indicators, the individual variants were compared. The evaluation was based on:

- Losses in the transmission system - given by the operation of 1 or 2 of the 400/110 kV transformers
- Losses in the distribution system - limitation of the operating voltage of the HV system to 117 kV
- Disturbance from other customers in the node area

The results of the comparison are summarized in Table 7.3. Therefore, variants A and B can be primarily recommended as the most promising variants of operation of the given area. Variants D and E, on the other hand, cannot be recommended.

| **Evaluation criteria** | Variant A | Variant B | Variant C | Variant D | Variant E | Variant F |
|---|---|---|---|---|---|---|
| Losses in the transmission system | - | - | - | + | + | - |
| Losses in the distribution system | + | + | - | - | - | - |
| Disturbation from other customers in the node area | + | + | + | - | - | + |
| **Final evaluation** | **+** | **+** | **0** | **-** | **-** | **0** |

*Table 7.3: Comparison of individual variants.*

## 7.3 Other potential measures

There are no longer many opportunities in the area to improve the power quality. On the part of the transmission and distribution system operator and the steelworks operator, all technically feasible measures leading to the improvement of the power quality were implemented.

The potential for further possible improvement can be found in compensation devices. With the current SVC compensation, there is the potential to use improved control methods to achieve a greater reduction factor of the flicker effect. Theoretically, the previous chapter 6 deals with these possibilities, and the following chapters 8 and 9 focus on estimating the real potential of the proposed improvements.

Another theoretical possibility is the use of STATCOM technology. However, this possibility is difficult to grasp from the point of view of the steelworks operator. The implementation of this technology would require high investment costs, which would not be offset by savings on the part of the production process. STATCOM technology would not increase productivity, efficiency, or other savings in the steelmaking process in an EAF (based on the existence of current SVC equipment). Some potential can be found in the variant considering the combination of the existing SVC technology with the STATCOM technology of low rated power (achievement of acceptable investment costs), which would have control algorithms designed exclusively to reduce the flicker effect.

# 8 Developed and tested strategies of FACTS utilization in the problematic area

## 8.1 Methodology for testing the FACTS performance

There are several options for testing the proposed improvements. The most commonly used simulations are based on mathematical models of nonlinear loads. The disadvantage of this approach is the considerable complexity of the whole modeled system and also the difficult simulation of the behavior of the EAF, as a nonlinear load, which this work focuses on.

A number of case studies using a mathematical model of an electric arc have been carried out in the field [64], [65], but it should be noted that these models do not capture the stochastic behavior of an electric arc furnace sufficiently. For this reason, the approach of design and creation of laboratory hardware model SVC and inverter simulating the real behavior of an EAF was chosen in this work on the basis of input reference data measured during real operation.

### 8.1.1 Description of measurements and overview of data files

Therefore, data measured from the joint operation of 60 t EAF (50 MVA furnace transformer) and 60 t LF (12 MVA furnace transformer) were used for testing purposes. Power quality analyzers were used for the measurements, which enabled the recording of voltage and current quantities in an aggregated sampling interval of 200 ms (possible recording length in the order of days) and in the transient mode with a sampling frequency of 9600 Hz (one recording of 64 seconds, started using trigger). Figure 8.1 illustrates the installation of measuring instruments in the substation of the steelworks.

*Figure 8.1: Power quality analyzers (ELCOM PNA560 and PNA571) installed in the HV substation of the steelworks.*

For experimental purposes, datasets were selected from practical measurements from EAF operation. In addition to changing the scale of quantities, 60-second measurement sections from various stages of the steel production process in EAF were always used. Figure 8.2 shows the apparent power of one EAF production cycle, indicating the datasets used in the experiments. Datasets A, B, D and F represent the typical behavior of EAF in the meltdown phase, where large dynamic changes occur. Datasets C, E, G and H represent the typical behavior of EAF in the quieter refining phase of the production process.

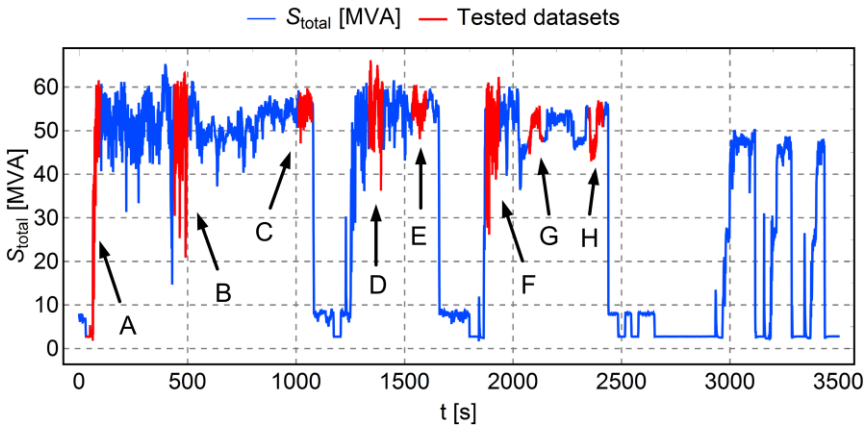


*Figure 8.2:. Apparent power of one EAF + LF production cycle with indicated testing datasets.*

### 8.1.2 Laboratory equipment

A laboratory physical model was designed and built for testing the improved SVC control system. A simplified diagram of the proposed model is illustrated in Figure 8.3. An ideal 3-phase AC programmable voltage source Chroma 1704 with a nominal frequency of 50 Hz and a nominal phase voltage of 25 V. To simulate the real behavior of the network, inductors were connected in series in the circuit behind the source. The magnitude of these inductances was chosen so that the ratio of the load power (EAF and LF) and the short-circuit power in the PCC was approximately the same for the real device and the assembled model. Another functional module connected to the model is a laboratory IGBT-based VSC converter Infineon Mipaq™, which simulates a load (EAF + LF). VSC takes active and reactive power from the modeled network, according to reference waveforms, which were obtained by measurements in real operation (with a reduced scale). To ensure sufficient dynamics and accuracy, the Model Predictive Direct Power Control [66] was applied using the MATLAB/Simulink Real Time Workshop environment implemented into the dSPACE™ control system DS1005. The tested functional module connected to the model is the laboratory model SVC. This model consists of a TCR unit and filters. Its control system was implemented as described in chapter 6 using the implementation in the MATLAB/Simulink Real Time Workshop environment. This environment made it possible to test different settings of the controller and different techniques of signal processing of control signals.

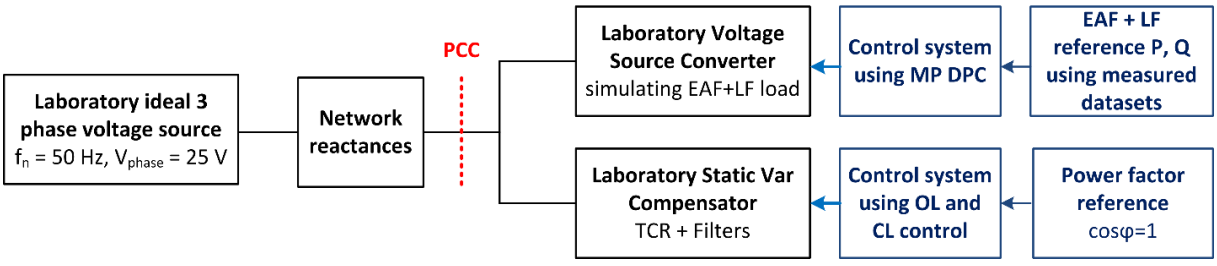


*Figure 8.3: Laboratory scale physical model of the EAF + LF with SVC compensation in industrial distribution system.*

Figure 8.4 shows a view of the control system user interface for SVC (including flicker measurement) and figure 8.5 of the control system user interface for VSC, which simulates EAF and LF loads based on input reference data (real data measured from EAF and LF operation).

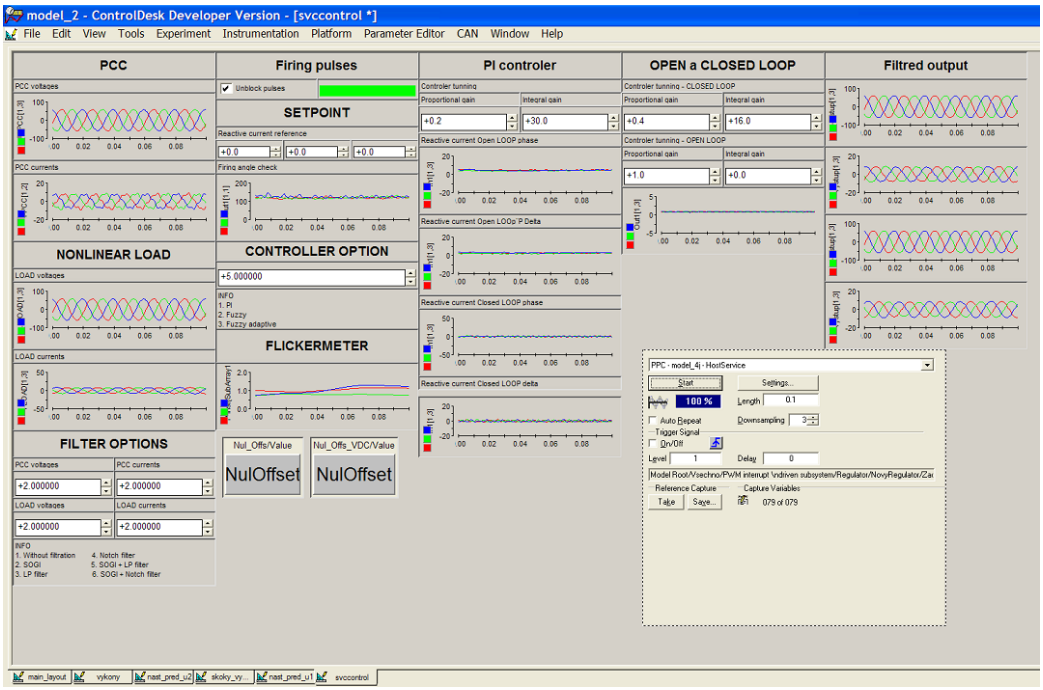


*Figure 8.4: Laboratory SVC control GUI.*

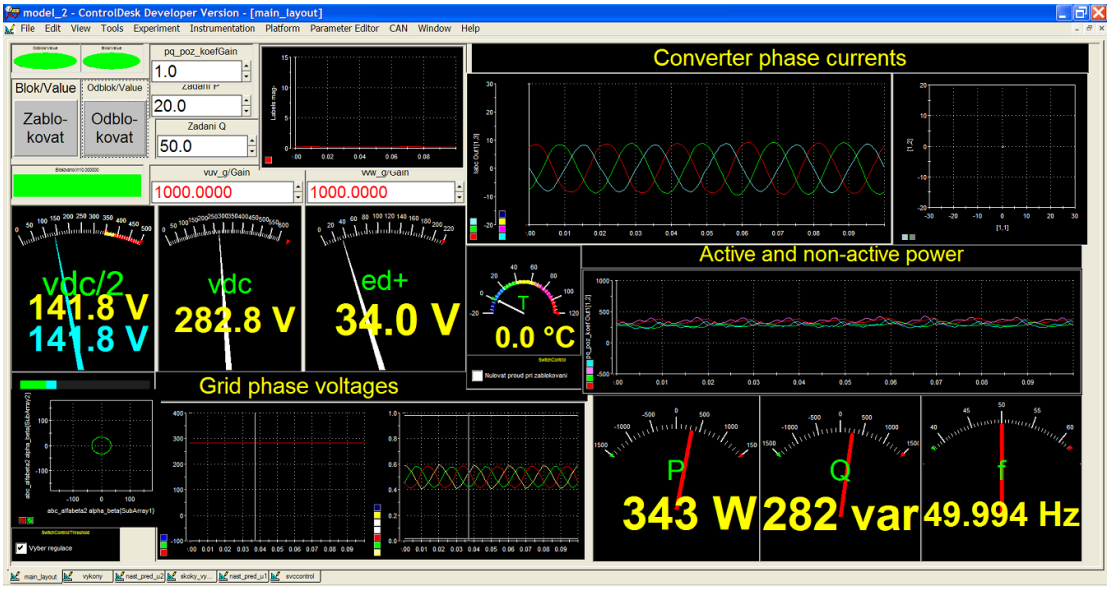


*Figure 8.5: Laboratory VSC (simulating EAF and LF load) control GUI.*

Figure 8.6 shows the power circuits of the laboratory set (TCR, filters, VSC and network reactances).

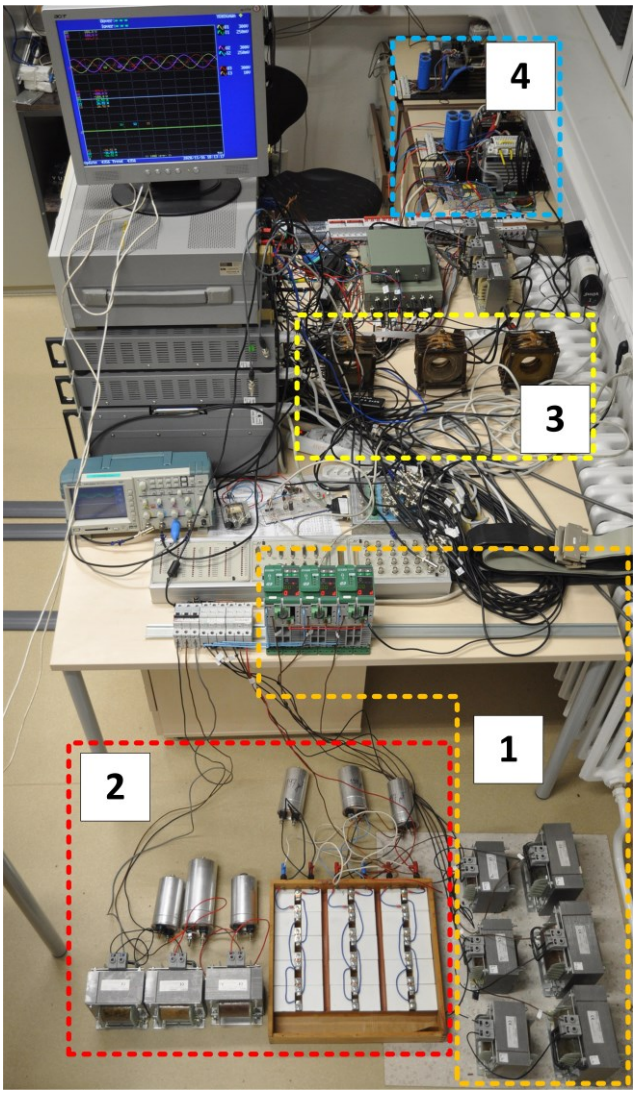


*Figure 8.6: Used laboratory hardware set (1 – TCR, 2 – filters, 3 – network reactances, 4 – laboratory VSC simulating EAF+ LF load).*

The specific parameters of the real system with EAF and LF and the laboratory physical model are summarized in Table 8.1. In order to achieve results with fair value, two basic assumptions need to be met. Real value means that the elements and parameters of the laboratory physical model are designed so that the behavior of the model and the real device is the same in terms of voltage fluctuations (flicker effect), higher harmonics, and other parameters. The first assumption is the resonant frequency (mutual resonance of the network and SVC filters). The second assumption is to maintain the ratio of load power and short-circuit power in the PCC.

| | Parameter | Real configuration | Laboratory model |
|---|---|---|---|
| SVC parameters | Phase voltage | 63,5 kV | 25 V |
| | Phase to Phase voltage | 110 kV | 43,3 V |
| | Filters reactive power | 45 MVAr | 606 VAr |
| | TCR reactive power | 90 MVAr | 716 VAr |
| | Filters reactance star connection equivalent (star connection) | 268,9 Ω | 3,1 Ω |
| | Filters capacity star connection equivalent (star connection) | 11,84 µF | 1029 µF |
| Network param. | PCC short circuit power | 1850 MVA | 25,41 kVA |
| | PCC short circuit reactance | 6,54 Ω | 0,0738 Ω |
| | PCC short circuit inductance | 20,83 mH | 0,235 mH |
| | Resonant frequency | **320,59 Hz** | **320,26 Hz** |

*Table 8.1: Parameters of real configuration and derived laboratory model.*

To prove that the laboratory model sufficiently reliably represents the real behavior of the EAF, a Fourier analysis of the voltages and currents of the tested datasets was performed on the values measured during real operation and on the values generated on the laboratory apparatus. Fourier analysis was performed using an FFT algorithm applied to a 60-second voltage or current record. Comparison of the obtained spectra confirms their sufficient agreement, with the exception of 5 and 7 harmonics. For experimental purposes, however, the key frequency band is characteristic of the flicker effect - 0 Hz - up to 50 Hz. In this band, the agreement between the real measurement and the laboratory apparatus is sufficient. The match is shown by selected illustrative images of harmonic spectra of the current in Figure 8.7 (melt-down) and Figure 8.8 (refining).

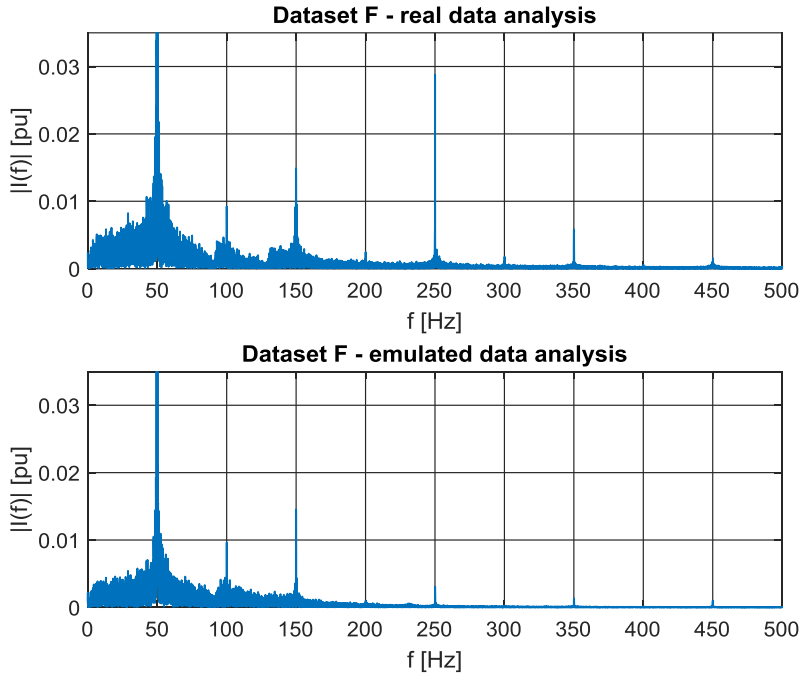


*Figure 8.7: Comparison of the current harmonic spectrums of dataset F (see Figure 8.2) representing melt-down process*

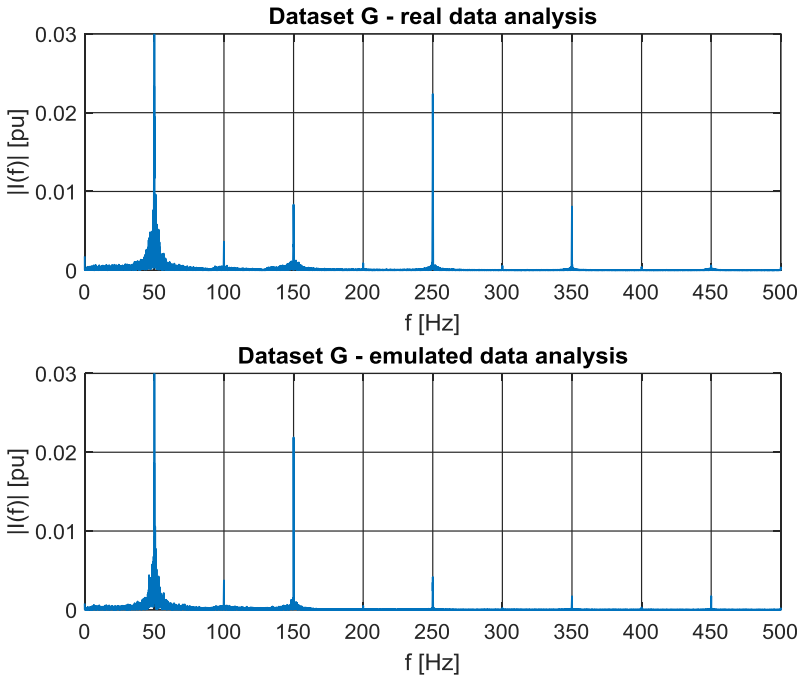


*Figure 8.8: Comparison of the current harmonic spectrums of dataset F( see Figure 8.2) representing refining process.*

## 8.2 Examples of input testing datasets

This subchapter aims to demonstrate the waveforms of voltages and currents of testing datasets. The waveforms shown are intended to demonstrate the different behavior of EAF at different stages of the production process (meltdown and refining). The samples consist of the waveform of instantaneous values for the selected time period and of the waveform of effective values of voltages and currents for entire datasets. In the meltdown phase, these are typically large and frequent dynamic changes in the current taken; in the refining phase, the waveforms are more stable but still with significant disturbances.

### 8.2.1 Meltdown phase

The meltdown phase is characterized by frequent dynamic changes, which are caused by the nature of this phase of the production process in EAF. In this phase, the electrodes are gradually remelted to the bottom of the EAF, where a bath of liquid molten metal is gradually formed. During this process, there are often scrap slides in the mass of gradually melted scrap, which results in two extreme states - the interruption of arcs, or a short circuit. The system of automatic electrodes positioning control system, which is usually built with the use of a hydraulic actuator, contributes to a partial reduction of the occurrence of these undesirable conditions. For short circuits, this system is equipped with a special function of fast electrode stroke, which shortens the duration of the short circuit. The consequence of these undesirable phenomena in terms of power quality is an increased rate of voltage fluctuations, increased harmonic distortion, and asymmetric consumption (negative sequence component). Figure 8.9 shows the time waveforms of the instantaneous values of voltages and currents from a selected part of the dataset F. Significant dynamic changes are observable, for example, at times of 1.55 s - 1.7 s.

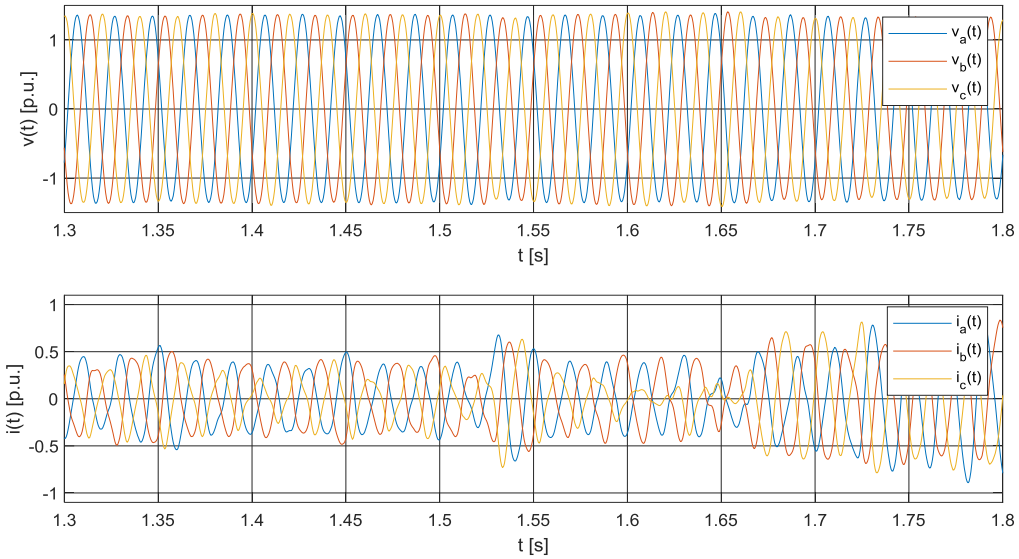


*Figure 8.9: Waveforms of instantaneous values of voltages and currents of the selected part of the dataset F.*

When looking at a longer period of time (e.g. 60, which corresponds to the length of each dataset), the dynamic changes depending on the nature of the melting process are clearly visible. Datasets A, B, D and F were chosen as test datasets for the meltdown phase. The courses of effective values of voltages and currents for these datasets are shown in Figure 8.10. Dataset A represents the beginning of the meltdown process of the first batch basket of the analyzed melt. This dataset shows a gradual increase in the power consumed by the electric arc furnace, including large dynamic changes. Within the first basket, these large dynamic changes visibly persist even during dataset B, but with a smaller range of dynamic changes. Datasets D and F represent the melting at the beginning of the meltdown process of the second and third batch baskets of scrap. Here, the nature of the process is similar to that of the first charge basket, but with a shorter duration, because there is already liquid metal in the bottom of the furnace from the molten previous charge.

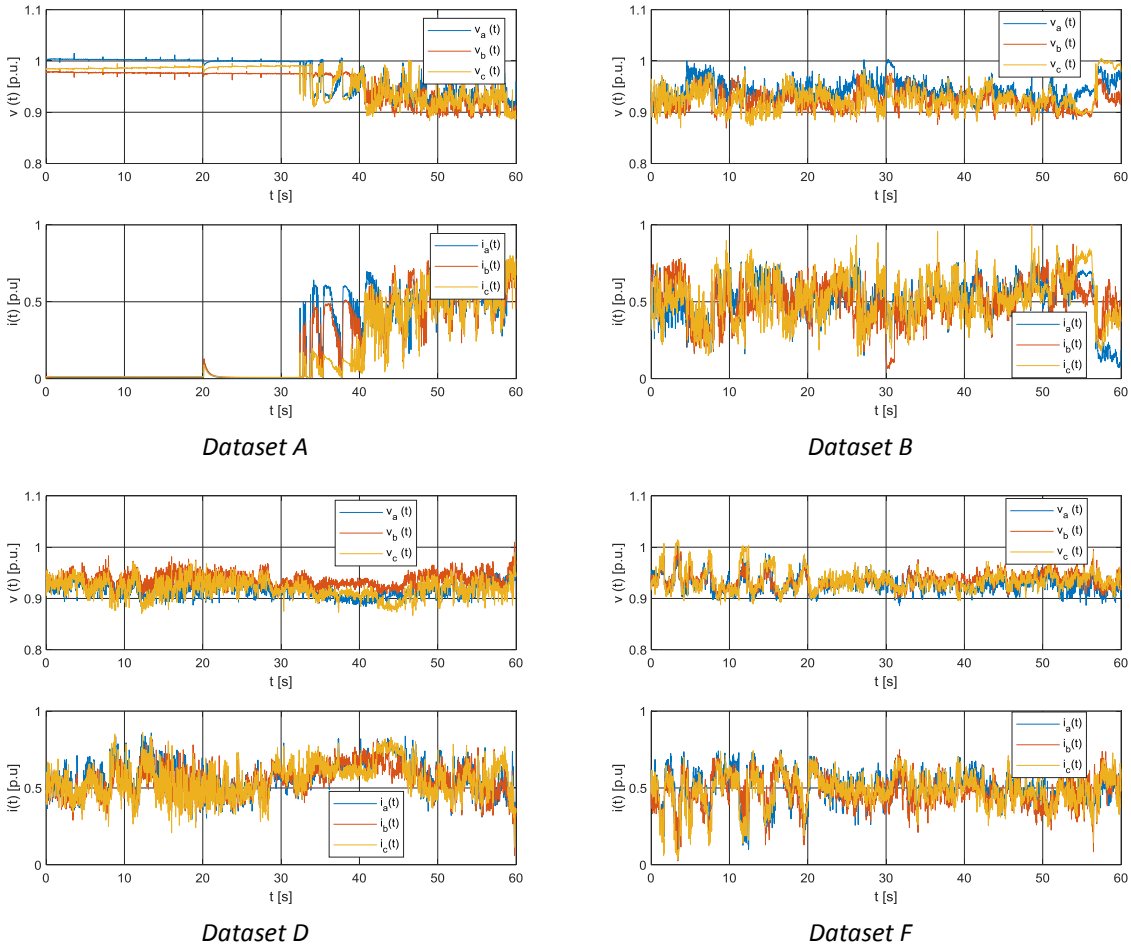


*Figure 8.10: Examples of used datasets, voltage and current of EAF during meltdown process.*

Detailed examples of entire datasets (60-second recording) are included in appendices B, C and D. The appendices contain waveforms of effective values of voltages, currents, active power, reactive power and apparent power. Appendix B shows the dataset of the initial meltdown phase of the EAF production process and Appendix C shows the dataset of the meltdown phase of the EAF production process.

### 8.2.2 Refining phase

The refining phase is a much quieter process compared to the melting phase. At this stage, the scrap is not melted into a liquid form, but the temperature of the liquid contents of the EAF is increased or maintained. The calmer character of this production phase is also contributed by the covering of electric arcs in the foamed slag on the surface of the melt. The formation of foamed slag is achieved by the addition of suitable slag-forming substances. In addition to calming the burning of electric arcs, the foamed slag also brings an increase in energy efficiency - a reduction in heat losses caused by flue gas extraction. The nature of the refining phase is illustrated in detail in Figure 8.11, where the waveforms of the instantaneous values of voltages and currents of a selected part of the test dataset C are shown.

Datasets C, E, G and H were chosen as test datasets for the refining phase. The RMS values of voltages and currents for these datasets are shown in Figure 8.12.

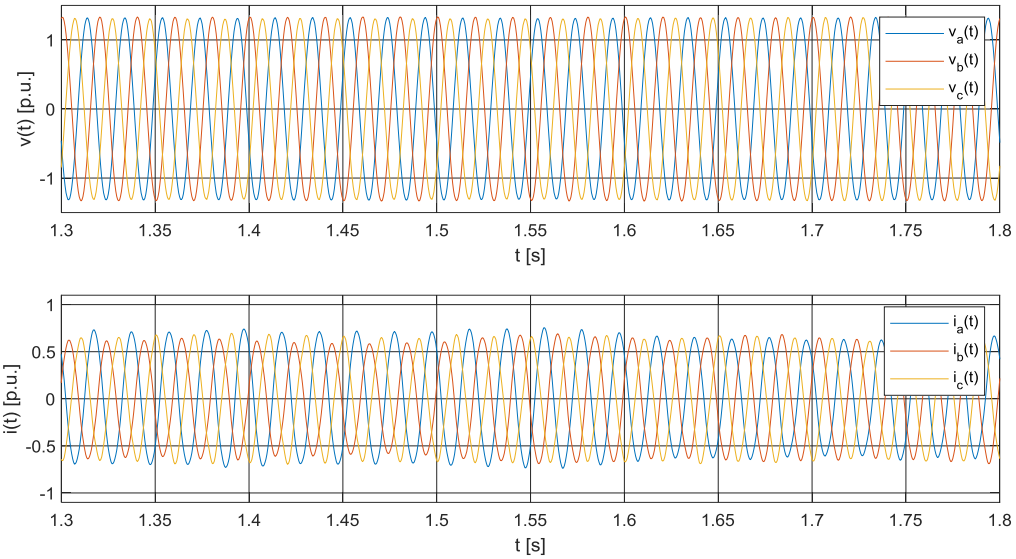


*Figure 8.11: Waveforms of instantaneous values of voltages and currents of the selected part of the dataset C.*

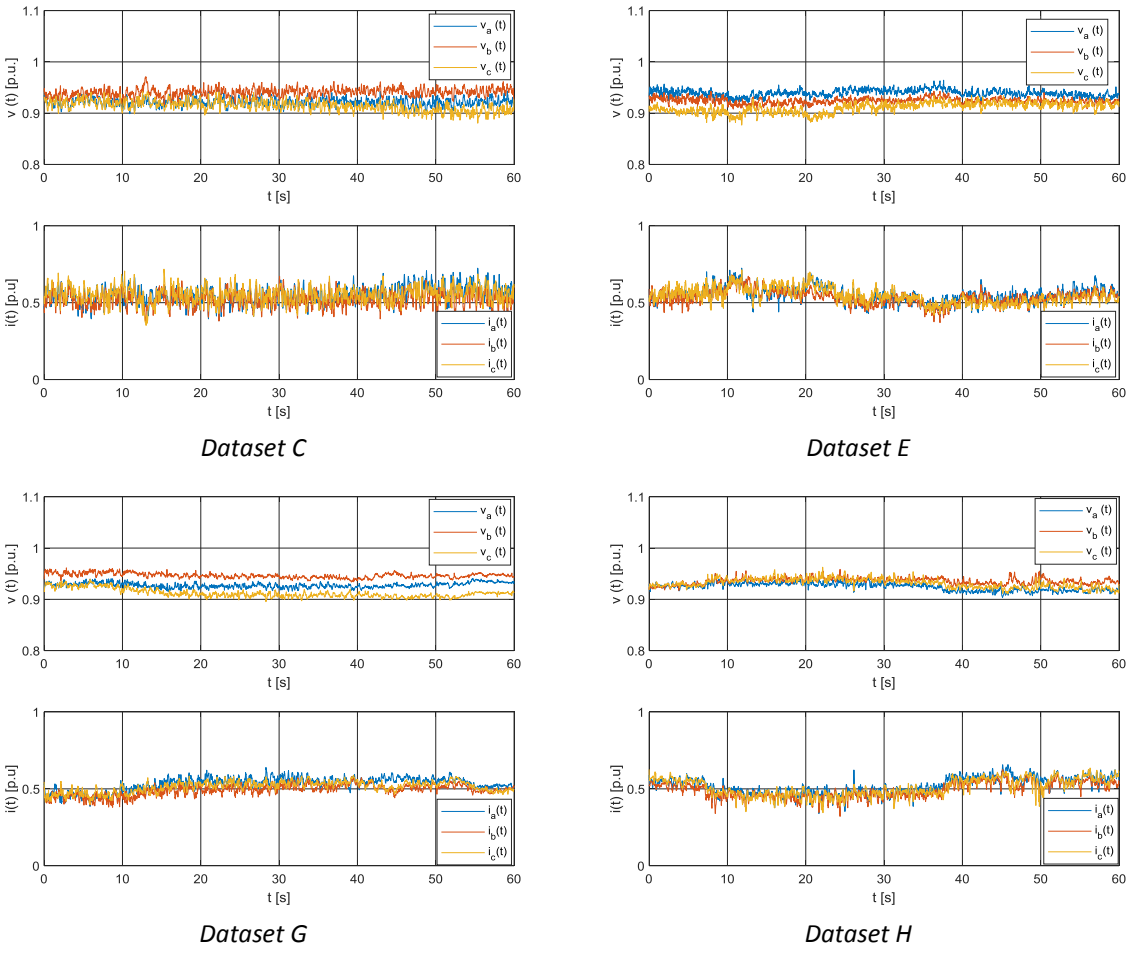


*Figure 8.12: Examples of used datasets, voltage and current of EAF during refining process.*

Appendix D shows the dataset of the initial refining phase of the EAF production process.

# 9 Evaluation of the result of simulations and measurements

Experiments using assembled laboratory equipment were performed for each dataset in several variants, including the basic variant, which does not consider the use of SVC. This chapter will summarize the basic overview of experiments, the methodology of evaluation of results for individual variants will be described, the obtained results will be presented in the form of numerical data and graphical outputs and at the end of this chapter, the results will be compared with other works, including discussion.

## 9.1 Overview of performed experiments

An overview of the performed experiments, including the parameters used, is given in Table 9.1. Regarding the parameters summarized in Table 9.1, $k$ is a conversion factor that expresses how many times the power of the real device $S_0$ (on which the test datasets were obtained by measurement) is higher than the power simulated on the $S_{\mathrm{real}}$ laboratory apparatus. The SVC/EAF ratio represents the ratio between the maximum size of the capacitive compensating laboratory SVC and the power of the simulated EAF consumption. The column labeled "SVC" indicates an indication of whether the SVC has been turned on or not. Experiments with the SVC turned off serve as a reference. The table also specifies the maximum power of the TCR and the maximum capacitive power of the filters. For the open and closed control loop, the constants of the proportional-integration controller (closed loop) or proportional controller (open loop) and the method of processing input signals for both loops are specified. The last column of the table induces the upstream mains inductance in the laboratory assembly to simulate certain short-circuit conditions at the connection point of the simulated EAF and SVC.

| | Test no. | Testing file | Output file | k [-] | $S_0$ [kVA] | $S_{real}$ [VA] | SVC/ EAF | SVC [-] | TCR [VAr] | C [VAr] | Closed loop | | | Open loop | | | $L_s$ [mH] |
|---|---|---|---|---|---|---|---|---|---|---|---|---|---|---|---|---|---|
| | | | | | | | | | | | $K_p$ [-] | $K_i$ [-] | Signal processing technique | $K_p$ [-] | $K_i$ [-] | Signal processing technique | |
| Dataset A | 1 | dats1.mat | 1.mat | 82490 | 50000 | 606 | 1 | Vyp. | 716 | -606 | NA | NA | NA | NA | NA | NA | 0,235 |
| | 2 | dats1.mat | 8.mat | 82490 | 50000 | 606 | 1 | Zap. | 716 | -606 | 0,4 | 16 | SOGI | 1 | 0 | FLICKER | 0,235 |
| | 3 | dats1.mat | 15.mat | 82490 | 50000 | 606 | 1 | Zap. | 716 | -606 | 0,4 | 16 | LP | 1 | 0 | FLICKER | 0,235 |
| | 4 | dats1.mat | 22.mat | 82490 | 50000 | 606 | 1 | Zap. | 716 | -606 | 0,4 | 16 | LP | 1 | 0 | LP | 0,235 |
| | 5 | dats1.mat | 29.mat | 82490 | 50000 | 606 | 1 | Zap. | 716 | -606 | 0,4 | 16 | SOGI | 1 | 0 | SOGI | 0,235 |
| Dataset B | 6 | dats7.mat | 1.mat | 82490 | 50000 | 606 | 1 | Vyp. | 716 | -606 | NA | NA | NA | NA | NA | NA | 0,235 |
| | 7 | dats7.mat | 8.mat | 82490 | 50000 | 606 | 1 | Zap. | 716 | -606 | 0,4 | 16 | SOGI | 1 | 0 | FLICKER | 0,235 |
| | 8 | dats7.mat | 15.mat | 82490 | 50000 | 606 | 1 | Zap. | 716 | -606 | 0,4 | 16 | LP | 1 | 0 | FLICKER | 0,235 |
| | 9 | dats7.mat | 22.mat | 82490 | 50000 | 606 | 1 | Zap. | 716 | -606 | 0,4 | 16 | LP | 1 | 0 | LP | 0,235 |
| | 10 | dats7.mat | 29.mat | 82490 | 50000 | 606 | 1 | Zap. | 716 | -606 | 0,4 | 16 | SOGI | 1 | 0 | SOGI | 0,235 |
| Dataset C | 11 | dats15.mat | 1e.mat | 82490 | 50000 | 606 | 1 | Vyp. | 716 | -606 | NA | NA | NA | NA | NA | NA | 0,235 |
| | 12 | dats15.mat | 8b.mat | 82490 | 50000 | 606 | 1 | Zap. | 716 | -606 | 0,4 | 16 | SOGI | 1 | 0 | FLICKER | 0,235 |
| | 13 | dats15.mat | 15b.mat | 82490 | 50000 | 606 | 1 | Zap. | 716 | -606 | 0,4 | 16 | LP | 1 | 0 | FLICKER | 0,235 |
| | 14 | dats15.mat | 22b.mat | 82490 | 50000 | 606 | 1 | Zap. | 716 | -606 | 0,4 | 16 | LP | 1 | 0 | LP | 0,235 |
| | 15 | dats15.mat | 29b.mat | 82490 | 50000 | 606 | 1 | Zap. | 716 | -606 | 0,4 | 16 | SOGI | 1 | 0 | SOGI | 0,235 |
| Dataset D | 16 | dats18.mat | 1.mat | 82490 | 50000 | 606 | 1 | Vyp. | 716 | -606 | NA | NA | NA | NA | NA | NA | 0,235 |
| | 17 | dats18.mat | 8.mat | 82490 | 50000 | 606 | 1 | Zap. | 716 | -606 | 0,4 | 16 | SOGI | 1 | 0 | FLICKER | 0,235 |
| | 18 | dats18.mat | 15.mat | 82490 | 50000 | 606 | 1 | Zap. | 716 | -606 | 0,4 | 16 | LP | 1 | 0 | FLICKER | 0,235 |
| | 19 | dats18.mat | 22.mat | 82490 | 50000 | 606 | 1 | Zap. | 716 | -606 | 0,4 | 16 | LP | 1 | 0 | LP | 0,235 |
| | 20 | dats18.mat | 29.mat | 82490 | 50000 | 606 | 1 | Zap. | 716 | -606 | 0,4 | 16 | SOGI | 1 | 0 | SOGI | 0,235 |
| Dataset E | 21 | dats21.mat | 1.mat | 82490 | 50000 | 606 | 1 | Vyp. | 716 | -606 | NA | NA | NA | NA | NA | NA | 0,235 |
| | 22 | dats21.mat | 8.mat | 82490 | 50000 | 606 | 1 | Zap. | 716 | -606 | 0,4 | 16 | SOGI | 1 | 0 | FLICKER | 0,235 |
| | 23 | dats21.mat | 15.mat | 82490 | 50000 | 606 | 1 | Zap. | 716 | -606 | 0,4 | 16 | LP | 1 | 0 | FLICKER | 0,235 |
| | 24 | dats21.mat | 22.mat | 82490 | 50000 | 606 | 1 | Zap. | 716 | -606 | 0,4 | 16 | LP | 1 | 0 | LP | 0,235 |
| | 25 | dats21.mat | 29.mat | 82490 | 50000 | 606 | 1 | Zap. | 716 | -606 | 0,4 | 16 | SOGI | 1 | 0 | SOGI | 0,235 |
| Dataset F | 26 | dats24.mat | 1.mat | 82490 | 50000 | 606 | 1 | Vyp. | 716 | -606 | NA | NA | NA | NA | NA | NA | 0,235 |
| | 27 | dats24.mat | 8.mat | 82490 | 50000 | 606 | 1 | Zap. | 716 | -606 | 0,4 | 16 | SOGI | 1 | 0 | FLICKER | 0,235 |
| | 28 | dats24.mat | 15.mat | 82490 | 50000 | 606 | 1 | Zap. | 716 | -606 | 0,4 | 16 | LP | 1 | 0 | FLICKER | 0,235 |
| | 29 | dats24.mat | 22.mat | 82490 | 50000 | 606 | 1 | Zap. | 716 | -606 | 0,4 | 16 | LP | 1 | 0 | LP | 0,235 |
| | 30 | dats24.mat | 29.mat | 82490 | 50000 | 606 | 1 | Zap. | 716 | -606 | 0,4 | 16 | SOGI | 1 | 0 | SOGI | 0,235 |
| Dataset G | 31 | dats27.mat | 1.mat | 82490 | 50000 | 606 | 1 | Vyp. | 716 | -606 | NA | NA | NA | NA | NA | NA | 0,235 |
| | 32 | dats27.mat | 8.mat | 82490 | 50000 | 606 | 1 | Zap. | 716 | -606 | 0,4 | 16 | SOGI | 1 | 0 | FLICKER | 0,235 |
| | 33 | dats27.mat | 15.mat | 82490 | 50000 | 606 | 1 | Zap. | 716 | -606 | 0,4 | 16 | LP | 1 | 0 | FLICKER | 0,235 |
| | 34 | dats27.mat | 22.mat | 82490 | 50000 | 606 | 1 | Zap. | 716 | -606 | 0,4 | 16 | LP | 1 | 0 | LP | 0,235 |
| | 35 | dats27.mat | 29.mat | 82490 | 50000 | 606 | 1 | Zap. | 716 | -606 | 0,4 | 16 | SOGI | 1 | 0 | SOGI | 0,235 |
| Dataset H | 36 | dats31.mat | 1.mat | 82490 | 50000 | 606 | 1 | Vyp. | 716 | -606 | NA | NA | NA | NA | NA | NA | 0,235 |
| | 37 | dats31.mat | 8.mat | 82490 | 50000 | 606 | 1 | Zap. | 716 | -606 | 0,4 | 16 | SOGI | 1 | 0 | FLICKER | 0,235 |
| | 38 | dats31.mat | 15.mat | 82490 | 50000 | 606 | 1 | Zap. | 716 | -606 | 0,4 | 16 | LP | 1 | 0 | FLICKER | 0,235 |
| | 39 | dats31.mat | 22.mat | 82490 | 50000 | 606 | 1 | Zap. | 716 | -606 | 0,4 | 16 | LP | 1 | 0 | LP | 0,235 |
| | 40 | dats31.mat | 29.mat | 82490 | 50000 | 606 | 1 | Zap. | 716 | -606 | 0,4 | 16 | SOGI | 1 | 0 | SOGI | 0,235 |
| Legend | | Meltdown | | | | | | | | | | | | | | | |
| | | Refining | | | | | | | | | | | | | | | |

*Table 9.1: Overview of performed experiments, including input parameters.*

## 9.2 Results evaluation methodology

For each experiment, the short-term flicker effect $P_{st}$ was calculated based on the procedure described in the standard for the standardized flicker meter [24] [61]. To evaluate the benefit of the analyzed modifications of the SVC control system, the flicker effect reduction coefficient using SVC $R_{SVC}$ is introduced in this work, which is defined according to equation (9.1).

$$R_{\mathrm{SVC}} = \frac{P_{\mathrm{st\_SVC\_off}}}{P_{\mathrm{st\_SVC\_on}}} \tag{9.1}$$

where $P_{st\_SVC\_off}$ (experiments no. 1, 6, 11, 16, 21, 26, 31, 36) is the calculated short-term flicker effect without SVC and a $P_{st\_SVC\_on}$ (remaining experiments) is the calculated short-term flicker effect for the

SVC use case. The $R_{SVC}$ coefficient is a key indicator for comparison with other works, which will be performed at the end of this chapter.

## 9.3 Summary of results achieved

For a clearer presentation of the achieved results, 3 variants of outputs are selected here:

- Short-term flicker effect values ($P_{st}$ determined for an interval of 1 minute).
- Waveforms of instantaneous values of perception of the flicker effect.
- Cumulative probability function composed of waveforms of instantaneous values of perception of the flicker effect.

### 9.3.1 Numerical evaluation of results

The evaluation of the short-term perception of the flicker effect $P_{st}$ (for the evaluation interval corresponding to the length of the datasets - 1 minute) and the reduction factor of the flicker effect using SVC $R_{SVC}$ are summarized in Table 9.2 for all performed experiments.

| Input data | | $P_{st}$ without SVC | SVC with SOGI + FF | | SVC with LP + FF | | SVC with LP + LP | | SVC with SOGI + SOGI | |
|---|---|---|---|---|---|---|---|---|---|---|
| **Dataset** | **Character** | | $P_{st}$ | $R_{SVC}$ | $P_{st}$ | $R_{SVC}$ | $P_{st}$ | $R_{SVC}$ | $P_{st}$ | $R_{SVC}$ |
| A | Meltdown | 8,07 | 4,55 | **1,78** | 5,04 | **1,60** | 5,22 | **1,55** | 4,55 | **1,77** |
| B | Meltdown | 8,58 | 5,11 | **1,68** | 5,73 | **1,50** | 5,94 | **1,44** | 4,83 | **1,78** |
| C | Refining | 3,15 | 1,83 | **1,73** | 1,88 | **1,67** | 2,00 | **1,58** | 1,77 | **1,78** |
| D | Meltdown | 8,32 | 4,12 | **2,02** | 4,64 | **1,79** | 4,91 | **1,69** | 4,56 | **1,83** |
| E | Refining | 2,35 | 1,33 | **1,77** | 1,63 | **1,44** | 1,56 | **1,51** | 1,57 | **1,49** |
| F | Meltdown | 7,32 | 4,13 | **1,77** | 4,52 | **1,62** | 4,74 | **1,55** | 4,21 | **1,74** |
| G | Refining | 1,53 | 0,89 | **1,72** | 1,04 | **1,47** | 1,04 | **1,48** | 0,94 | **1,63** |
| H | Refining | 1,90 | 0,94 | **2,03** | 1,12 | **1,70** | 1,08 | **1,76** | 1,07 | **1,78** |

*Table 9.2: Results of the experiments, short time flicker effect and flicker reduction factor for various datasets and various signal processing techniques.*

### 9.3.2 Graphical outputs

The waveforms of the instantaneous values of perception of the flicker effect for all performed experiments and datasets are illustrated in Figure 9.1. The figure shows the partial waveforms for each dataset with a comparison of the techniques used and the basic reference variant without the use of SVC.

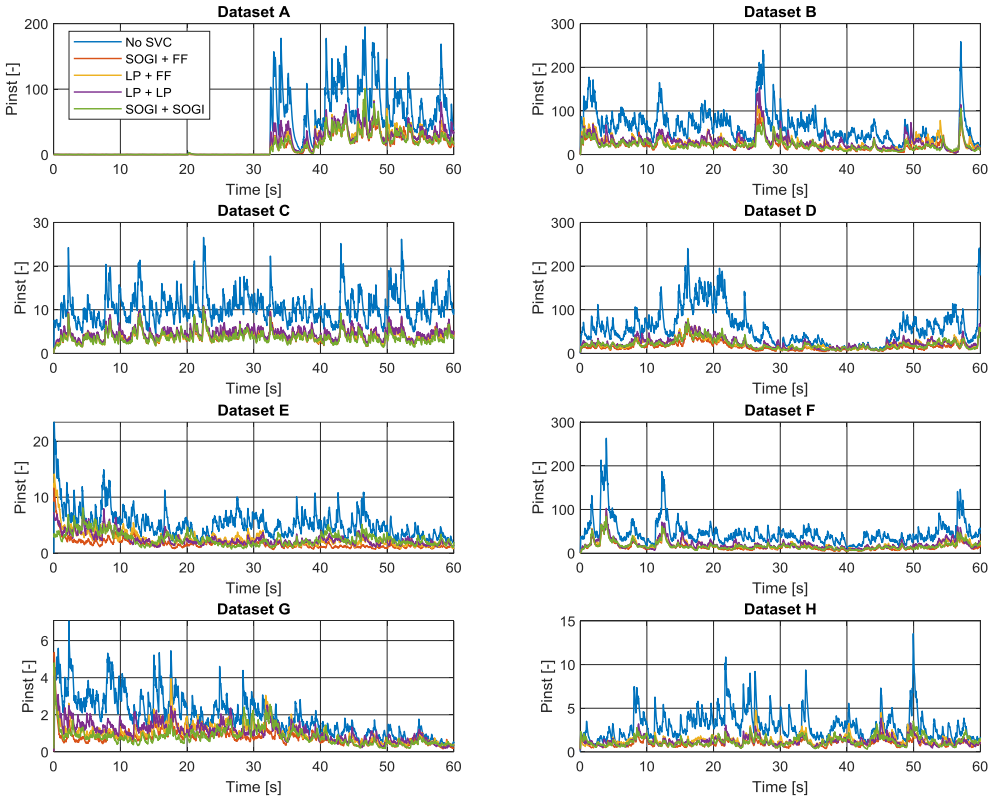


*Figure 9.1: Instantaneous flicker effect for various datasets and various signal processing techniques.*

Another way of visualizing the results is cumulative probability functions compiled from the courses of instantaneous values of the perception rate of the flicker effect $P_{st}$. When comparing these functions, the differences between the individual applied techniques are more visible. The cumulative probability functions are illustrated in Figure 9.2.

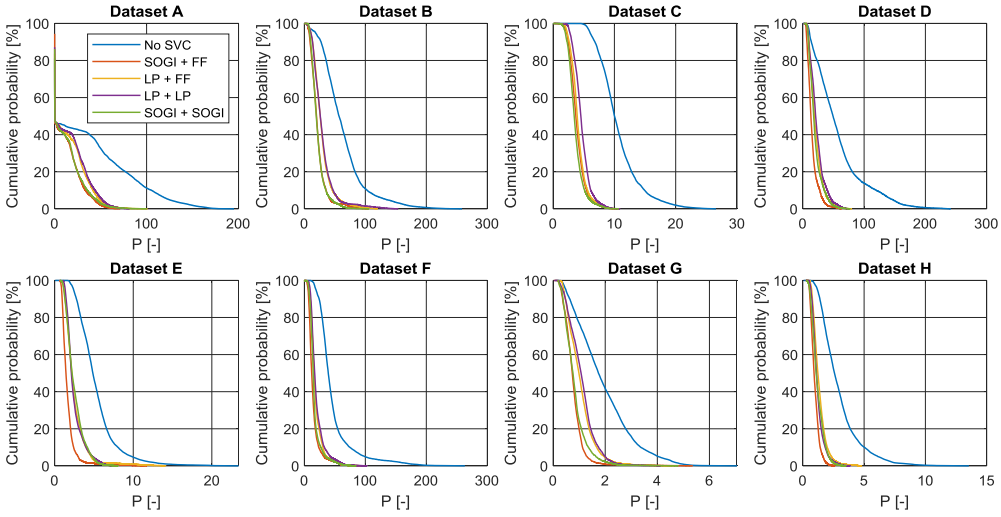


*Figure 9.2: Cumulative probability function of the flicker effect for various datasets and various signal processing techniques.*

## 9.4 Discussion

The results of the performed experiments show that the flicker reduction factor differs depending on the phase of the EAF production process and depending on the used processing method of the open loop and closed loop control signals of the SVC controller.

For the production phase of meltdown, the best results are achieved by a variant where open loop signals are filtered using FF and closed loop signals are filtered using SOGI. The flicker reduction factor, in this case, ranges from 1.68 (dataset B) to 2.02 (dataset D). The variant where open loop and closed loop signals are filtered using SOGI also achieves good results. The flicker reduction factor $R_{SVC}$, in this case, ranges from 1.74 (dataset F) to 1.83 (dataset D). The conventional technique of using low pass filters (Closed loop) and FF (Open loop) achieves lower values of flicker reduction factor $R_{SVC}$ 1.5 (dataset B) to 1.79 (dataset D). In the case of using low pas filters for open loop and closed loop, the values of the flicker reduction factor $R_{SVC}$ are even lower, from 1.44 (dataset B) to 1.69 (dataset D).

For the production phase of refining, the best results are also achieved by the variant where open loop signals are filtered using FF and closed loop signals are filtered using SOGI. The flicker reduction factor $R_{SVC}$ in this case ranges from 1.72 (dataset G) to 2.03 (dataset H). The conventional technique of using low pass filters (Closed loop) and FF (Open loop) achieves lower values of the flicker reduction factor $R_{SVC}$ 1.44 (dataset E) to 1.70 (dataset H) even in this case. In the case of using low pas filters for open loop and closed loop, the values of the flicker reduction factor $R_{SVC}$ are similar, from 1.48 (dataset G) to 1.76 (dataset H).

## 9.5 Comparison of results with other works

The achieved results were compared with the results of previous works. Several key factors need to be looked at to ensure the relevance of the comparison. The first factor for evaluating the possibility of reducing the flicker effect using SVC is the way of testing the proposed measures. Significant differences may occur between field measurement-based experiments and EAF modeling simulations. The differences are caused by different techniques for modeling the dynamic behavior of EAF, where the chaotic behavior of the electric arc is often not sufficiently taken into account. The second factor is the differences in the ratio of the rated power of the EAF and the possible LF to the compensating power of the SVC. When the SVC performance is significantly higher than the EAF performance in a given application, the flicker effect is more significantly reduced than when the SVC performance is comparable to the EAF performance. Another factor is the external conditions, among which it is possible to include short-circuit conditions in the PCC, the occurrence of other problematic devices in the same part of the network. The last factor is the way of evaluating the flicker effect, whether it is a short-term flicker effect ($P_{st}$) or a long-term flicker effect ($P_{lt}$). In addition, the use of supporting technologies of metallurgical processes in EAF (oxygen burners, natural gas burners, electrodes positioning system performance, quality of input material, foaming slag, etc.) can play an important role. Taking into account these factors, an overview of the results achieved in other previous works was prepared. Table 9.3 shows a comparison of the achieved results with previous works. The table also summarizes the input parameters that suggest the comparability of the results.

| Authors | Year | Furnaces configuration | Furnaces rating | SVC rating | SVC control strategy | EAF simulation/field data | Flicker reduction factor |
|---|---|---|---|---|---|---|---|
| M. F. Alves et al. [67] | 2010 | EAF | 30 MVA | 25,8 MVAr (TCR), 50 MVAr (filters) | Compensation of all negative sequence currents and the imaginary part of the positive sequence currents | Simulation: Model Chua's circuit | 1,73 |
| S. Morello et al. [68] | 2015 | EAF + LF | 30 MVA (EAF) + 15 MVA (LF) | 80 MVAr (TCR), 80 MVAr (filters) | Not specified | Field measurement | 1,98 |
| S. Morello et al. [69] | 2017 | EAF + LF | 50 MVA (EAF) + 15 MVA (LF) | 80 MVAr (TCR), 80 MVAr (filters) | Not specified | Field measurement | 1,62 |
| T. J. Dionise [70] | 2014 | EAF + LF | 50 MVA (EAF) + 14 MVA (LF) | 231 MVAr (TCR), 273 MVAr (filters) | Not specified | Field measurement | 1,19 |
| X. Zhu et al. [71] | 2016 | EAF + LF | 28 MVA (EAF) + 12,5 MVA (LF) | 15 MVAr (TCR), 18 MVAr (filters) | Not specified | Simulation: chaotic behavior | 1,53 |
| S. Prinz et al. [72] | 2005 | 2xEAF+LF | 85 MVA (EAF1) + 120 MVA (EAF2) + 24 MVA (LF) | 180 MVAr (TCR), 180 MVAr (filters) | Closed loop reactive control | Simulation: chaotic behavior | 1,79 |
| | | | | 150 MVAr (TCR), 150 MVAr (filters) | Closed loop reactive control | | 1,39 |
| | | | | 150 MVAr (TCR), 150 MVAr (filters) | Closed loop reactive control with anti-windup | | 1,67 |
| H. Samet et al. [73] | 2018 | EAF | 90 MVA (standard power system) | 108 MVAr (TCR), 97,2 MVAr (filters) – Rated power of 1 of 2 SVCs, not specified if 1 or 2 SVCs were used | Closed loop reactive power control | Simulation: field measured data based numerical model | 1,69 |
| | | | | | Closed loop reactive power control + Prediction block | | 2,32 |
| | | | 90 MVA (weak power system) | | Closed loop reactive power control | | 2,26 |
| | | | | | Closed loop reactive power control + Prediction block | | 4,07 |
| This work | 2020 | EAF + LF | 50 MVA (EAF) + 12 MVA (LF) | 59 MVAr (TCR), 50 MVAr (filters) | Closed loop (SOGI), open loop (FF) | Simulation: field measured data based experimental model | 1,68 - 2,03 (1,81 in average) |
| | | | | | Closed loop (LP), open loop (FF) | | 1,44 - 1,79 (1,60 in average) |
| | | | | | Closed loop (LP), open loop (LP) | | 1,44 - 1,76 (1,57 in average) |
| | | | | | Closed loop (SOGI), open loop (SOGI) | | 1,49 - 1,83 (1,72 in average) |

*Table 9.3: Comparison of achieved results with results achieved in previous works.*

Work [68] achieves significantly better results than the remaining strategies. This difference can be achieved by the disparity between the power of SVC (80 MVAr) and the power of EAF (30 MVA) + LF (15 MVA) in the case [68]. The advantage of [68], [69], [70] is that the results are based on field measurement. In [67], [71], [72] the simulation of chaotic behavior was used. Comparison of the results shows that the method proposed in this thesis (closed loop using SOGI and open loop using flicker weighting function) achieves better results than works [67], [69], [70], [71], [72]. Work in this thesis was based on a field measured data-based experimental model. The work [68] shows better results, but with a significant disproportion between the performance of EAF + LF and the performance of SVC. The work [73] uses more advanced techniques based on the Gray - ANN-based prediction method to reduce the flicker effect. These techniques show better results, but for example the work [74] focused on the prediction of high power nonlinear loads using NARX neural networks concludes that the

prediction works with good reliability only in selected phases of the EAF production cycle. Good results have been obtained in the refining phase, which is not as critical in terms of the flicker effect as the melting phase. According to [74], the melting phase is difficult to predict due to the dependence on the composition (consistency) of the input material (steel scrap), which can vary considerably from cycle to cycle. Other factors are the inputs of random anomalies such as short-circuiting (scrap landslides in EAF), electric arc extinguishment, electrode breakage, the utilization of supporting technologies such as natural gas burners or oxygen burners, etc.

# 10 Conclusions

The dissertation was divided into three levels. The first level consists of introductory chapters, which provide an overview of the current state of the issue and define the focus of the dissertation on improving the control system of SVC equipment in order to more effectively reduce the flicker effect in industrial distribution systems. The introductory chapters focus on the introduction and definition of the framework of power quality, including demonstrative examples, the issue of electric arc furnaces in terms of power quality in industrial distribution systems, including demonstrative examples, basic options for improving electricity quality in industrial distribution systems, including demonstrative examples and part focused on the use of compensation devices. The second level of work consists of chapters that focus on the flicker effect on the extended possibilities of using compensation devices, where the potential for improving the SVC control system is presented, as well as case studies of problem areas where the results of practical exercises demonstrate the effectiveness of basic measures to improve the quality of electricity. The chapter focused on the use of FACTS in the problematic area focused on verifying the effectiveness of the proposed improvements using the developed laboratory design of SVC with the implementation of data from the real operation of EAF. The third level of the work is focused on the presentation of the achieved results and their comparison with other scientific works in the segment. The conclusion of this part is a discussion of the achieved results.

## 10.1 Evaluation of the fulfillment of work objectives

The conclusions of this work are conceived as an evaluation based on the objectives set out in the introductory subchapter 1.3.

The first objective was met in Chapters 2 and 3. Chapter 2 contains a description of the legislative framework on which the issue of power quality is based, presents the parameters of power quality, and specifies the requirements for measuring the power quality. Due to the focus of work on industrial distribution systems, this chapter also contains illustrative examples of the disturbance, more precisely disturbing appliances typical for this type of electrical system. Chapter 2 also presents mechanisms for the propagation of disturbances (higher harmonics and flicker effect) in industrial distribution systems, which are important for the effective planning of measures leading to the improvement of power quality. Due to the definition of the work on the issue of flicker effect in connection with the EAF, a necessary part of the first goal is also Chapter 3, focused on the technology of EAF. This chapter provides an overview of EAF technology with a focus on the electrical part of the technology. In terms of power quality, this chapter focuses on the derivation of operating characteristics and their comparison with data from real operation, based on which it is possible to master the principle of flicker effect due to EAF operation.

The second objective would be met in Chapter 4, which focuses on the basic possibilities of improving the power quality without the use of compensating devices. Possibilities of modification of basic system components and system configuration are considered as basic tools. In the case of an EAF and flicker effect, the short-circuit power in the PCC and the type of arc furnace play the most important role. The concept of industrial distribution systems also plays an important role, which considers the isolation of consumers with a significant degree of disturbance emission into a separate part of the distribution system. The model examples point to the fundamental importance of this measure, which makes it possible to reduce the level of perception of the flicker effect for other end customers by up to 85%. Another model example is focused on assessing the effect of active loads, which brings a reduction in the perception of the flicker effect by approximately 1.2% (the value is strongly dependent on local conditions and the relative proportion of active loads). In fulfilling this goal, the possibilities of modifying the technological process of production in the EAF were also taken

into account. The technologies described in Chapter 4, in addition to improving the quality of metallurgical technological processes, also contribute to reducing the flicker effect resulting from the operation of the EAF.

The third goal is met in Chapter 5, which focuses on an overview of compensation devices. Chapter preview on the benefits of compensating devices for flicker effect mitigation. Compensation devices are divided according to several criteria and in terms of their properties, the selected technologies are adequate to mitigate the flicker effect in industrial distribution systems and EAF. SVC and STATCOM devices are the most suitable for a given application. The chapter contains a description of these technologies, including operational aspects (investment intensity and space requirements).

The fourth goal is met in Chapter 6, which focuses on the possibilities of improving the SVC system to more effective mitigation of the flicker effect. The chapter describes the philosophy of the SVC control system in applications for the transmission system and then describes the philosophy of the SVC control system for applications in industrial distribution systems. In this embodiment, the chapter contains a more detailed description of the system, including the identification of the potential for improvement in terms of flicker effect mitigation, which consists of suitable signal processing methods of the input control signals. By default, low pass filters are used for this purpose. In order to improve, this work analyzes the use of the so-called "flicker filter", which is based on the sensitivity function of the flicker effect and the SOGI technique in various combinations.

The fulfillment of the fifth goal is contained in Chapter 7, which is focused on a case study in a problematic area. An analysis of the historical development in the area of disturbance - flicker effect was performed in the selected industrial distribution system with EAF. This chapter confirms the hypotheses expressed mainly in Chapter 4. A very valuable part of this chapter is the evaluation of the impact of transmission and distribution system configuration based on real measurements, which were carried out in research cooperation of steelworks operator, distribution system operator, distribution system operator and university research team. The evaluation points to the fundamental influence of short-circuit power in the PCC and the isolation of problematic appliances (consumer’s technologies) from other customers in the distribution system.

The fulfillment of the last, sixth goal is contained in Chapters 8 and 9. Chapter 8 focuses on testing the improvements of the control system of the SVC compensation device. For testing purposes, a laboratory setting was developed containing a hardware model of SVC, including a parameterizable control system, a power supply point taking into account the real characteristics of the distribution system and a VSC converter, which was used as an element simulating non-linear load. The behavior of the load (VSC inverters) was based on reference test datasets, which were obtained by measurements during real operation of 60 t EAF. In the designed and implemented laboratory setting, the behavior was verified almost the same as in the case of a real system on the basis of relative comparison of input parameters and on the basis of a comparison of frequency spectra. Several datasets were used to evaluate partial variants of the SVC control system improvements, representing variously different phases of the production process in the EAF. The evaluation was based on 40 reference experiments (5 variants for each of the 8 datasets). The short-term rate of perception of the flicker effect (60 s interval) was evaluated, and subsequently, based on the reference experiments (state without the use of SVC), the coefficients of reduction of the flicker effect were evaluated. The best results were demonstrated for the SOGI variant (closed loop, reactive current control in PCC) + flicker filter (open loop, fast control of dynamic changes in the reactive current of the HV EAF terminal). The obtained results were compared with the results of other researchers and research groups. It should be noted that the comparison is a relatively elusive task, given that there are a number of differences in individual cases, such as the magnitude of the short-circuit power in the PCC and the power ratio of the EAF and SVC. Another factor that raises a number of questions is how to verify the benefits of each technique. The most reliable are the results verified on the basis of measurements

from real operation, the results obtained on the basis of models using real data also have a high informative value. On the contrary, due to the nature of the chaotic behavior of EAF, simulation models may have less informative value. The results of the comparison, including comments on the individual references, are summarized in Chapter 9.

## 10.2 Recommendations and suggestions for further work

In the future, the flicker effect and EAFs related topics are expected to develop in the following ways:

1. The concept of joint use of SVC and STATCOM technology. The idea should be based on maintaining the existing SVC equipment and supplementing the compensation system with a STATCOM unit with lower-rated power. The SVC would be operated with full use of its potential, the STATCOM unit would be used to compensate for phenomena that are outside the functionality of the SVC (compensation of changes in active power, use of better dynamic response).
2. The concept of compensating devices with the possibility of accumulating electricity. STATCOM technology theoretically allows the accumulation of electricity. This functionality would bring more expanded options for compensating for changes in active power.
3. More accurate quantification of the impacts of EAF's supporting metallurgical technologies on flicker effect mitigation.
4. Optimization of the EAF energy balance based on the price, availability and acceptability of individual types of input energy. It is therefore the ratio of electricity and chemical energy (oxygen, natural gas and other elements) in the production process in EAF. A reduction in the share of electricity would be expected to mitigate the flicker effect.

# References


[1] A. Meier, Electric Power Systems: A Conceptual Introduction, Hoboken: Wiley-IEEE Press, 2006.

[2] E. Abdelaziz, R. Saidur and S. Mekhilef, "A review on energy saving strategies in industrial sector," *Renewable and Sustainable Energy Reviews,* vol. 15, no. 1, pp. 150-168, January 2011.

[3] B. Mecrow and A.G. Jack, "Efficiency trends in electric machines and drives," *Energy Policy,* vol. 36, no. 12, pp. 4336-4341, December 2008.

[4] M. Bollen, "What is power quality?," *Electric Power Systems Research,* vol. 66, no. 1, pp. 5-14, July 2003.

[5] J. Dawson, A. Marvin and C. Marshman, "Electromagnetic Compatibility," in *Encyclopedia of Physical Science and Technology (Third Edition)*, Academic Press, 2003, pp. 261-275.

[6] J. Hernández, M. Ortega, J. D. l. Cruz and D. Vera, "Guidelines for the technical assessment of harmonic, flicker and unbalance emission limits for PV-distributed generation," *Electric Power Systems Research,* no. 81(7), pp. 1247-1257, 2011.

[7] F. Ferdowsi, S. Mehraeen and G. B. Upton, "Assessing distribution network sensitivity to voltage rise and flicker under high penetration of behind-the-meter solar.," *Renewable Energy,* no. 152, pp. 1227-1240, 2020.

[8] F. Girbau-Llistuella, A. Sumper, F. Díaz-González and S. Galceran-Arellano, "Flicker mitigation by reactive power control in wind farm with doubly fed induction generators," *International Journal of Electrical Power & Energy Systems,* no. 55, pp. 285-296, 2014.

[9] S. Abulanwar, A. Ghanem, M. E. Rizk and W. Hu, "A proposed flicker mitigation scheme of DFIG in weak distribution networks," *Alexandria Engineering Journal,* no. 58(2), pp. 677-687, 2019.

[10] M. Maksić and I. Papič, "Calculating flicker propagation in a meshed high voltage network with interharmonics and representative voltage samples," *International Journal of Electrical Power & Energy Systems 2012,* no. 42(1), pp. 179-187, 2012.

[11] World Steel Association AISBL, "Worls Steel in Figures 2019," Brussels, 2020.

[12] J. Madias, "Electric Furnace Steelmaking," in *In Treatisein Process Metallurgy*, Oxford, Elsevier, 2014, pp. 271-286.

[13] S. R. Mendis, M. T. Bishop and J. F. Witte, "Investigations of voltage flicker in electric arc furnace power systems," *IEEE Industry Applications Magazine,* vol. 2, no. 1, pp. 28-34, Jan.-Feb. 1996.

[14] M. Kovačič, K. Stopar, R. Vertnik and B. Šarler, "Comprehensive Electric Arc Furnace Electric Energy Consumption Modeling: A Pilot Study," *Energies,* no. 12(11), p. 2142, 2019.

[15] G. Manchur and C. C. Erven, "Development of a model for predicting flicker from electric arc furnaces," *IEEE Transactions on Power Delivery,* vol. 7, no. 1, pp. 416-426, January 1992.

[16] S. Ambra, S. Jan and L. Tomas, "Power-electronic solutions to power quality problems," *Electric Power Systems Research,* vol. 66, no. 1, pp. 71-82, July 2003.

[17] R. E. Brown, Electric Power Distribution Reliability, Boca Raton: CRC Press, 2017.

[18] Sbírka zákonů České Republiky, *Zákon č. 458/2000 Sb. Zákon o podmínkách podnikání a o výkonu státní správy v energetických odvětvích a o změně některých zákonů (energetický zákon),* 2000.

[19] Sbírka zákonů České Republiky, *Zákon č. 670/2004 Sb. Zákon, kterým se mění zákon č. 458/2000 Sb., o podmínkách podnikání a o výkonu státní správy v energetických odvětvích a o změně některých zákonů (energetický zákon), ve znění pozdějších předpisů,* 2004.

[20] Sbírka zákonů České Republiky, *Vyhláška č. 540/2005 Sb. Vyhláška o kvalitě dodávek elektřiny a souvisejících služeb v elektroenergetice,* 2005.

[21] Úřad pro technickou normalizaci, metrologii a státní zkušebnictví, *ČSN EN 50160. Charakteristiky napětí elektrické energie z veřejných distribučních síti,* 3. dopl. vyd. ed., Praha, 2011.

[22] International Electrotechnical Commission, *IEC TR 61000-2-8. Electromagnetic compatibility (EMC) Part 2-8: Environment Voltage dips and short interruptions on public electric power supply systems with statistical measurement results,* 2002.

[23] Úřad pro technickou normalizaci, metrologii a státní zkušebnictví, *ČSN EN 61000-4-30. Elektromagnetická kompatibilita (EMC) – Část 4-30: Zkušební a měřicí technika – Metody měření kvality energie. 3. dopl. vyd.,* Praha, 2017.

[24] Úřad pro technickou normalizaci, metrologii a státní zkušebnictví, *Elektromagnetická kompatibilita (EMC) – Část 4-15: Zkušební a měřicí technika – Flikrmetr – Specifikace funkce a dimenzování. 2. dopl. vyd.,* Praha, 2011.

[25] Úřad pro technickou normalizaci, metrologii a státní zkušebnictví, *ČSN EN 61000-4-7. Elektromagnetická kompatibilita (EMC) - Část 4-7: Zkušební a měřicí technika - Všeobecná směrnice o měření a měřicích přístrojích harmonických a meziharmonických pro rozvodné sítě a zařízení připojovaná do nich. 2. dopl. vyd.,* Praha, 2003.

[26] J. Schlabbach, D. Blume and T. Stephanblome, Voltage quality in electrical power systems, London: Institution of Electrical Engineers, 2001.

[27] C. Surajit, M. Madhuchhanda and S. Samarjit, Electric Power Quality, Dordrecht: Springer Netherlands, 2011.

[28] A. B. Baggini, Handbook of power quality, Hoboken, NJ: John Wiley, 2008.

[29] Mathworks, "Documentation - Thyristor Rectifiers.," [Online]. Available: https://www.mathworks.com/help/physmod/sps/ug/thyristor-rectifiers.html. [Accessed 15 1 2021].

[30] J. C. Das, Power System Harmonics and Passive Filter Designs, Hoboken: John Wiley & Sons, Inc., 2015.

[31] H. Renner and M. Sakulin, "Flicker Propagation in Meshed High Voltage Networks," in *Ninth International Conference on Harmonics and Quality of Power*, Orlando, 2000.

[32] R. W. Crandall, "From competitiveness to competition: The threat of minimills to large national steel companies," *Resources Policy,* no. 22(1-2), pp. 107-118, 1996.

[33] J. R. Stubbles, "The Minimill Story," *Metallurgical and materials transactions,* no. 40B, pp. 134-144, 2009.

[34] International Electrotechnical Commission, *IEC TR 61000-3-7:2008. Electromagnetic compatibility (EMC) - Part 3-7: Limits - Assessment of emission limits for the connection of fluctuating installations to MV, HV and EHV power systems,* 2008.

[35] The Institute of Electrical and Electronics Engineers, *IEEE 1453.1-2012 - IEEE Guide-Adoption of IEC/TR 61000-3-7:2008, Electromagnetic compatibility (EMC)-Limits--Assessment of emission limits for the connection of fluctuating installations to MV, HV and EHV power systems,* 2012.

[36] A. J. P. Rosentino, I. N. Gondim, J. R. Macedo and A. C. Delaiba, "A Practical Electric Arc Furnace Model For Flicker Assessment," *J Control Autom Electr Syst,* no. 26, pp. 68-79, 2015.

[37] A. Singh, R. K. Singh and A. K. Singh, "Power Quality Issues of Electric ArcFurnace and their Mitigations-A Review," *International Journal of Advanced Engineering Research and Science (IJAERS),* no. 4, pp. 22-41, 2017.

[38] Úřad pro technickou normalizaci, metrologii a státní zkušebnictví, *ČSN EN 60909-0-ed.2 (333022). Zkratové proudy v trojfázových střídavých soustavách - Část 0: Výpočet proudů.,* Praha, 2016.

[39] T. Wieczorek, M. Blachnik and K. Mączka, "Building a Model for Time Reduction of SteelScrap Meltdown in the Electric Arc Furnace(EAF): General Strategy with a Comparison ofFeature Selection Methods," in *Artificial Intelligence and Soft Computing - ICAISC 2008*, Zakopane, Polsko, 2008.

[40] A. A. Nikolaev, P. G. Tulupov and G. V. Astashova, "The comparative analysis of electrode control systems of electric arc furnaces and ladle furnaces," in *2016 2nd International Conference on Industrial Engineering, Applications and Manufacturing (ICIEAM)*, Chelyabinsk, Rusko, 2016.

[41] M. Kirschen, K. Badr and H. Pfeifer, "Influence of direct reduced iron on the energy balance of the electric arc furnace in steel industry," *Energy,* no. 36(10), 2011.

[42] Primetals Technologies, "EAF RCB Injection Technology," [Online]. Available: https://www.primetals.com/portfolio/technologie-packages/detail/eaf-rcb-injection-technology. [Accessed 9 2 2021].

[43] P. Rathaba, I. Craig and P. Pistorius, "Influence of Oxyfuel Burner Subsystem on the EAF Process," *IFAC Proceedings Volumes,* no. 37(15), pp. 215-220, 2004.

[44] J. D. Hernandez, L. Onofi and S. Engell, "Model of an Electric Arc Furnace Oxy-Fuel Burner for dynamic simulations and optimisation purposes," *IFAC-Papers On Line,* no. 52(14), pp. 30-35, 2019.

[45] A. Luz, A. T. Martinez, F. López, P. Bonadia and V. Pandolfelli, "Slag foaming practice in the steelmaking process," *Ceramics International,* no. 44(8), pp. 8727-8741, 2018.

[46] C. Sedivy and R. Krump, "Tools for foaming slag operation at EAF steelmaking," *Archives of Metallurgy and Materials,* no. 53(2), 2008.

[47] V. Ganesh, S. Periasamy and D. Sivakumar, "Proposal Technique for an Static VarCompensator," *IOSR Journal of Electrical and Electronics Engineering (IOSR-JEEE),* no. 5(7), pp. 1-7, 2013.

[48] Q. Yu, P. Li, W. Liu and X. Xie, "Overview of STATCOM technologies," in *2004 IEEE International Conference on Electric Utility Deregulation, Restructuring and Power Technologies*, Hong Kong, 2004.

[49] T. Zaveri, B. Bhajla and N. Zaveri, "Load compensation using DSTATCOM in three-phase, three-wire distribution systemunder various source voltage and delta connected load conditions," *Electrical Power and Energy Systems,* no. 41, pp. 34-43, 2012.

[50] ABB, *ABB Grids and Power Quality solutions - Automatic voltage control & digital developments,* Bucharest: ABB, 2019.

[51] M. Claus, D. Retzmann, K. Uecker and A. Zenker, *Improvement inVoltage Qualityfor Power Systems–with SVC PLUS®,* Internationaler ETG-Kongress 2009, 2009.

[52] S. Schneider and B. Strong, *Voltage Stability improvement using FACTS devices: SVC and STATCOM,* Siemens AG, 2019.

[53] E. Spanic, O. Kuhn, A. Rentschler, M. Delzenne, M. Schwan and Y. E. Jazouli, "Inertia and Voltage Challenges in Future Power Grids - Impact of SVC PLUS Frequency Stabilizer," in *CIGRE Egypt - The Future of Electricity Grids 2019*, Cairo, 2019.

[54] E. B. Martínez and C. Á. Camacho, "Technical comparison of FACTS controllers in parallel connection," *Journal of Applied Research and Technology,* pp. 36-44, 2017.

[55] ABB, *FACTS - SVC for mitigation of flicker from electric arc furnaces,* Västerås: ABB, 2011.

[56] N. G. Hingorani and L. Gyugyi, Understanding FACTS: Concepts and Technology of Flexible AC Transmission Systems, New York: The Institute of Electrical and Electronics Engineers, 1999.

[57] The Institute of Electrical and Electronics Engineers, *IEEE Guide for the Functional Specification of Transmission Static Var Compensators," in IEEE Std 1031-2011(Revision of IEEE Std 1031-2000),* The Institute of Electrical and Electronics Engineers, 2011, pp. 1-89.

[58] B. V. M. Torabian Esfahani, "Development of optimal shunt hybrid compensator based on improving the measurement of various signals," *Measurement,* no. 69, pp. 250-263, 2015.

[59] I. M. M. P. Haidar Samet, "New reactive power calculation method for electric arc furnaces," *Measurement,* no. 81, pp. 251-263, 2016.

[60] T. J. E. Miller, Reactive Power Control in Electric Systems, New York: John Wiley and Sons, 1983.

[61] International Electrotechnical Commission, *Electromagnetic compatibility (EMC) - Part 4-15: Testing and measurement techniques - Flickermeter - Functional and design specifications,* International Electrotechnical Commission, 2010.

[62] P. Šimek, J. Škramlík and V. Valouch, "A frequency locked loop strategy for synchronization of inverters used in distributed energy sources," *International Journal of Electrical Power & Energy Systems,* no. 107, pp. 120-130, 2019.

[63] P. Rodriguez, I. C. A. Luna, R. Mujal, R. Teodorescu and F. Blaabjerg, "Multiresonant frequency-locked loop for grid synchronization of power converters under distorted grid conditions," *IEEE Transactions on Industrial Electronics,* no. 58(1), pp. 127-135, 2011.

[64] A. T. Teklić, B. Filipović-Grčić and I. Pavić, "Modelling of three-phase electric arc furnace for estimation of voltage flicker in power transmission network," *Electric Power Systems Research,* no. 146, pp. 218-227, 2017.

[65] D. C. Bhonsle and R. B. Kelkar, "Analyzing power quality issues in electric arc furnace by modeling," *Energy,* no. 115(1), pp. 830-839, 2016.

[66] M. Čerňan, M. Müller, Z. Müller, J. Tlustý and V. Valouch, "Model Predictive Direct Power Control of Four-Switch-Based Inverter Connected to Unbalanced Grid System," in *2018 IEEE International Conference on the Science of Electrical Engineering in Israel (ICSEE)*, Eilat, Izrael, 2018.

[67] M. F. Alves, Z. M. A. Peixoto, C. P. Garcia and D. G. Gomes, "An integrated model for the study of flicker compensation in electrical networks," *Electric Power Systems Research,* no. 80(10), pp. 1299-1305, 2010.

[68] S. Morello, T. J. Dionise and T. L. Mank, "Comprehensive Analysis to Specify a Static VarCompensator for an Electric Arc Furnace Upgrade," *IEEE Transactions on Industry Applications,* no. 51(6), pp. 4840-4852, 2015.

[69] S. Morello, T. J. Dionise and T. L. Mank, "Installation, Startup, and Performance of a Static VARCompensator for an Electric Arc Furnace Upgrade," *IEEE Transactions on Industry Applications,* no. 53(6), pp. 6024-6032, 2017.

[70] T. J. Dionise, "Assessing the Performance of a Static Var Compensator for an Electric Arc Furnace," *IEEE Transactions on Industry Applications,* no. 50(3), pp. 1619-1629, 2014.

[71] X. Zhu, H. Chen, P. Hu and R. Chen, "Reactive compensation for AC electric arc furnace considering power quality constraints," in *2016 17th International Conference on Harmonics and Quality of Power (ICHQP)*, Belo Horizonte, 2016.

[72] S. Prinz, H. Pietzsch and D. Stade, "Optimal control of static VAr compensators in power supply systems with electrical arc furnaces," in *2005 European Conference on Power Electronics and Applications*, Dresden, 2005.

[73] H. Samet, A. Mojallal, T. Ghanbari and M. Farhadi, "Enhancement of SVC performance in electric arc furnace for flicker suppression using a Gray-ANN based prediction method," *International Transactions on Electrical Energy Systems,* no. 29(4), 2018.

[74] K. Bhaskar and S. N. Singh, "AWNN-Assisted Wind Power Forecasting Using Feed-Forward Neural Network," *IEEE Transactions on Sustainable Energy,* no. 3(2), pp. 306-315, 2012.

[75] Č. Martin, Z. Müller, T. Josef and V. Viktor, "An improved SVC control for electric arc furnace voltage flicker mitigation," *International Journal of Electrical Power & Energy Systems,* no. 129, July 2021.

# List of author's publications

**Journal Publications (indexed in Web of Science) related to the dissertation topic**

1. Čerňan, M.; Müller, Z.; Tlustý, J.; Valouch, V.. An improved SVC control for electric arc furnace voltage flicker mitigation. *International Journal of Electrical Power and Energy Systems*. 2021, **129** ISSN 0142-0615. DOI 10.1016/j.ijepes.2021.106831.
   ***Citations: 1***

**Conference Publications (indexed in Web of Science) related to the dissertation topic**

1. Čerňan, M.; Müller, M.; Müller, Z.; Tlustý, J.; Valouch, V.. Model Predictive Direct Power Control of Four-Switch-Based Inverter Connected to Unbalanced Grid System. In: *2018 IEEE International Conference on the Science of Electrical Engineering in Israel*. Eilat, 2018-12-12/2018-12-14. Tel Aviv: IEEE, 2018. ISBN 978-1-5386-6378-3. DOI 10.1109/ICSEE.2018.8646186.

2. Čerňan, M.; Tlustý, J.. Study of the susceptance control of industrial Static Var Compensator. In: *2015 16th International Scientific Conference on Electric Power Engineering (EPE)*. Kouty nad Desnou, 2015-05-20/2015-05-22. Ostrava: VŠB - Technical University of Ostrava, 2015. s. 538-541. ISSN 2376-5623. ISBN 978-1-4673-6788-2. DOI 10.1109/EPE.2015.7161150.
   ***Citations: 2***

3. Čerňan, M.; Tlustý, J.. Model of Electric Arc Furnace for Designing of Power Quality Improvement Equipment. In: *Proceedings of the 2014 15th International Scientific Conference on Electric Power Engineering*. Electric Power Engineering 2014, Brno, 2014-05-12/2014-05-14. Brno: Vysoké učení technické v Brně, 2014. s. 187-192. ISSN 2376-5623. ISBN 978-1-4799-3807-0. DOI 10.1109/EPE.2014.6839465.
   ***Citations: 1***

**Other Publications related to the dissertation topic**

4. Čerňan, M.; Tlustý, J.; Müller, Z.; Müller, M.. Experience with Reconstruction of Industrial SVC Analogue Controller. In: Cigre 2020 e-Session. online, 2020-08-24/2020-09-03. Paris: Cigre, 2020.

5. Čerňan, M.; Tlustý, J.; Müller, Z.; Procházka, R.. Ferroresonance Phenomena in Medium Voltage Systems. In: 19th International Symposium on High Voltage Engineering. Pilsen, 2015-08-23/2015-08-28. Pilsen: University of West Bohemia, 2015. ISBN 978-80-261-0477-3.

6. Čerňan, M.; Tlustý, J.; Müller, Z.; Brabec, D.. Srovnání různých přístupů ke zlepšování parametrů SAIFI a SAIDI v distribučních sítích vysokého napětí. In: 19. konference ČK CIRED. CK CIRED 2015, Tábor, 2015-11-10/2015-11-11. Tábor: Český komitét CIRED, 2015. ISBN 978-80-905014-4-7.

7. Čerňan, M.; Müller, Z.; Tlustý, J.. Increase of Voltage Quality in Industrial Distribution Systems. *Renewable Energies & Power Quality Journal (RE&PQJ)*. 2015, **1**(13), 704-707. ISSN 2172-038X. DOI 10.24084/repqj13.459.
8. Čerňan, M.; Tlustý, J.. Návrh filtrov vyšších harmonickcých pre objekty s rozsiahlou káblovou sieťou. In: *Konference ČK CIRED 2014*. CIRED 2014, Tábor, 2014-11-04/2014-11-05. Praha: CIRED, 2014. ISBN 978-80-905014-3-0.

9. Čerňan, M. Odporové prstence vzduchových tlmiviek. In: *Proceedings of ELEN 2014*. ELEN 2014, Praha, 2014-09-11/2014-09-12. Praha: ČVUT FEL, Katedra elektroenergetiky, 2014. ISBN 978-80-01-05654-7.

10. Čerňan, M. Time Domain Model of Electric Arc Furnace for Study Power Quality in Industrial Networks. In: FOREN 2014. Bucharest, 2014-06-22/2014-06-24. Bukurešť: WEC - Romanian National Committee, 2014.

**Other Publications**

11. Čerňan, M.; Müller, Z.; Tlustý, J.; Halaška, J.. Critical infrastructure and the possibility of increasing its resilience in the context of the energy sector. In: Proceedings of *2020 21st International Scientific Conference on Electric Power Engineering (EPE)*. Prague, 2020-10-19/2020-10-21. 2020. ISSN 2376-5631. ISBN 978-1-7281-9479-0. DOI 10.1109/EPE51172.2020.9269175.

12. Čerňan, M.; Müller, Z.; Tlustý, J.; Halaška, J.. Methodology of electricity supplying of critical infrastructure in crisis situations. In: Proceedings of *2020 21st International Scientific Conference on Electric Power Engineering (EPE)*. Prague, 2020-10-19/2020-10-21. 2020. ISSN 2376-5631. ISBN 978-1-7281-9479-0. DOI 10.1109/EPE51172.2020.9269257.

13. Alshammari, A.; Čerňan, M.; Müller, Z.. Potential of technical losses reduction in low voltage feeder using small photovoltaics. In: Proceedings of *2020 21st International Scientific Conference on Electric Power Engineering (EPE)*. Prague, 2020-10-19/2020-10-21. Prague: Czechoslovakia Section IEEE, 2020. ISSN 2376-5631. ISBN 978-1-7281-9479-0. DOI 10.1109/EPE51172.2020.9269214.

14. Valouch, V.; Čerňan, M.; Šimek, P.; Škramlík, J.. Fault identification at microgrid-connected converter and its ride-through capability. In: *Proceedings of the 9th International Scientific Symposium on Electrical Power Engineering ELEKTROENERGETIKA 2017*. ELEKTROENERGETIKA 2017, Stará Lesná, 2017-09-12/2017-09-14. Košice: Technical University of Košice, 2017. pp. 68-71. ISBN 978-80-553-3195-9.

15. Melkior, U.; Čerňan, M.; Müller, Z.; Tlustý, J.; Kasembe, A.. The Reliability of the System with Wind Power Generation. In: Proceedings of *2016 17th International Scientific Conference on Electric Power Engineering (EPE 2016)*. 17th International Scientific Conference on Electric Power Engineering, Praha, 2016-05-16/2016-05-18. New York: IEEE, 2016. International Scientific Conference on Electric Power Engineering. ISBN 978-1-5090-0907-7. DOI 10.1109/EPE.2016.7521833.

16. Müller, Z.; Müller, M.; Tuzikova, V.; Tlustý, J.; Čerňan, M.; Beck, Y.; Golan, G.. Novel method of optimization of losses in power grid. In: *IEEE International Conference on the Science of Electrical Engineering*. 2016 IEEE International Conference on the Science of Electrical Engineering, Eilat, 2016-11-16/2016-11-18. Tel Aviv: IEEE, 2016. ISBN 978-1-5090-2152-9. DOI 10.1109/ICSEE.2016.7806044.
***Citations: 1***
17. Müller, Z.; Švec, J.; Čerňan, M.; Kyncl, J. The Use of Regression Methods for Measurement and Diagnostics in Electrical Power Engineering. In: Proceedings of the 13th International Scientific Conference EPE 2012. Brno: VUT v Brně, Fakulta elektrotechniky a komunikačních technologií, 2012. pp. 413-417. ISBN 978-80-214-4514-7.
***Citations: 5***

# A. Appendix A

| Element | Parameter | Units | Value |
|---|---|---|---|
| PCC | $S_{ks}$ | MVA | 1500 |
| | $V_{ns}$ | kV | 119 |
| HV transformer | $S_n$ | MVA | 63 |
| | $V_{n1}$ | kV | 110 |
| | $V_{n2}$ | kV | 23 |
| | $z_k$ | % | 11,85 |
| Furnace reactor | $X_n$ | Ω | 0 - 2,5 |
| Furnace transformer | $S_n$ | MVA | 50 |
| | $V_{n1}$ | kV | 22 |
| | $V_{n2}$ | kV | 400 - 800 |
| | $r_k$ | % | 0,54 - 1,11 |
| | $x_k$ | % | 6,8 - 11,2 |
| Short current path | X | mΩ | 6,2 |
| | R | mΩ | 0,4 |

*Table A.1: Parameters for compiling the theoretical characteristics of EAF.*

# B. Appendix B- Character of EAF – initial meltdown phase

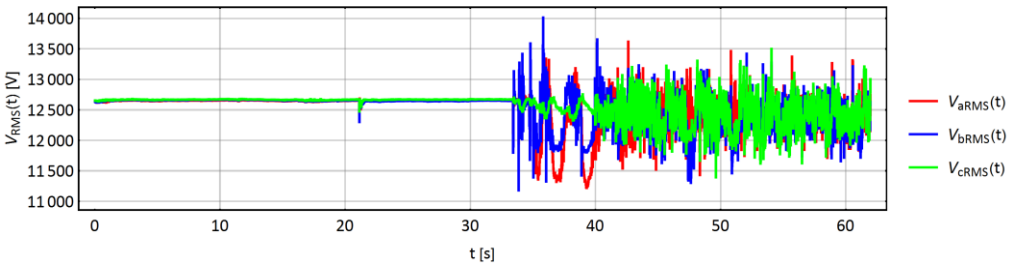


*Figure B.1: EAF MV section voltages during the initial meltdown phase.*

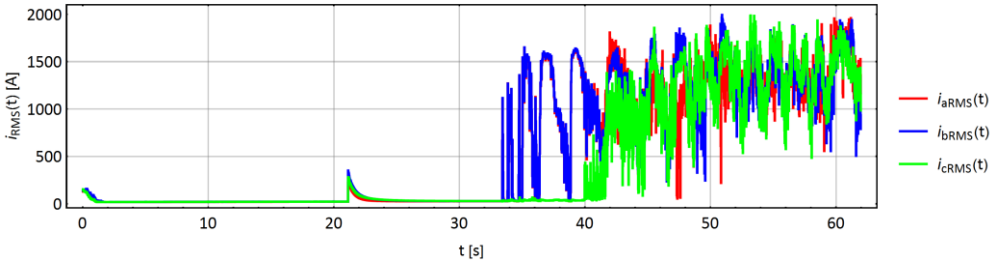


*Figure B.2: EAF MV section currents during the initial meltdown phase.*

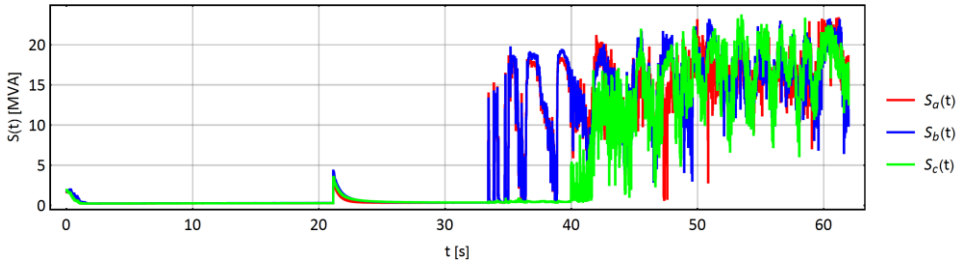


*Figure B.3: EAF MV section apparent powers during the initial meltdown phase.*

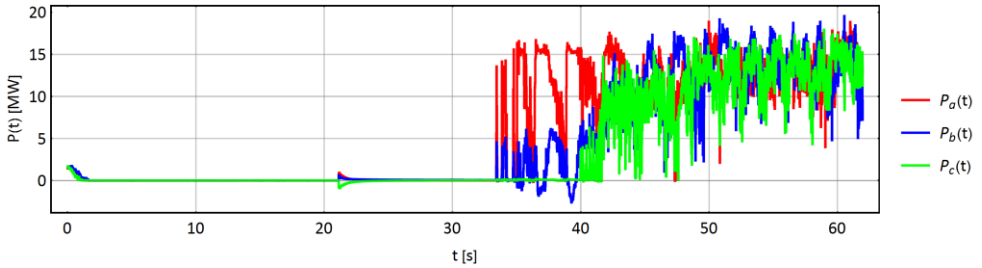


*Figure B.4: EAF MV section active powers during the initial meltdown phase.*

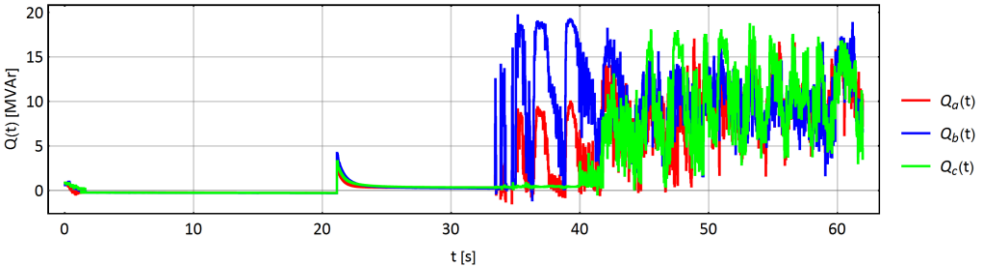


*Figure B.5: EAF MV section reactive powers during the initial meltdown phase.*

# C. Appendix C - Character of EAF – meltdown phase

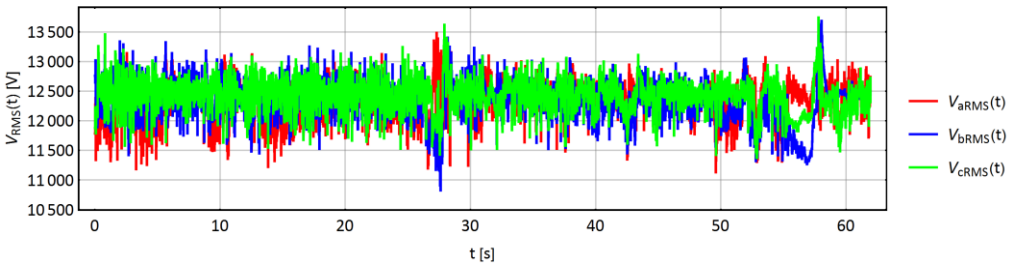


*Figure C.1: EAF MV section voltages during the meltdown phase.*

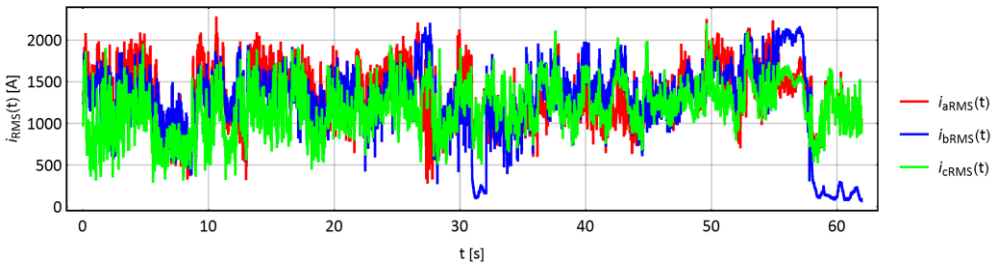


*Figure C.2: EAF MV section currents during the meltdown phase.*

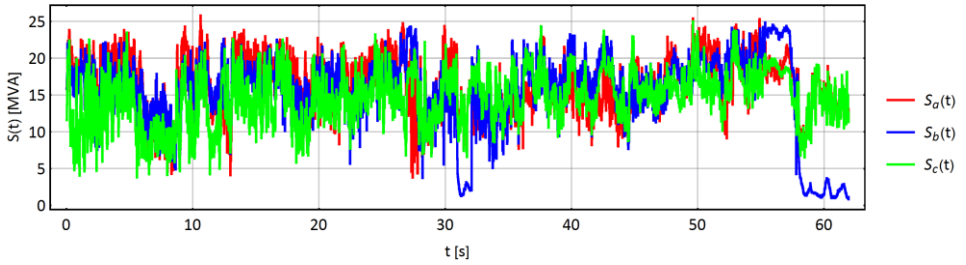


*Figure C.3: EAF MV section apparent powers during the meltdown phase.*

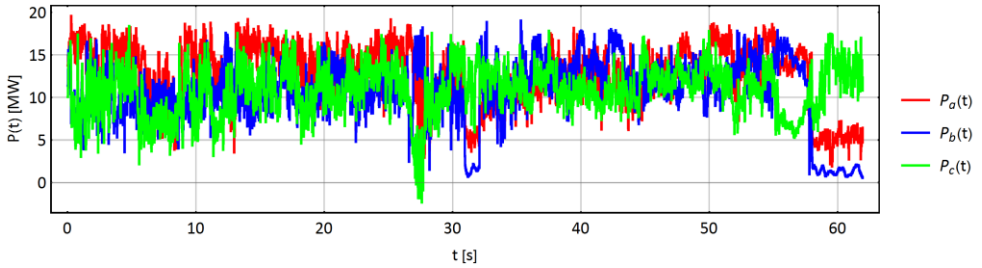


*Figure C.4: EAF MV section active powers during the meltdown phase.*

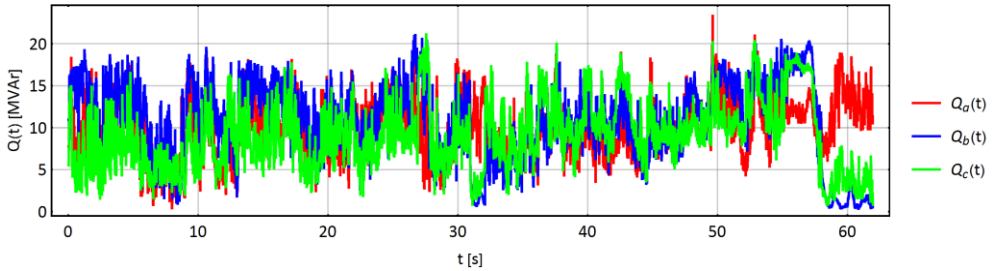


*Figure C.5: EAF MV section reactive powers during the meltdown phase.*

# D. Appendix D - Character of EAF – refining phase

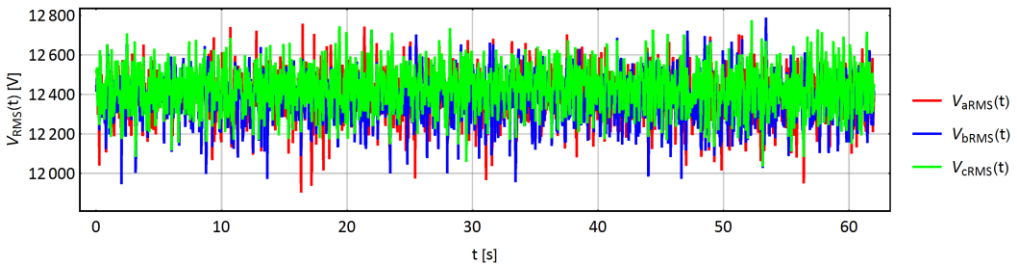


*Figure D.1: EAF MV section voltages during the refining phase.*

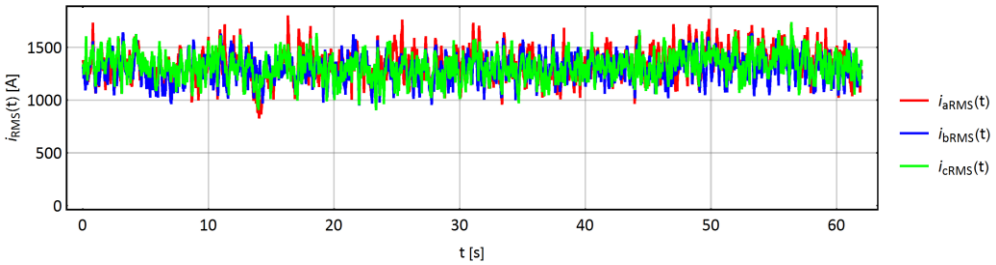


*Figure D.2: EAF MV section currents during the refining phase.*

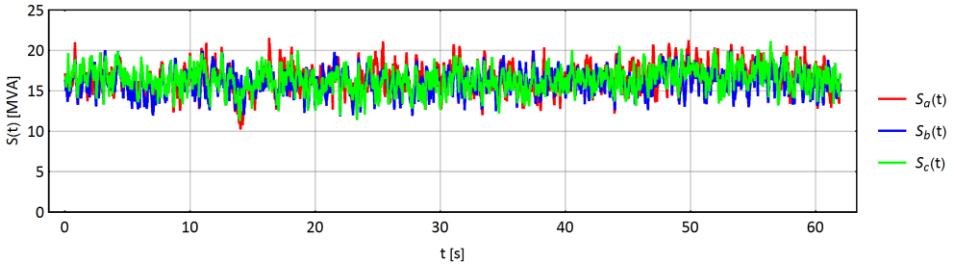


*Figure D.3: EAF MV section apparent powers during the refining phase.*

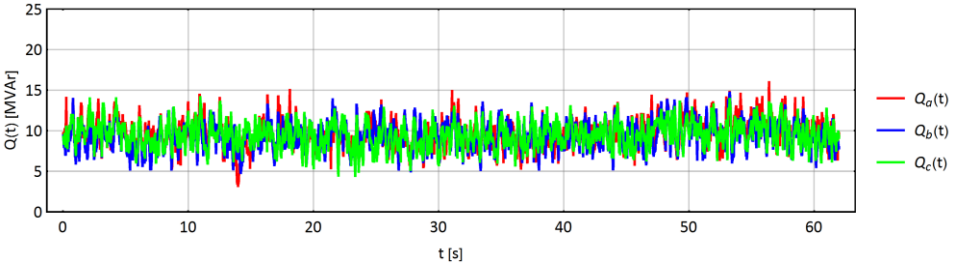


*Figure D.4: EAF MV section active powers during the refining phase.*

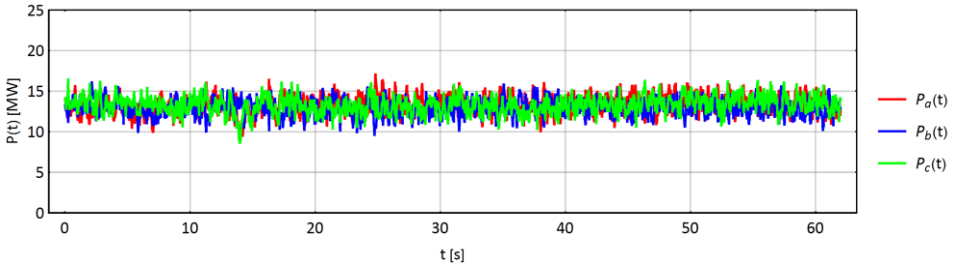


*Figure D.5: EAF MV section reactive powers during the refining phase.*